Ocean Barramundi Expansion Project - Integrated Modelling Report

Customer	Tassal
Project	000608.003
Deliverable	1
Version	1
	16 July 2024

Document Control

Document Identification

Title	Ocean Barramundi Expansion Project - Integrated Modelling Report
Project No	000608.003
Deliverable No	1
Version No	1
Version Date	16 July 2024
Customer	Tassal
Classification	BMT (OFFICIAL)

Author	Gayan Gunaratne, Ashrafur Rahman
Checked By	Harrison Carmody
Approved By	Louise Bruce
Project Manager	Harrison Carmody

Amendment Record

The Amendment Record below records the history and issue status of this document.

Version	Version Date	Distribution	Record
A	27 March 2022	Internal	Docx
0	03 May 2022	Client	PDF
1	16 July 2024	Internal	Docx

Contents

Tables

Figures

1 Introduction

1.1 Background

Tassal Operations Pty Ltd (referred to as Tassal hereafter) is proposing to implement an expansion of its current ocean barramundi farming operations in Cone Bay, West Kimberley to the broader Buccaneer Archipelago (Figure 1.1). This expansion will allow Tassal to increase production to approximately 17,500 tonnes per annum, reaching a maximum of ~4,500 tonnes per site before harvesting.

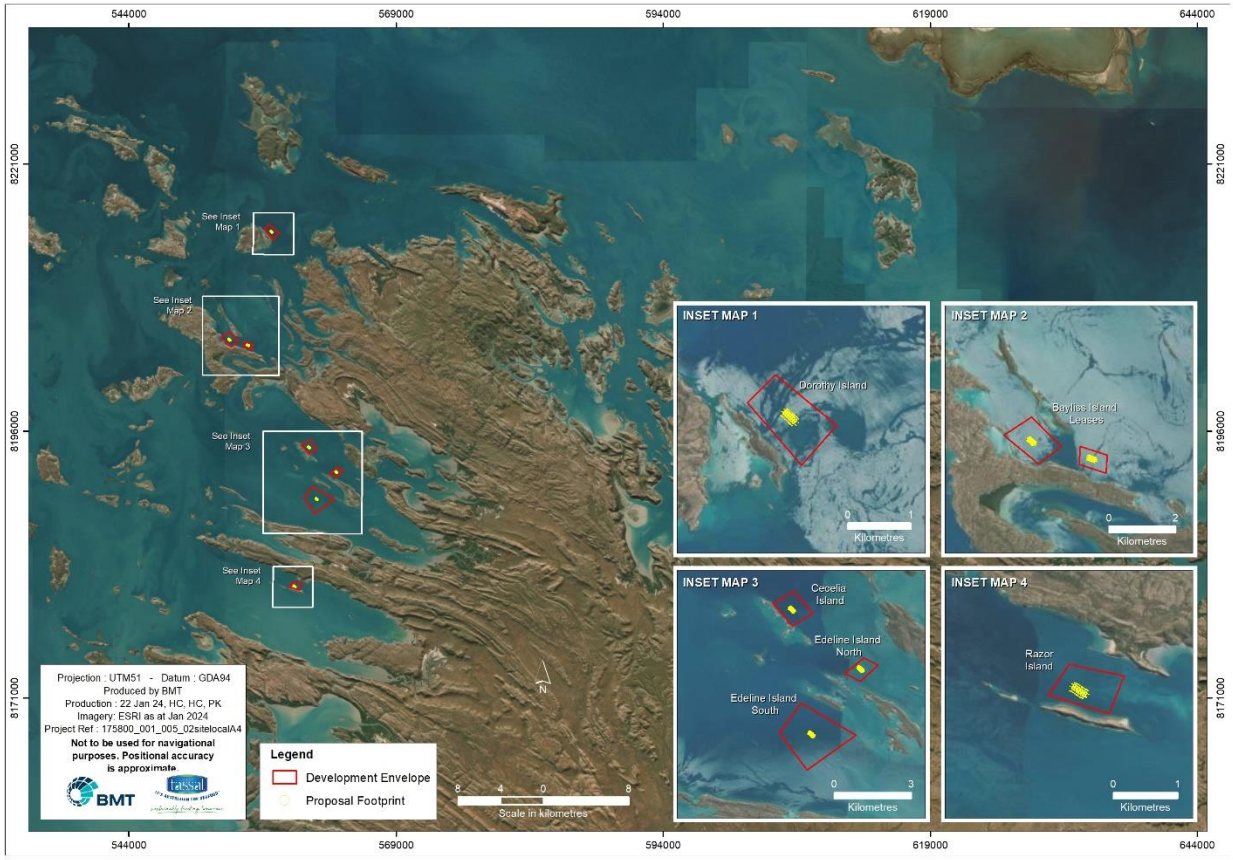

Figure 1.1 Seven proposed farm locations

A review of potential environmental impacts of the prosed expansion included the development of an integrated aquaculture model to quantify the potential impacts of aquaculture activities on water quality parameters (e.g., nutrient concentrations, chlorophyll concentrations, etc.) and examine underlying sediments under different operational scenarios. The region surrounding the proposed leases is a dynamic system influenced by largescale to local processes. Simulating such an environment is challenging, as a model must resolve the dynamic processes affecting the area on a regional scale (e.g., regional currents), the mesoscale (e.g., eddy formation) and the local scale (e.g., the influence of local bathymetric features on current velocities).

An integrated hydrodynamic and water quality model of the Buccaneer Archipelago and regional marine environment was first developed to reproduce the baseline or “pre-farming” conditions for the region of interest. The methods and results from the model calibration and verification process against baseline field monitoring is presented in BMT (2024a).

The purpose of this document is to summarise the findings of the operational scenario modelling study that includes hydrodynamic, particle tracking, water quality and sediment diagenesis modelling outcomes. Results are provided in the context of marine (benthic and open water) environments in and around the proposed sites for the additional sites.

1.2 Field sampling program and simulation period

Baseline hydrodynamic, water and sediment quality monitoring programs were conducted between February-August 2021, with further water and sediment quality monitoring conducted in 2023 and 2024. The purpose of the program was to effectively capture the seasonal and spatial variability in the collected parameters across the area of interest, providing a comprehensive set of observation data to calibrate the parameters used in the water quality baseline model. Full detail of the monitoring program is provided in BMT (2024b).

The integrated model was used to study the impact of proposed farming under typical environmental forcing, including variation in tides and meteorological conditions (typical sea breeze and seasonal synoptic conditions, i.e., winter and summer). It was important that the period simulated by the model should overlap with the baseline monitoring program from which thresholds for impact assessment were derived. A four month warm up and twelve-month simulation period was selected to provide seasonal variation and ensure sufficient time to accumulate environmental impacts of proposed fish farms. Scenario model results were extracted from May 2020 to May 2021 to cover the baseline monitoring and calibration period.

2 Model Approach

This section summarises the methods applied, and assumptions made that underpin the integrated aquaculture model used in this study, including a technical overview of the integrated modelling methods, the model set-ups for each of the model components and the rationale supporting the model assumptions.

2.1 Integrated model overview

The integrated approach to modelling the dynamic feedback between biotic and physical processes was used to simulate ecosystem response to sea pen aquaculture and assess risk levels for environmental impact. The fully integrated model resolved the regional hydrodynamics of the Buccaneer Archipelago, the dispersal and deposition of waste products from fish pens, the organic and inorganic nutrient contents of these wastes, the associated impact on water and sediment quality and the rate of benthic recovery following cessation and/or relocation of aquaculture operations. There are five key components of the integrated model: 1) hydrodynamic, 2) water quality, 3) fish farm waste, 4) particle transport and 5) sediment diagenesis (Figure 2.1) as described in detail below. Zones of impact were mapped using outputs from the water quality, particle transport and sediment diagenesis models.

Figure 2.1 Components of the integrated aquaculture model

2.2 Hydrodynamic model

The primary aim of the hydrodynamic model was to provide a precise representation of currents for determining the fate of the waste released from the sea-pens. The hydrodynamic model was dynamically coupled to the water quality model driving ecosystem processes such as the magnitude of nutrient fluxes estimated by the sediment diagenesis model through to the temperature dependence of primary productivity.

The hydrodynamic modelling was undertaken using the TUFLOW FV software, which is developed and distributed by BMT. TUFLOW FV is a numerical hydrodynamic model solving the two-dimensional (2D)

and three-dimensional (3D) Non-Linear Shallow Water Equations (NLSWE). The model is suitable for simulating a wide range of hydrodynamic systems ranging in scale from open channels and floodplains, through estuaries to coasts and deep offshore. The three-dimensional model was deployed in this study.

The Finite-Volume (FV) numerical scheme employed by TUFLOW FV solves the NLSWE on unstructured meshes comprised of triangular and quadrilateral elements. The flexible mesh allows for seamless boundary fitting along complex coastlines or channels as well as accurately and efficiently representing complex bathymetries with a minimum number of computational elements. The flexible mesh capability is particularly efficient at resolving a range of scales in a single model without requiring multiple domain nesting. In the present study, a flexible mesh of triangular elements with varying spatial resolution has been employed. Furthermore, the models developed by BMT incorporate a hybrid (fixed z-sigma) coordinate scheme. While the fixed layers are used to capture the necessary pycnoclines, and sigma coordinates placed above fixed layers adjust with the water's surface.

2.2.1 Domain and model mesh bathymetry

The hydrodynamic model covers the proposed ocean barramundi expansion project to ≈180 km radius off the coast adjacent to the leased areas. The domain extends from Carnot Bay in southwest to Brunswick Bay in northeast including King Sound and Cone Bay. The large extent of the domain used was necessary to accurately capture tidal signals and allow the development of the large tidal amplitudes that dominate the hydrodynamics in the nearshore.

A digital elevation model (DEM) was developed using a high-resolution depth model for Northern Australia obtained from Geosciences Australia with a 30 m resolution, Electronic Navigation Chart extracted from MIKE CMAP and supplied to BMT from MPA, and locally acquired high resolution single beam sonar data supplied by MPA. All the datasets were converted to mean sea level (MSL), interpolated to the grid locations and the final bathymetry adopted in this study is as shown in Figure 2.2 and Figure 2.3.

Figure 2.3 depicts a high-resolution mesh bathymetry of the area of interest around the proposed sites. Depths increase from ~30 m in Buccaneer Archipelago to ~100 m offshore in the northwest. Careful consideration was therefore given to ensure the model resolution captured the transitions from deep to shallow water, especially relatively deep channels flanked by shallower islands and sandbars.

Two mesh configurations covering the same domain with similar performance against observed baseline were selected for the study. The selection was based on the need to resolve small scale bathymetry and flow features affecting the waste discharge underneath the pen. The first mesh configuration was used in the particle tracking model to derive the outer extent and footprint of the particulate waste footprints beneath the pen. The second mesh configuration, designed for the water quality model was created with refinement within the zones of impact to effectively capture the release of nutrients from the pens and nutrient fluxes from the sediments beneath.

The first mesh configuration consisted of ~52,000 horizontal triangular mesh cells of varying dimensions. At the open ocean boundary and in remote deeper areas the element side lengths were in the order of 15km. The second mesh configuration consisted of ~43,000 horizontal mixed triangular and quadrilateral mesh cells of varying dimensions. The mesh size in the vicinity of the pens was reduced to ~ 60 m while the mesh size in remote deeper areas was increased to ~17 km. In both configurations, the mesh resolution was gradually increased towards the areas of interest with further resolution within the site boundaries. Around the Buccaneer Archipelago, the mesh had typical element side lengths of 150 – 300 m with minimum lengths sides along the coastline reduced to 75 m.

The hydrodynamic model was undertaken in 3D baroclinic mode adopting a hybrid sigma/z-coordinate layer scheme. Five sigma layers were applied above -8.5 m AHD and had the ability to vary in their thicknesses depending on the water surface elevation changes. The vertical coordinates were fixed relative to Australian Height Datum (AHD) and comprised of 20 fixed-depth layers (z layers) of variable depth, starting at -8.5 m AHD. The z-grid layers were organised as follows:

- -8.5 to -18.0 mAHD (6 layers): ~1.5 m.
- -18.0 to -26.0 mAHD (3 layers): ~3.0 m.
- -26.0 to -30.0 mAHD (1 layer): ~4 m.
- -30.0 to -50.0 mAHD (2 layers): ~10 m.
- -50.0 to -100.0 mAHD (2 layers): ~25 m.
- -100 to -200 mAHD (2 layers): ~50 m.
- -200 to -500 mAHD (1 layer): ~300 m.
- -500 to -2000 mAHD (3 layers): ~500 m.

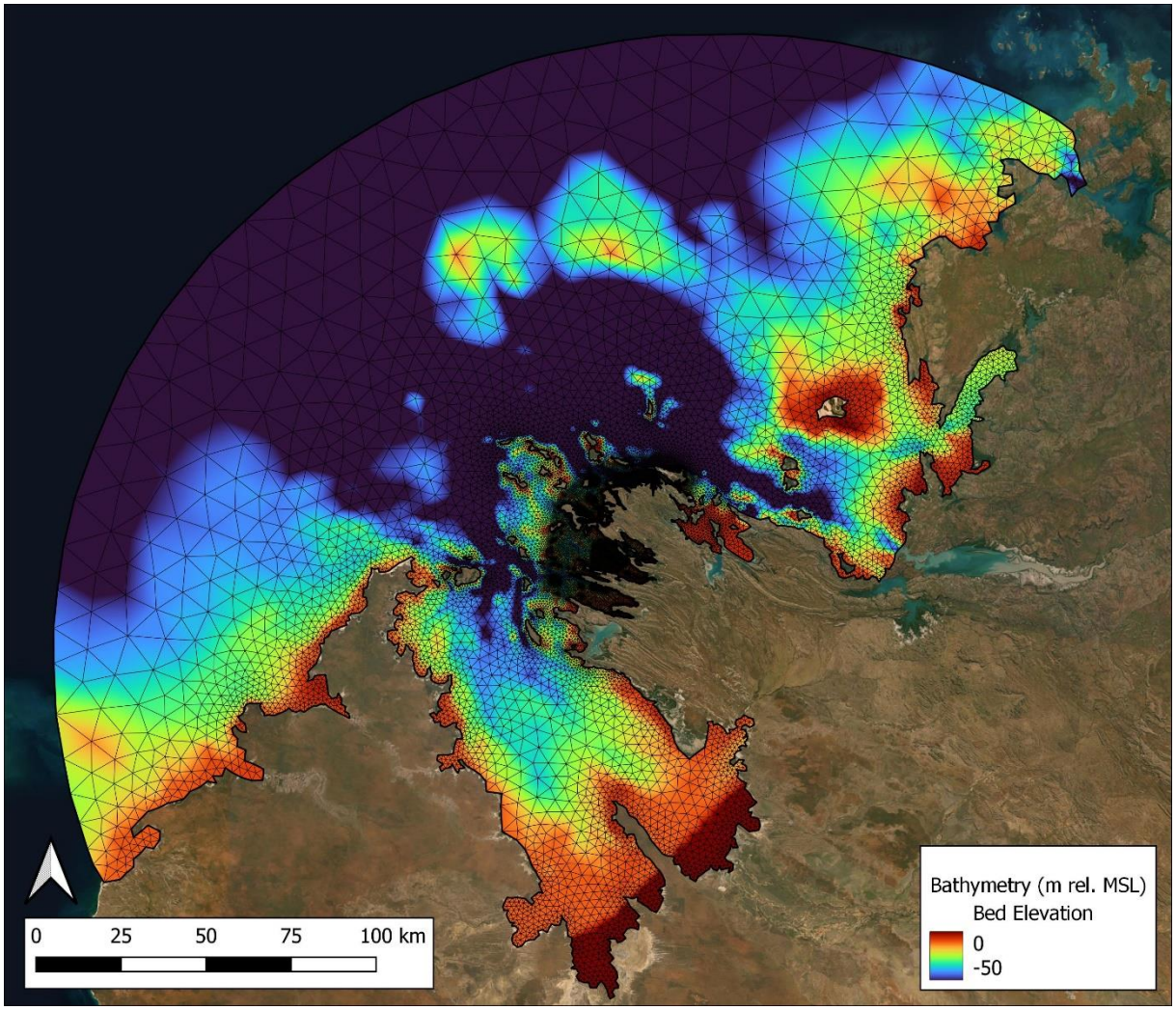

Figure 2.2 TUFLOW FV hydrodynamic model mesh and bathymetry

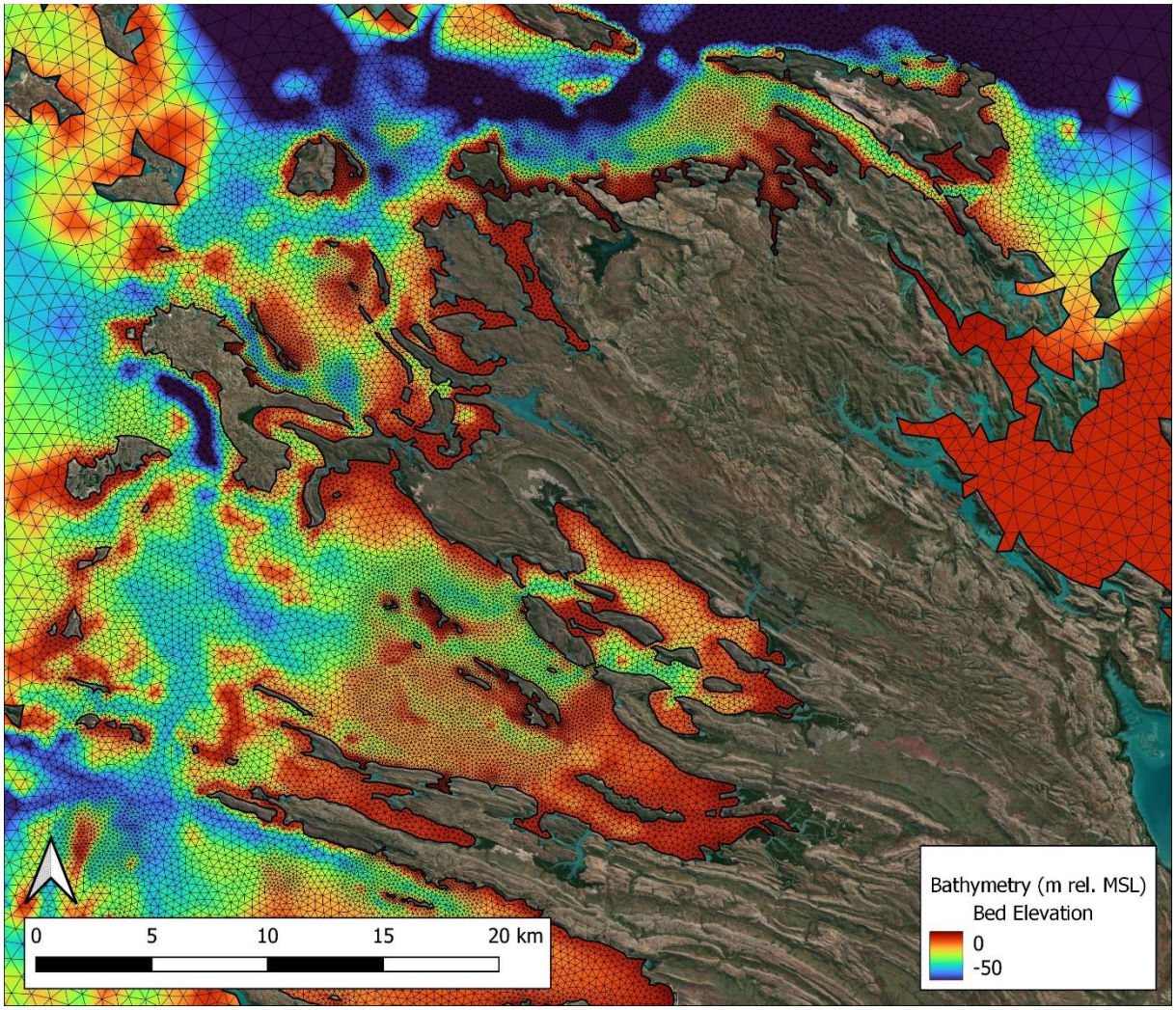

Figure 2.3 TUFLOW FV hydrodynamic model mesh and bathymetry around the primary area of interest.

2.2.2 Boundary conditions

2.2.2.1 Open boundary

The open ocean boundary conditions were forced with tidal variations and general oceanic recirculation for temperature, salinity, current speed and direction.

Tidal water-levels with temporal and spatial variations were applied at the model boundaries based on harmonic constituents from the Finite Element Solution – Global Tide Model FES2014 (2016).

The tidal model was based on a 0.0625° x 0.0625° spatial resolution and included 34 harmonic constituents. Water-levels were generated and transferred to the model at a temporal resolution of 15 minutes covering the period of simulation. The model solution used both in-situ tidal data sources as well as satellite mounted altimeter observations from Topex/ Poseidon, Jason-1, Jason-2, TP interleaved -J1 interleaved, ERS-1, ERS-2, and Envisat. The time series of the water-levels applied at the western-most and eastern-most points along the ocean boundary are presented in Figure 2.4. The figures depict the semi-diurnal tidal pattern and the strong spatial variation in the tidal amplitude within the model domain.

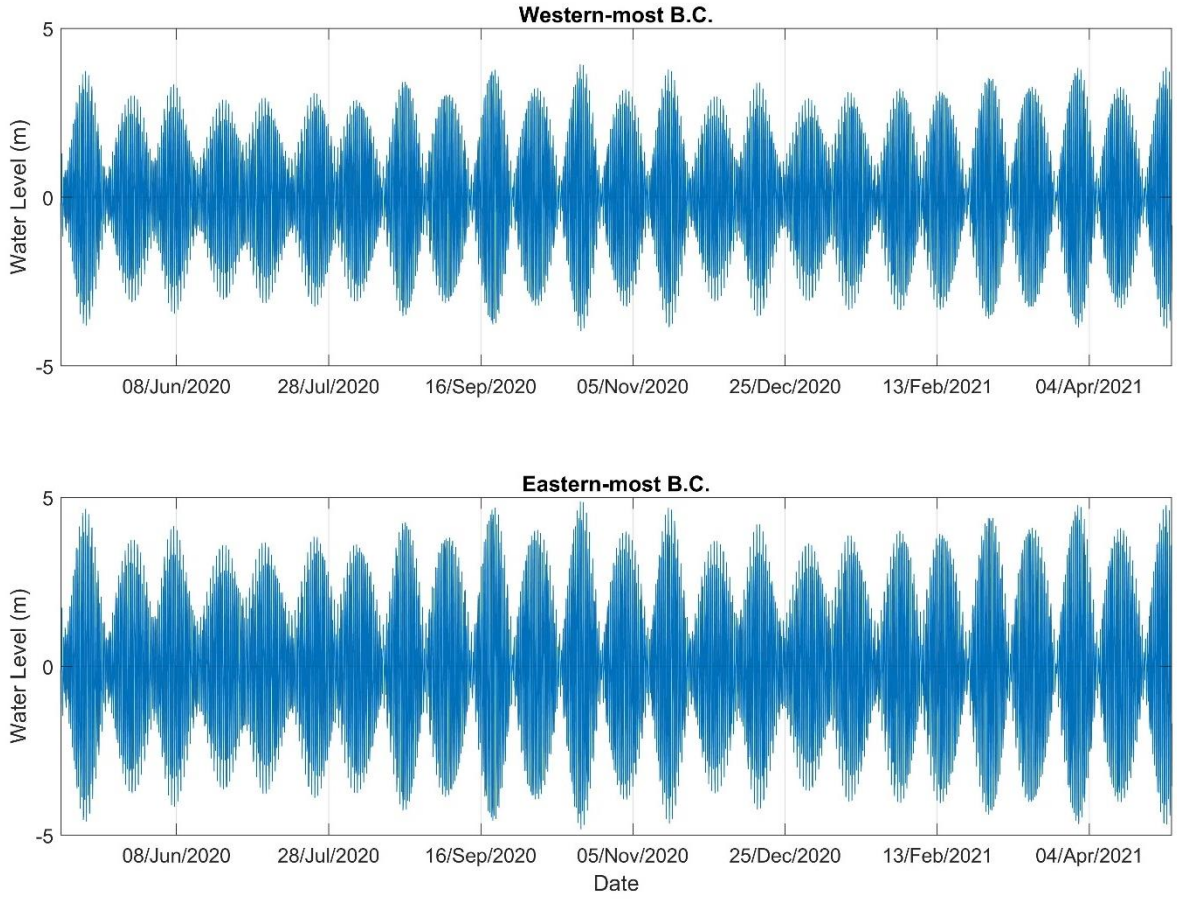

Figure 2.4 Tidal water level along the open ocean boundary

Regional current forcing (residual water level, current magnitude and direction) and profiles of temperature and salinity were also applied on the model open ocean boundary. These were derived from the ocean general recirculation Hybrid Coordinate Ocean Model HYCOM with variation in both space (horizontal and vertical) and time (HYCOM 3.1).

HYCOM 3.1 is a general circulation model providing wind driven and geostrophic flows with vertical coordinates that are isopycnic in the open ocean. The analysis dataset used in this study covers from 2014 onwards and uses data assimilation to improve the accuracy of the prediction by ‘relaxing’ the solution towards observed data from a variety of sources (e.g., in-situ monitoring devices and satellite altimetry).

The HYCOM model spatial resolution used was approximately 5 km horizontally (non-uniform spacing over the vertical) with a temporal resolution of 6 hours. The water level specified on the model boundary was a linear superposition of the HYCOM water level and the tidal water level from FES2014. At each time step the velocity profiles at the open ocean boundary were specified as a superposition of the HYCOM velocity profile and the depth-averaged tidal current and then relaxed barotropically using an active Flather-type (Flather,1976) condition. This approach was used as it minimises the reflection of outward propagating barotropic waves at the model open boundaries (allows for the over-specification of the boundary condition).

Sea-surface elevation, velocity, salinity, and temperature along the ocean boundary of the domain were applied by extracting HYCOM model output and converting to a TUFLOW FV boundary condition format.

2.2.2.2 Atmospheric boundary

A gridded atmospheric data forcing was required to ensure the hydrodynamic model capture the variation between the nearshore and offshore conditions. Atmospheric datasets were applied as gridded (spatially and temporally varying) and interpolated to the TUFLOW FV model mesh. The hourly datasets with 0.25° spatial resolution were sourced from the European Centre for Medium-Range Weather Forecasts' (ECMWF) ERA5 global atmospheric reanalysis model. The ECMWF ERA5 product includes data assimilation techniques to incorporate historical observations of atmospheric variables. Atmospheric forcing included in the model were:

- 10 m wind speed vector,
- Relative humidity,
- Mean sea level pressure,
- Mean surface downward short-wave radiation,
- Mean surface long wave radiation flux, and
- Air temperature (at a height of 2m above sea-level).

To check consistency of the atmospheric forcing with local observations, the reanalysis datasets were compared with the local meteorological data from a nearby station. Comparison of wind speed and direction indicated that the ERA5 datasets are representative of the local observations at the Broome Airport station of proximity to the study area (Figure 2.5).

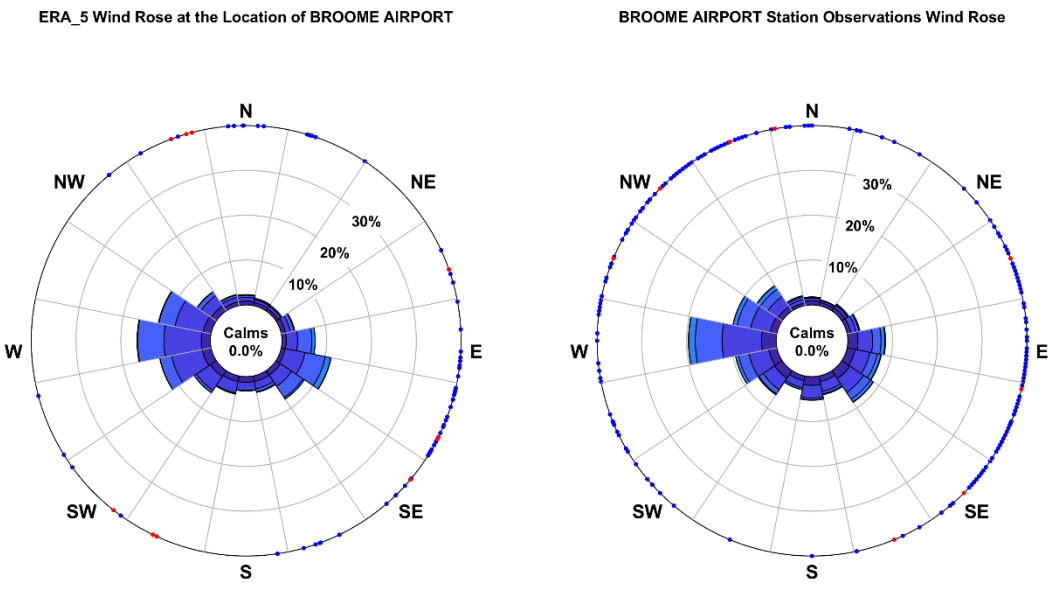

Figure 2.5 Wind roses showing comparison between ERA5 (left) and observations at Broome Airport Station (right) (~ 9 km distance apart)

2.2.2.3 River inflows

To represent catchment nutrient loads, three key river discharges were included in model simulations:

- Fitzroy River
- Isdell River
- Lennard River.

River flow and river water quality data were extracted for the past 15 years (2006-2021) from the Water Information Reporting (WIN) tool (DWER, 2021). Data were extracted from the three most downstream gauging locations with the river flows entering the model domain (Figure 2.6).

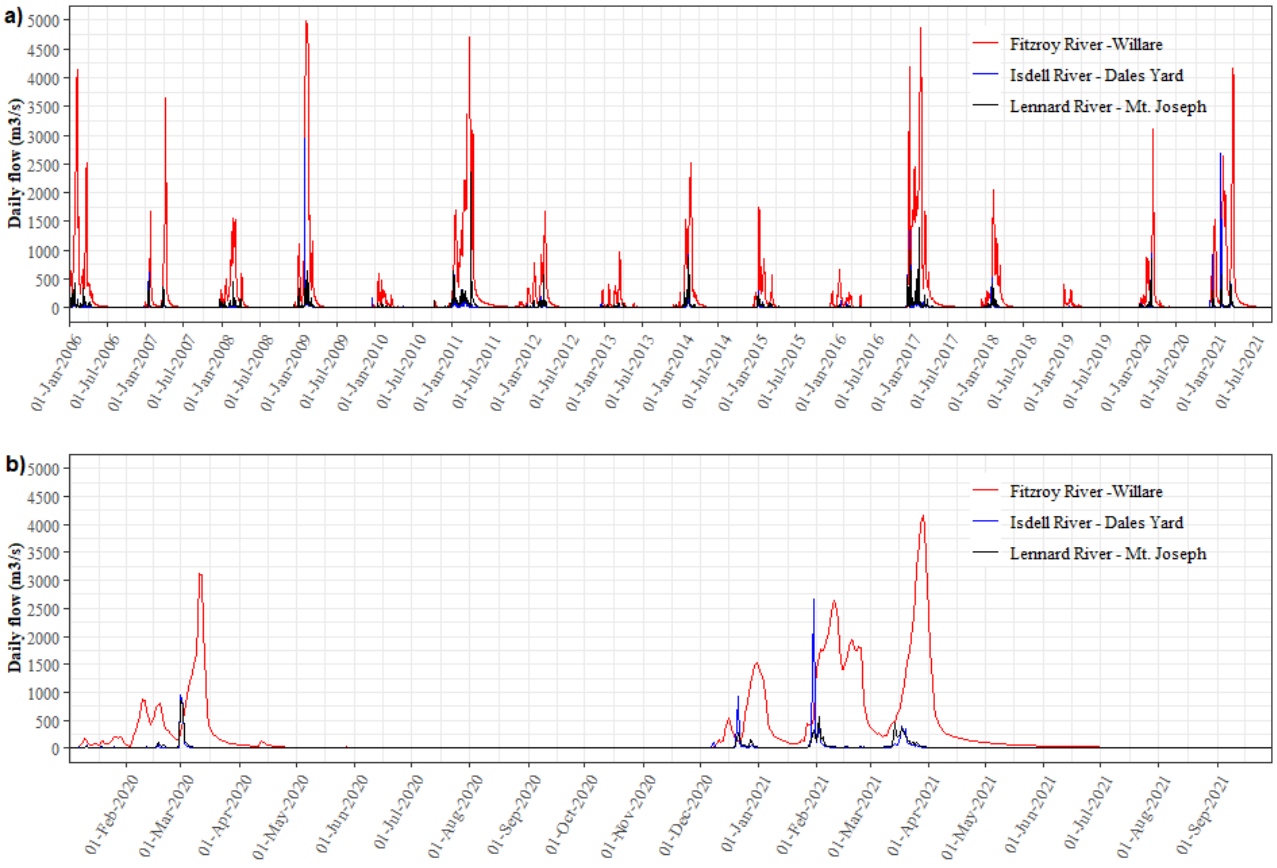

Figure 2.6 Daily flow data from the three main rivers located in the model catchment a) from 2006 to 2021; b) from Jan 2020 to May 2021 (includes the simulation period)

2.2.2.4 Bed roughness

Bottom roughness used to represent bed scale turbulence was assigned based on the regional marine habitat map, described in BMT (2024b). A default global default bottom roughness length scale coefficient (ks) of 0.06 was used for all material types except habitats such as mangroves, rocks and reefs, where ks was set to 0.5 m. Further adjustment of local values for ks was undertaken as part of the hydrodynamic calibration process as described in BMT (2024a).

2.2.2.5 Initial conditions and model warm-up

The hydrodynamic conditions for temperature, salinity and currents were initialised from the open ocean boundary conditions and run for a 4-month warm-up period to allow the model to reach equilibrium state. Initial conditions for water quality parameters were set to observed data from the closest sampling period and particle tracking was initialised at zero.

2.3 Water quality model

The TUFLOW FV Water Quality (WQ) Module offers advanced capabilities for the simulation of water quality and ecological processes within a diverse range of aquatic environments. Integrated into the TUFLOW FV framework, this module supports both 2D and 3D modelling, addressing the complex dynamics of natural and constructed waterways. These include lakes, tidal estuaries, river systems, and coastal oceans, where precise and dependable water quality modelling is essential.

The WQ Module is designed with exceptional flexibility, allowing users to customize its setup to meet specific application requirements and complexities. This adaptability enables the module to tackle a broad spectrum of water quality issues, such as nutrient cycling, algae dynamics, contaminant transport, and sediment interactions.

2.3.1 Boundary conditions

2.3.2.1 Open boundary

The concentrations of water quality variables at the open ocean boundary were derived from a combination of observed data collected as part of the baseline monitoring program (BMT 2024a), chlorophyll concentrations from NASA Earth Observations (NEO) data and parameters chosen to represent a typical oligotrophic marine environment.

The water quality variables at the open boundary were derived as follow:

- Total and inorganic nutrient concentrations, were calculated from observed median values collected at the offshore water quality stations (Boundary 1, Boundary 2, Boundary 3, and Boundary 4, see Figure 2.7) of the baseline sampling program interpolated and extrapolated to a full 12-month period.
- The Chlorophyll-*a* concentration at the open boundary were derived from weekly observations from the Moderate Resolution Imaging Spectroradiometer (MODIS) on NASA's Aqua satellite. Data were downloaded from the Chlorophyll Concentration (AQA/MODIS) page 25/08/2021 (NASA Earth Observations 2014).
- The particulate and dissolved organic nutrients were estimated from the observed inorganic and total nutrient concentration with speciation based on observations and assumptions of global ocean trends (Murray 2000).
- Dissolved oxygen concentrations were calculated based on a fully saturated assumption derived from the boundary conditions for temperature and salinity, atmospheric pressure with the dependence in the vapour pressure neglected following Riley and Skirrow (1974).

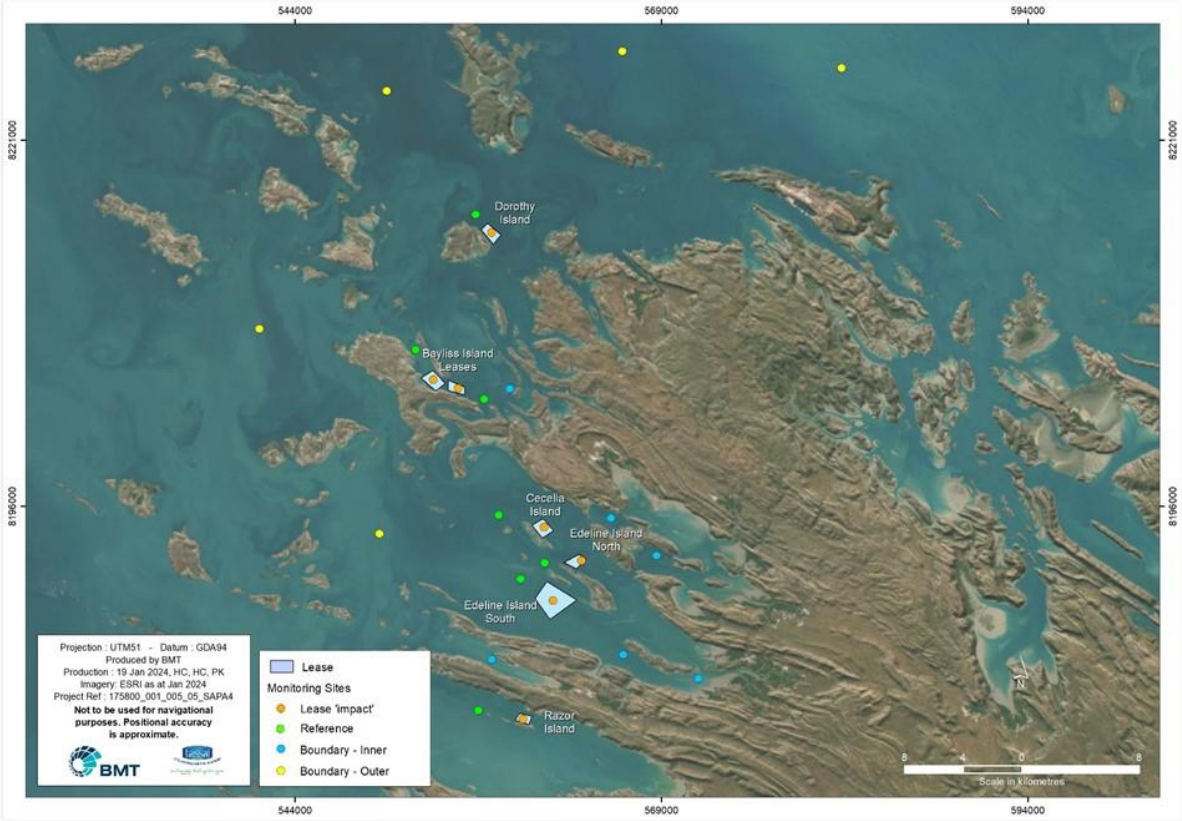

Figure 2.7 Water quality monitoring sites used for the model verification

2.3.2.2 River inflows

Daily river flow rates sourced from three rivers (Figure 2.6) were extrapolated using statistical techniques to obtain data at river outlets. Due to the paucity of river water quality data for the simulated period, available data sampled over the past 15 years were extrapolated to create time series data for corresponding river boundary conditions (Figure 2.8 and Figure 2.9).

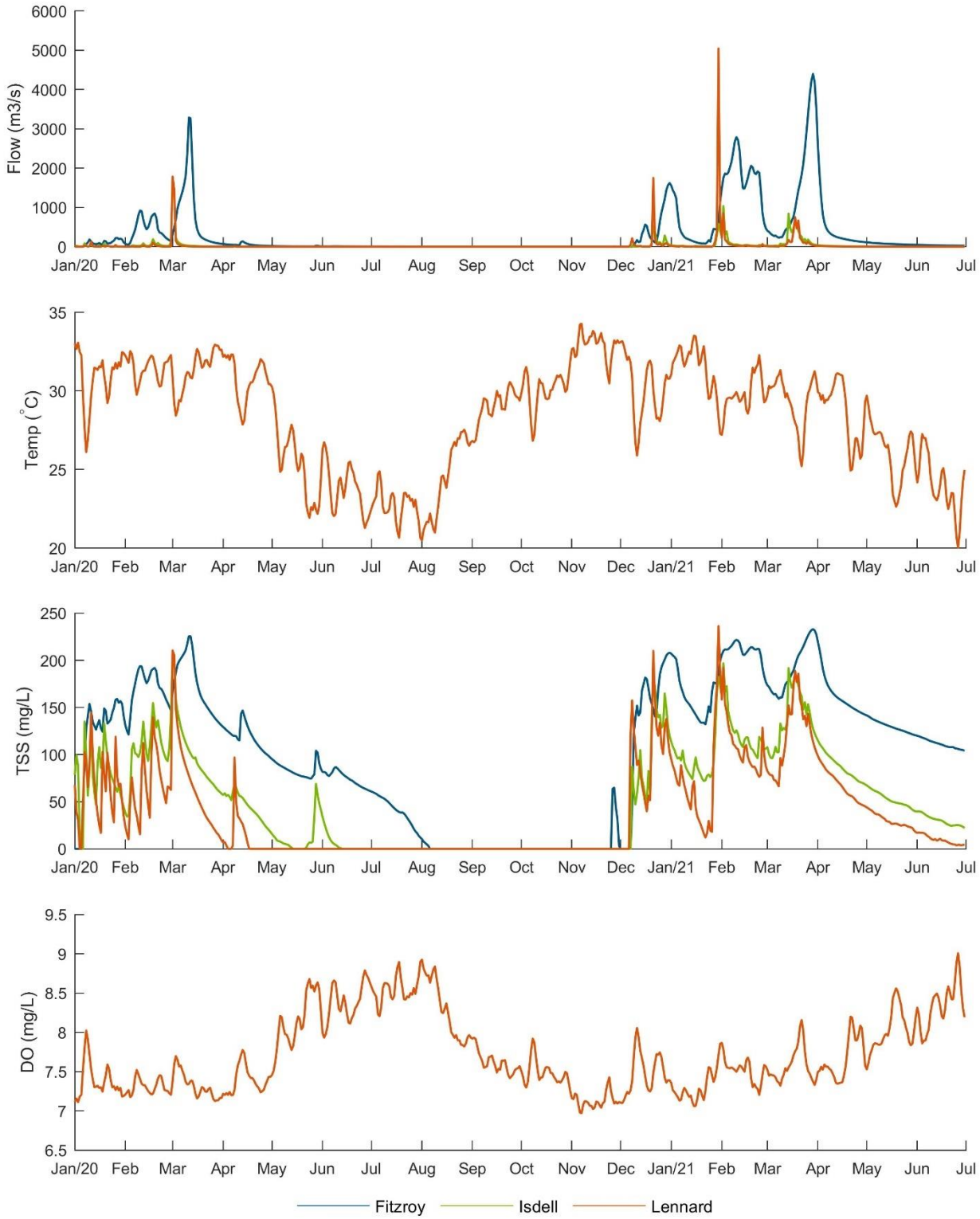

Figure 2.8 Timeseries for daily flow rate, temperature, Total Suspended Solids (TSS) and dissolved oxygen (DO) applied to river boundaries

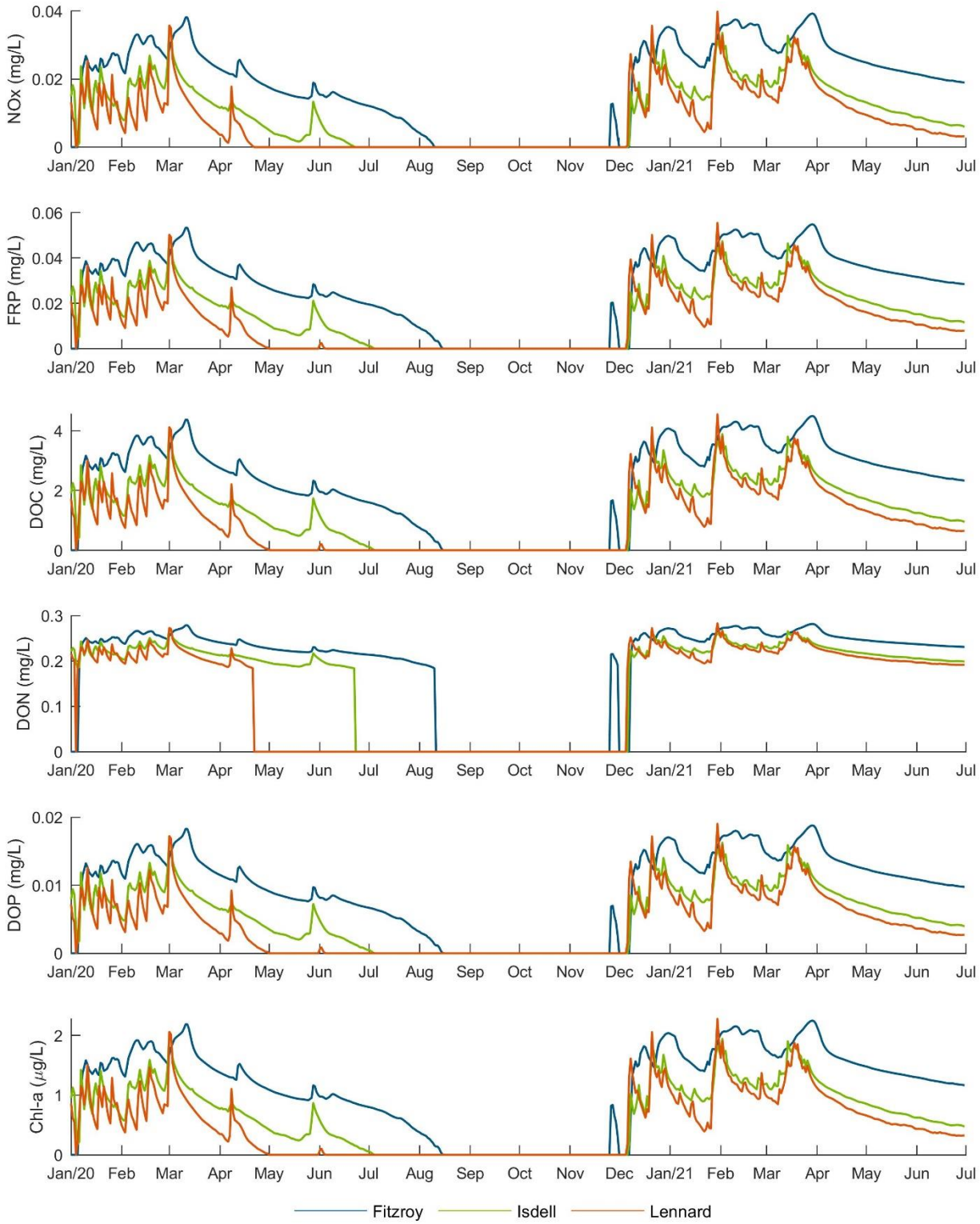

Figure 2.9 Timeseries for dissolved nutrients (N, P,C) and Chlorophyl-a applied to river boundaries

2.3.2.3 Sediment fluxes

Sediment fluxes (including sediment oxygen demand) resulting from decomposition of organic matter and nitrification (i.e., transformation of ammonia into nitrate) in the benthic sediments, lead to oxygen depletion in the hypolimnion and thus play a key role in the biological and chemical processes occurring in the benthic layer.

The sediment fluxes prior to the commencement of fish farming (baseline condition) were calculated based on the following:

- Seven zones corresponding to the habitat maps and representative sediment flux values were assigned through the calibration process.
- The sediment fluxes were calibrated to meet the baseline observations within the model domain using data collected during the period of February to July 2021. The water quality model verification is detailed in BMT (2024a).

As sediment fluxes are determined by benthic organic content and the microbial community, the sediment fluxes under the proposed fish farming scenarios were influenced by the food conversion ratio (FCR) and standing biomass. Values calculated were based on the following assumptions:

- Particulate organic nutrients in fish farm waste eventually deposit, decompose in the benthic layer and get released into the water column under hypoxic conditions.
- For each scenario, sediment fluxes were calculated for the zones underneath and adjacent to sites corresponding to regions of high, medium and low organic footprints. These footprints were derived from particle tracking model (PTM) maps (refer section 2.2).
- The sediment fluxes for the zones of impact were calculated from sediment diagenesis model output (Paraska et al. 2015) based on the rate of deposition of particulate organic carbon (Section 2.2).

2.3.2.4 Sea-pen discharges

Fish waste released from sea-pens were represented as point source boundary conditions with concentration of dissolved inorganic nitrogen and phosphorous (DIN & DIP); and particulate organic carbon, nitrogen and phosphorus (POC, PON and POP) derived from the fish waste model. The following assumptions were made:

- Concentrations were assumed constant with time and uniformly released from the top 10 m depth at the location of the sea-pens.
- The base case was simulated with zero sea-pen waste discharge.

2.4 Fish waste model

A fish waste model was developed by BMT based on advice given by Skretting Australia (https://www.skretting.com/en/) and scientific literature. Skretting is a consultancy providing innovative and sustainable nutritional solutions and services for the aquaculture industry. Skretting has production facilities in 18 countries on five continents and manufactures and delivers high quality feeds from hatching to harvest for more than 60 species. The model is based on the metabolism and the nutrient and carbon outputs of Barramundi species under typical conditions of the Kimberly coastal waters (Skretting, 2024). In this study, the fish waste model predicted the daily mass of waste for a given standing biomass of fish and assumed FCR. Results from the fish waste model were used to set the boundary condition parameters for the water quality and the particle transport models.

The fish waste model resolves the proportion of nitrogen, phosphorus and carbon in farm waste, as well as the solid and the dissolved fractions (Table 2.1). Nutrient speciation is based on the following assumptions:

- The PTM tracks solid waste outputs as four size fractions ranging in density from light to heavy
- Dissolved organic and inorganic nutrients are included as boundary condition in TUFLOW FV Water Quality Module (WQM).
- Speciation of TN and TP were calculated using the fractions described by Herbeck et al., (2013) and Rodela (2013) as:
  - 100% of dissolved P was composed of PO_4,
  - 38% of dissolved N was excreted in organic form
  - 100% of dissolved inorganic N was excreted as NH_4.

Table 2.1 Fish waste model parameters for Barramundi grown in the marine waters of the Kimberley, Western Australia

Description			Parameter values under two different FCRs		Units	Data Source
Feed Conversion ratio (FCR)			2.3	1.5		
Biomass	Licenced Standing Biomass (per pen)		375	375	tonnes	
		as percent of licenced standing biomass	100.0	100.0	Percent	
	Capacity	Net Standing Biomass	375	375	tonnes	
			0.63	0.63	% Body weight/ day	
Mass Balance	Feed rate	Daily feed amount	2.363	2.363	tonnes	
	Input:	Total Input	2.363	2.363	tonnes	
		Metabolic Oxygen Demand	2.639	2.334	tonnes of O_2 per day	Estimated from salmon model
		C as CO_2	0.469	0.276		78% respiration from Bermudes et al (2010)
		Total Waste Load	1.335	0.788	tonnes of waste per day	
		Total load C (T/day)	0.601	0.354	Based on 45% C ratio in Feed	
		Total excretion load	1.335	0.788		78% respiration from Bermudes et al (2010)
Waste	Solid waste	Feed	0.027	0.015	tonnes/day	
		Faecal 1	0.327	0.193	tonnes/day	Based on salmon model

Description		Parameter values under two different FCRs		Units	Data Source
	Faecal 2	0.419	0.247	tonnes/day	Based on salmon model
	Faecal 3	0.562	0.331	tonnes/day	Based on salmon model
Nutrients	POC	0.132	0.078	tonnes C/day	22% ration taken from Bermudes et al 2010
	PON	0.021	0.008	tonnes N/day	Based on SKA Barramundi grower - Nova FF-v10.
	POP	0.018	0.007	tonnes P/day	Based on SKA Barramundi grower - Nova FF-v10
	DIN	0.116	0.044	tonnes N/day	Based on SKA Barramundi grower - Nova FF-v10
	DIP	0.008	0.003	tonnes P/day	Based on SKA Barramundi grower - Nova FF-v10
	Total Carbon Loss	0.601	0.354	tonnes C/day	
	Total Nitrogen Loss	0.137	0.052	tonnes N/day	
	Total Phosphorus Loss	0.026	0.010	tonnes P/day	

2.5 Particle tracking model

The coupled hydrodynamic-particle tracking model (TUFLOW FV PTM) (Figure 2.10) was simulated to study the dispersal and deposition of particulate wastes from 7 aquaculture sites. The Particle Transport Module (PTM) was used to resolve both the vertical and horizontal transport of particulate aquaculture wastes, while accounting for differing size fractions and settling velocities of waste particles (i.e. waste feed and faecal material). The PTM is based on a Lagrangian particle tracking scheme driven by three-dimensional currents and wave fields from the TUFLOW FV model (BMT, 2020). The Lagrangian particle movements included a deterministic component derived from modelled currents and a stochastic 'random walk' component to represent vertical and horizontal dispersive processes due to unresolved turbulence scales. The processes of deposition and resuspension from the seabed due to wave and current induced shear stresses were also resolved using standard boundary layer and sediment transport calculations. A very large number of Lagrangian particles (~1.5 million) were released over a 12-month simulation period in order to integrate over a broad ensemble of environmental conditions, including stochastic dispersion processes.

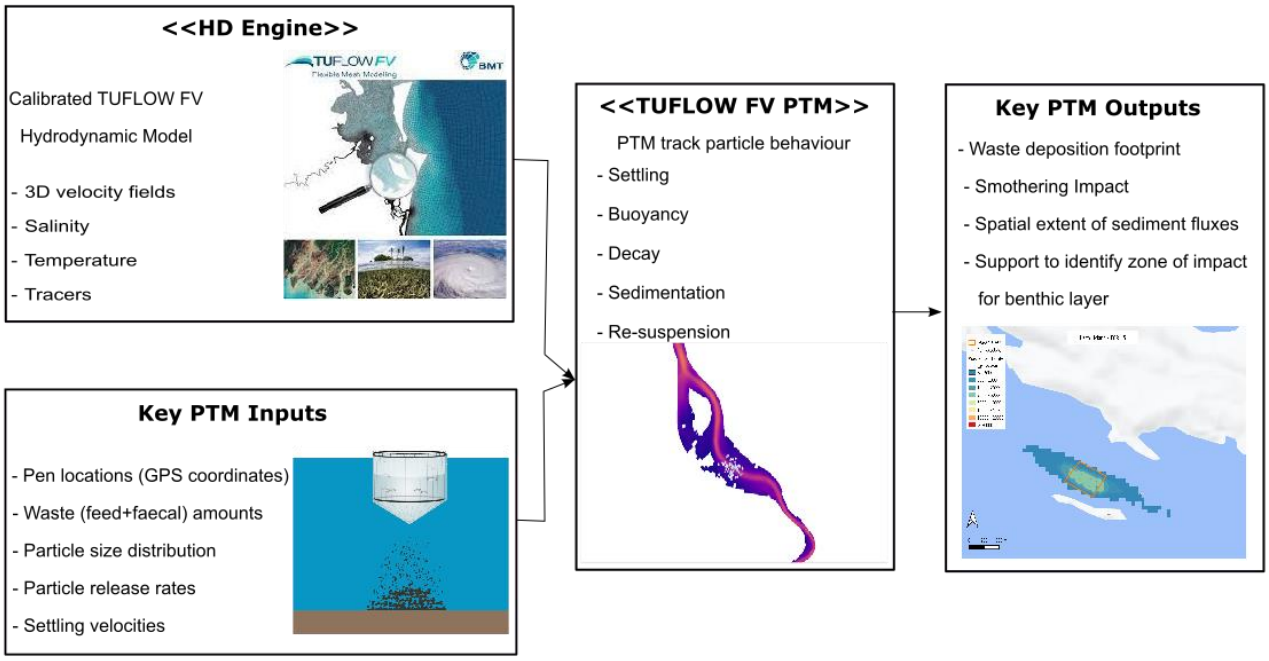

Figure 2.10 Schematic for the coupling of the hydrodynamic model (TUFLOW FV) and particle tracking module (TUFLOW FV PTM), key input data used and PTM mapped outputs.

The PTM calculated the transport of particles away from the sea-pens and quantified the waste deposition footprint as waste area density near and far from the sea-pens. The Lagrangian PTM approach allowed for high resolution 'meshless' representation of the particle advection, dispersion, deposition and resuspension dynamics. The particle size, settling rates, ratio of nitrogen, phosphorus and carbon in the waste material was held at a constant rate, based on the outputs from the fish waste model described above. Particles that had settled out of suspension were tracked on the seabed and remained available for resuspension when wave and current induced shear stresses exceeded prescribed thresholds. No particle breakdown or burial processes were considered in the PTM simulations although burial was incorporated in the sediment diagenesis model.

The approach used here for aquaculture particulate waste dispersal models coupled with benthic impact estimation, TUFLOW FV PTM (BMT, 2020) has been used in a number of applications from

Australia and the UAE (BMT 2016, BMT 2018, Gunaratne et al 2021). This model is routinely used by BMT, as a modelling tool to support aquaculture EIA and determine ecological carrying capacity for sustainable operating practice.

The particle tracking model was parameterised with data relevant to the local environment and fish species. The main parameters include setting model, setting velocity, release rates, release times, release depths, seeding mechanism, erosion parameters and dispersion parameters (Table 2.2).

Table 2.2 Key parameters used in the PTM

Parameter Name	Description	Parameter Value	Remarks
Settling model	Calculates the sediment fraction settling velocity (m/s) at each HD model computational cell.	Constant	Constant settling velocity through the water column
Settling velocity	Different constant settling velocities for feed and faecal matter were used	Feed – 0.121 Faecal 1 – 0.015 Faecal 2 – 0.035 Faecal 3 – 0.059	Units are in m/s. Values adapted from Tanner et al. 2007, DHI 2013, Cromey et al. 2002, Chen et al. 1999.
Release times	Based on feeding times, 2 X 3-hr windows were selected per day	07:00 to 10:00 15:00 to 18:00	Particles were released in every second during these windows
Release amount	In total 1.5 million particles were released over 12 months	Feed – 0.5 Faecal 1 – 6.0 Faecal 2 – 7.7 Faecal 3 – 10.3	Units are number of particles per window (3hr)
Avg. release rates (Actual) - FCR 1.5	Actual rates were calculated, based on fish waste model. Converted tonnes/day to g/s	Feed – 0.46414 Faecal 1 – 5.6857 Faecal 2 – 7.2870 Faecal 3 – 9.7701	Units are in g/s.
Avg. release rates (Actual) - FCR 2.3	Actual rates were calculated, based on fish waste model. Converted tonnes/day to g/s	Feed – 0.787509 Faecal 1 – 9.6469 Faecal 2 – 12.3638 Faecal 3 – 16.5771	Units are in g/s.
Release rates (Simulated) – FCR 1.5	For modelling purposes actual release rates were scaled down to reduce model output size based on 1.5 million particle release over a year. The Calculation based on particle release amount per window	Feed – 4.52997 x 10^{-5} Faecal 1 – 55.5 x 10^{-5} Faecal 2 – 71.1 x 10^{-5} Faecal 3 – 95.4 x 10^{-5}	Units are in g/s. Factored by 10246 during post processing
Release rates (Simulated) – FCR 2.3			Units are in g/s. Factored by 17384 during post processing

Parameter Name	Description	Parameter Value	Remarks
Seeding mechanism	Particles released from a point source at a certain depth	12-point sources in each cluster at 5m depth	
Horizontal dispersion model	Describes Gaussian random walk component that can be applied as a function	Model – Constant Dispersion coefficient - 1	Dispersion coefficient units are m^2/s
Vertical dispersion model	Random walk component including higher-order terms to improve accuracy in the case of strong vertical concentration gradients.	Model – HD model Dispersion scale factor - 1	If scale factor is 1.1, that would increase HD Vertical dispersion by 10%
Deposition model	The Deposition model is used to calculate suspended sediment deposition fluxes to the bed	Ws0	Typically applied to non-cohesive sediments.
Erosion model	The Mehta model is a simple shear stress excess formula used to calculate the erosion flux from bed layer to water column	0.015, 0.2, 1.0	Erosion rate constant, critical shear stress for erosion and power coefficient

The PTM accounts for the differences in size fractions and settling velocities of waste particles, which includes the waste from the feed and the faecal material. In this study, the particle size, the settling rates, as well as the ratio of nitrogen, phosphorus and carbon in the waste material were all held at constant values. The ratios of N, P and C were based on the outputs from the fish waste model described in Section 2.3.

The science of particle transport through the water column is complex and only a few studies address the specifics of fish faeces. The settling velocity of fish waste leaving a sea-pen varies depending on the feed type, fish health, species, fish size, and the general farming practices (Chen et al. 1999, Felsing et al. 2005, Moccia et al. 2007, Moran et al. 2009). The settling velocities of the different particle sizes assumed in this study were based on the Farmér concept (Tanner et al. 2007), which predicts that the largest proportion of particles falls beneath or close to the pens, with increasingly smaller proportions falling further from the pens.

The difference between the volume of waste leaving a sea-pen and the volume reaching the seafloor is also complex, and depends on biological and physical factors, such as the current speeds and the extent of secondary consumption by scavengers beneath the pens (Felsing et al. 2005). For this study, the fish waste was partitioned into waste feed (commercial aquaculture pellets) and waste faecal material. Faecal material was further partitioned into three size fractions, following Chen et al. (1999), Cromey et al. (2002) and DHI (2013) four types of particles were modelled with different settling characteristics as shown in (Table 2.2). Seven pen clusters were simulated for PTM, and each cluster had 12 sea-pens with a single particle release point.

2.6 Sediment transport model

The TUFLOW FV sediment transport module (STM) is a coupled hydrodynamic and sediment transport modelling tool designed to simulate the movement and distribution of sediments in aquatic environments. It integrates advanced numerical methods to model sediment transport, and related processes in both two and three dimensions. STM is particularly effective in predicting total suspended solids (TSS) by accounting for different sediment fractions, such as fine silts, clays, and larger particulate matter. By simulating the interactions between water currents, suspended particles, and environmental conditions, the model predicted TSS concentrations and distribution. The STM was parameterised with data relevant to the TSS in the local environment with one sediment fraction (Table 2.3).

Table 2.3 TUFLOW FV Sediment Transport Model configuration with key parameters

Section	Parameter	Description/Value
Simulation Config Commands	Bed roughness model	ks
	Bed roughness parameters	0.0020 (currents), 0.0015 (waves)
	Erosion Depth Limits	0.05, 0.15
Sediment Fraction Commands	Fraction	fines (Sediment Fraction 1 Name)
	d50	40.0e-6 m (Median Sediment Diameter)
	particle density	2650 kg/m^3
	Settling model	constant
	settling parameters	0.0015 m/s (Settling Velocity)
	Erosion Model	Mehta
	Erosion parameters	0.05 (Erosion rate, g/m^2/s), 5.0 (Critical shear stress, N/m^2), 1.0 (Exponent)

2.7 Sediment diagenesis model

The sediment diagenesis model developed by UWA (Paraska et al 2015) was used to resolve the benthic biogeochemistry of leases and to estimate the nutrient flux into and out of the sediments under a range of waste deposition scenarios. It was then coupled to the hydrodynamic and water quality models to ensure the nutrient cycling pathways including phytoplankton growth incorporated cumulative sources of nutrients, both directly from fish respiration and indirectly via sediment mineralisation processes.

Recovery times were estimated by calculating the time required for the benthic environment to return to base conditions following the mineralisation of organic carbon waste and the time taken for oxygen and sulphide levels to return to pre-farming levels. The approach was previously applied to the Midwest Aquaculture Development Zone project (BMT 2016) in Australia and Delma Island Aquaculture Project in UAE (BMT 2019), where the module was used to inform likely fallowing times and the size of the zone required to sustain ongoing aquaculture operations based on an annual production in excess of 10 000 tonnes per annum (BMT 2016; BMT 2019).

The sediment diagenesis model is an Aquatic Ecodynamics (AED) Model Library module (Hipsey 2013) for carbon and nutrient diagenesis adopting CANDI, an extension of the numerical code written by Boudreau (1996 & 1997) and widely used across a range of marine and coastal environments (Paraska et al. 2014). The configuration of the model was guided by previously published sediment biogeochemical model applications in finfish aquaculture (Brigolin et al. 2009). Additional sources used to parameterise the sediment diagenesis model are listed in Table 2.4. For an overview of the theory and applications of the sediment diagenesis model refer to the review by Paraska et al. (2014) and methodology detailed in Paraska et al. (2015).

Table 2.4 Sources of literature used in the sediment diagenesis model

Reference	Study location
Macleod & Forbes 2004	Salmon farms in Tasmania
Tanner & Fernandes 2010	Yellowtail kingfish farms in Fitzgerald Bay in Spencer Gulf, South Australia
Fernandes &Tanner 2008	
Brigolin et al. 2009	Salmon farms in Loch Creran, Scotland
Volkman et al. 2009	Salmon farms in the Huon Estuary and D'Entrecasteaux Channel, Tasmania
Skretting 2024 (Personal communication)	Barramundi in Cone Bay leases, Western Australia

The chemical reactions simulated in the model can be broadly defined as primary and secondary reactions; these are summarised in Figure 2.11. Primary reactions are the microbially-driven breakdown reactions of organic matter via a series of oxygen reduction (redox) pathways. Primary reactions are the driving force of most of the other chemical reactions that occur in the sediment. Inputs of fish feed and faecal matter serve to quickly shift chemical concentrations away from the equilibrium that occurs in marine waters, especially those which are naturally nutrient poor.

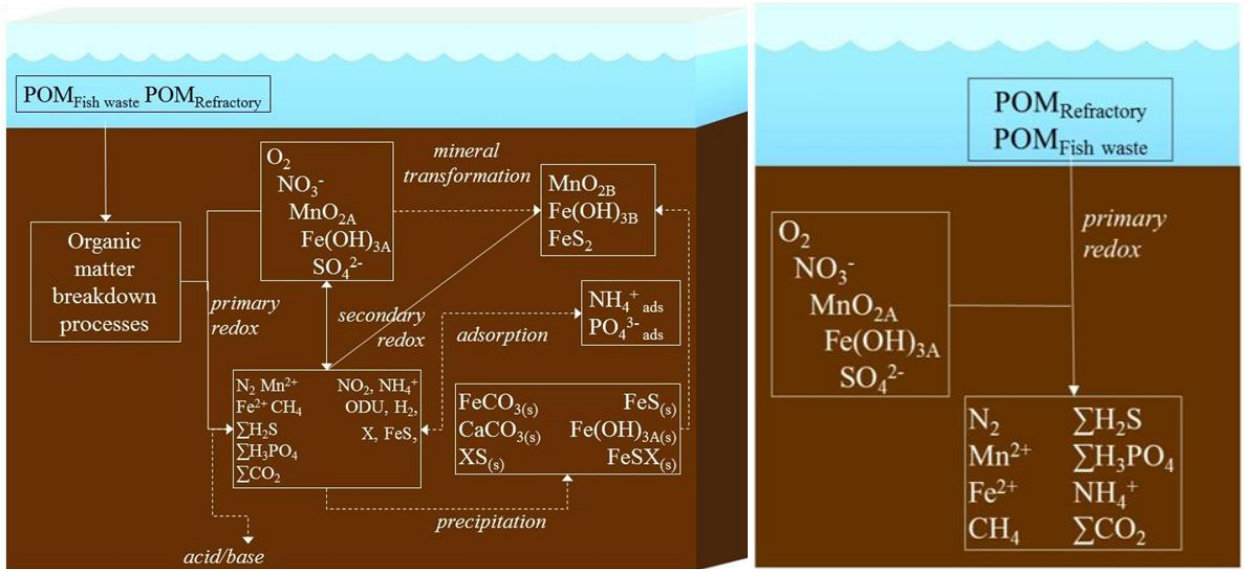

Note:

1. POM = particulate organic matter

Figure 2.11 Processes simulated in the carbon and nutrient diagenesis-Aquatic Ecodynamics sediment diagenesis model

2.8 Threshold Criteria

2.8.1 Water quality thresholds

The water quality model interrogation faced challenges in directly modelling the recovery of the water column to baseline levels due to uncertainties regarding the lethal and sub-lethal thresholds of endemic species and their recovery timing following exposure to aquaculture stressors such as organic material and inorganic nutrients. Using EPA (2017) guidelines, annual thresholds for water column oxygenation, algal growth potential, and nutrient enrichment were applied. Baseline values at Razor Island, which differed significantly from other proposed leases, warranted separate assessment criteria. For oxygenation, thresholds based on EPA (2017) required dissolved oxygen levels to be maintained at 80% and 90% saturation for over six weeks, aligning with moderate and high level of ecological protection (Table 2.5). Inorganic nutrient thresholds addressed algal growth potential and nutrient enrichment, utilizing 95th and 80th percentile baseline values to reflect moderate and high protection levels, respectively, with distinct criteria for Razor Island.

Table 2.5 Water quality thresholds

Parameter	Moderate ecological protection	High ecological protection
Oxygenation[1]	DO saturation in the bottom half of water column not to fall below 80% for a period exceeding 6 weeks	DO saturation in the bottom half of water column not to fall below 90% for a period exceeding 6 weeks
Algal growth potential[2] Razor Island	DIN concentration not to exceed 0.035 mg/L more than 50% of the time	DIN concentration not to exceed 0.01 mg/L more than 50% of the time

Parameter	Moderate ecological protection	High ecological protection
Algal growth potential[2] Remaining leases[3]	DIN concentration not to exceed 0.022 mg/L more than 50% of the time	DIN concentration not to exceed 0.014 mg/L more than 50% of the time
Nutrient enrichment[2] Razor Island	Chlorophyll-a not to exceed 1.1 µg/L more than 50% of the time	Chlorophyll-a not to exceed 0.9 µg/L more than 50% of the time
Nutrient enrichment[2] Remaining leases[3]	Chlorophyll-a not to exceed 1.2 µg/L more than 50% of the time	Chlorophyll-a not to exceed 0.8 µg/L more than 50% of the time

Notes:
1. Thresholds are based respectively on the EPA's EQGs for moderate and high ecological protection (EPA 2017). Threshold assumes continuous exceedance for a period exceeding six weeks.
2. Thresholds are based on the EPA's EQGs for moderate (95th percentile baseline data) and high (80th percentile baseline data) ecological protection (EPA 2017).
3. Remaining leases = Edeline Island South, Edeline Island North, Cecelia Island, Bayliss Island, Bayliss Island Extra, Dorothy Island

2.8.2 Soft sediments thresholds

The Proposal's potential adverse effects on the benthic marine environment, particularly soft sediments, were evaluated using criteria based on physico-chemical stressors such as dissolved oxygen and hydrogen sulphide, referencing EPA (2016) and Hargrave et al. (2008). This method is considered best practice globally for assessing marine finfish farm impacts on soft sediments (EPA Tasmania 2022). Impacts were predicted based on sediment oxygenation and hydrogen sulphide concentrations and depths. Ecological protection levels were defined by oxygen and sulphide concentrations within the top 5 cm of sediment, designating areas with hypoxia as MEPA and areas with waste-affected sediments, but without significant chemical alteration, as HEPA. Chemical indicators were preferred over biological indicators due to their more reliable and identifiable trajectories. For metals, thresholds were based on whether sediment concentrations of copper and zinc exceeded EPA's Environmental Quality Guideline (EQG) trigger values (EPA 2017), with areas exceeding EQGs designated as MEPA/HEPA (Table 2.6).

Table 2.6 Thresholds applied to soft sediments

Parameter	MEPA	HEPA
Hydrogen sulphide Oxygenation	Conditions of hypoxic stress, resulting in potential reductions of infauna taxa of no more than 50%. This occurs when the upper 2 cm H_2S concentration remains within the 100-300 µM L-1 range.	Where the rate of deposition is sufficiently low so as not to contribute material affects to sediment chemistry and/or infauna species richness. Following Hargrave et al. (2008) this category requires that H_2S remains below 100 µM L-1 Top 5 cm of sediment remain oxygenated
Metals (Zn and Cu)[1]	Sediment concentrations of Zn and Cu exceed the EPA EQGs[2,3]	Sediment concentrations of Zn and Cu exceed the EPA EQGs[2,3]

Notes:
1. Zinc (Zn) and Copper (Cu) are the metals present in feeds in the highest proportion and those with EPA (2017) triggers.
2. EQG = Environmental Quality Guideline
3. Per EPA (2017), the values for high/moderate protection are the same

2.9 Model Assumptions

A conservative approach was adopted to ensure the outputs of modelling were equivalent to 'worst case' outcomes. As such, the impacts predicted in this document are more extensive than might be expected on average but are nevertheless within the upper range of impacts reported in the literature (Brooks et al. 2004). The assumptions underpinning the development and execution of the integrated model are summarised below:

- The hydrodynamic model was calibrated and validated against multiple Metocean datasets collected over the months April and May 2021 and the water quality model was validated against grab samples collected over the period of February to July 2021 (water quality model was also compared to data collected in the additional baseline monitoring program, but validation only against the 2021 period noting this was the actual period modelled directly). The conditions during the data collection phase were considered normal and captured the summer to winter seasonal transition of changing winds, waves and oceanographic currents. Although the Metocean data collection period captured typical seasonal patterns, no significant storm or other extreme events were captured.
- The sediment flux rates used by the water quality model were based on predictions from the sediment diagenesis model following five years of continuous fish farming.
- An Arrhenius temperature factor was applied to the predicted sediment fluxes with greater flux simulated in the warmer months.
- The modelled response of phytoplankton follows the WQM method in which inputs of N and P are converted to phytoplankton biomass using stoichiometric relationships and the Redfield ratio. The model simulated changes in phytoplankton were guided by the calibration process (BMT 2024a).
- The projected waste outputs from the fish farm model are conservative and likely greater than the outputs that can be achieved once the farms are established using best practice waste management.
- It was assumed that particulate nutrient loadings were discharged two times a day based on a typical feeding schedule distributed by a period of three hours per feed. The dissolved nutrient loadings were discharged continuously, at a constant rate (Table 2.2).
- No particle breakdown or burial processes were considered in the PTM simulations. Once the particulate portion settles, it is subject to mineralisation, as simulated by the early diagenesis (biogeochemistry) model.
- Following a conservative approach, the total particulate portion of the waste was added to the water quality model from the sea-pen discharges as well as to the diagenesis model (according to the distribution simulated by the PTM model). The total dissolved and particulate portions of the waste, therefore, undergoes biochemical transformations in the water column, as simulated by the water quality model (WQM). The total particulate portion of the waste also undergoes biochemical transformations in the sediment, as simulated by the diagenesis model.
- Feed rates were calculated as a percent of standing biomass per day. No allowances were made for annual fluctuations in standing biomass due to harvesting of stock.
- Scenarios with monthly (step-function) build-up of standing biomass over a 12-month period due to growth were modelled.

3 Model Scenarios

3.1 Description of scenarios and modelling period

The models were run for a typical 12-month operation from 01/05/2020 to 01/05/2021 coinciding with the original baseline field data collection. The 12-month simulation period was selected to include seasonal variations, particularly in the wet season runoff and wind.

Modelling scenarios were agreed in consultation with Tassal. Scenarios were based on a conservative assessment of the proposed farming methods Tassal is looking to implement for the expansion project, as described in Table 3.1.

Table 3.1 Aquaculture infrastructure assumptions

Infrastructure components	Details
Pen diameter (m)	36
Pen circumference (m)	120
Pen depth – anti predator netting (m)	13-16
Pen depth – fish netting (m)	10-13
Pen volume (m^2)	~12,600
Other assumptions	12 pens per site Simultaneous production in every site Continuous release of feed and associated wastes

In addition to the baseline simulation, two operational scenarios were modelled in total. Scenarios 1 and 2 both modelled an increasing standing biomass ranging from 1570 tonnes to a maximum of 4500 tonnes per lease, with Food Conversion Ratios (FCRs) varying between 1.5 and 2.3 for scenarios 1 and 2 respectively. FCRs were used to determine the amount of particulate and dissolved wastes excreted from farmed fish and is based on determining how much of the feed is converted to waste material. The lower the FCR, the less waste produced by the farmed fish.

The modelling included an associated increase in feed and waste outputs throughout the model period as biomasses increased. The standing biomass of 4500 tonnes was selected in consultation with Tassal, with this value equating to the absolute maximum biomass that will be present on a given site prior to harvesting. Scenario 1 is representative of the most likely operating conditions for the Proposal, with Tassal committing to a target FCR of 1.5, while Scenario 2 is provided to indicate worst-case impacts.

Figure 3.1 depicts monthly standing biomass during a typical operational period of 19 months. For scenarios, a stepwise increment in the standing biomass has been used from month 7 to month 18 for the 12-month simulated period.

Table 3.2 Modelled operation scenarios

Scenario	Initial standing biomass (t/cluster) *	Final standing biomass (t/cluster)	Feed conversion ratio (FCR)	Operating period (months)	Modelling assumption
0 (Base)	NA	NA	NA	12 months	NA
SCE 1	1570	4510	1.5	12 months (Month 7 to Month 18) **	Stepwise monthly increase in feed inputs and waste**
SCE 2			2.3		

*** t/cluster = tonnes per cluster; 12 sea-pens in each cluster;**

- **Base -** represents the predicted conditions of the site using the verified hydrodynamic and water quality model (BMT 2024a). This scenario provided the baseline for comparison of impacts from each of the following operational scenarios.

- **Scenario 1 - 2:** These scenarios assumed a stepwise monthly increase in the standing biomass from 1570 tonnes/cluster to 4510 tonnes/cluster over the 12-month simulation period. Feed inputs and waste outputs were also assumed to vary with the standing biomass.

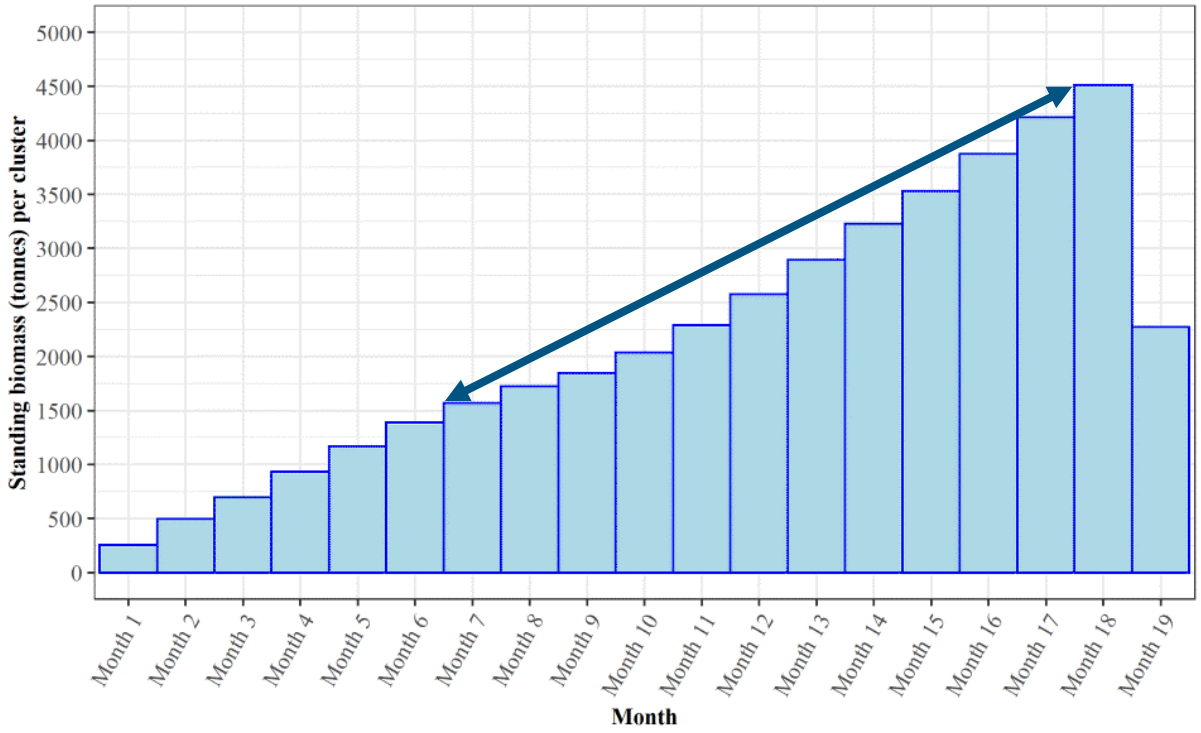

Figure 3.1 Operational standing biomass per cluster

3.2 Presentation of results

Results in Section 4 are presented by comparing each of the scenarios with the baseline conditions to study the relative impact of different operational factors on water quality and benthic habitats.

Comparisons between the FCR scenarios were made using 50th percentile concentrations (or the concentrations expected to be achieved 50% of the time over a 12-month period).

4 Model Results

4.1 Overview

An integrated hydrodynamic, particle transport, water quality and sediment diagenesis model was used to simulate a total of six scenarios, in addition to the base case. The following sections describe the predicted impacts of each of these scenarios on the marine environment, in reference to hydrodynamics, regional water quality and sediments.

4.2 Regional ecosystem nutrient budget

Despite the increased levels of nutrient discharges from the catchment during the summer months (December to March) and nutrient upwelling from the Indian Ocean, the existing environment in the vicinity of the leases can be still considered as oligotrophic. Natural fluctuations associated with seasonal variations are characteristic of the Buccaneer Archipelago with increased nutrients during the wet season (MPC, 2008)

The proposed aquaculture operations are predicted to add a nutrient perturbation to the system and has been a key subject of investigation in this study. This perturbation takes the form of both an immediate nutrient load to the water column (via waste and feed excess) and a delayed load via organically enriched sediment nutrient remineralisation. A simulated projected mass analysis of estimated annual nutrient fluxes for the existing (baseline) and impacted conditions (post-aquaculture) for the FCR 1.5 scenario (Scenario 1, Table 3.2) provides a conceptual overview of the anticipated level of impact from the nutrient perturbation (Figure 4.1).

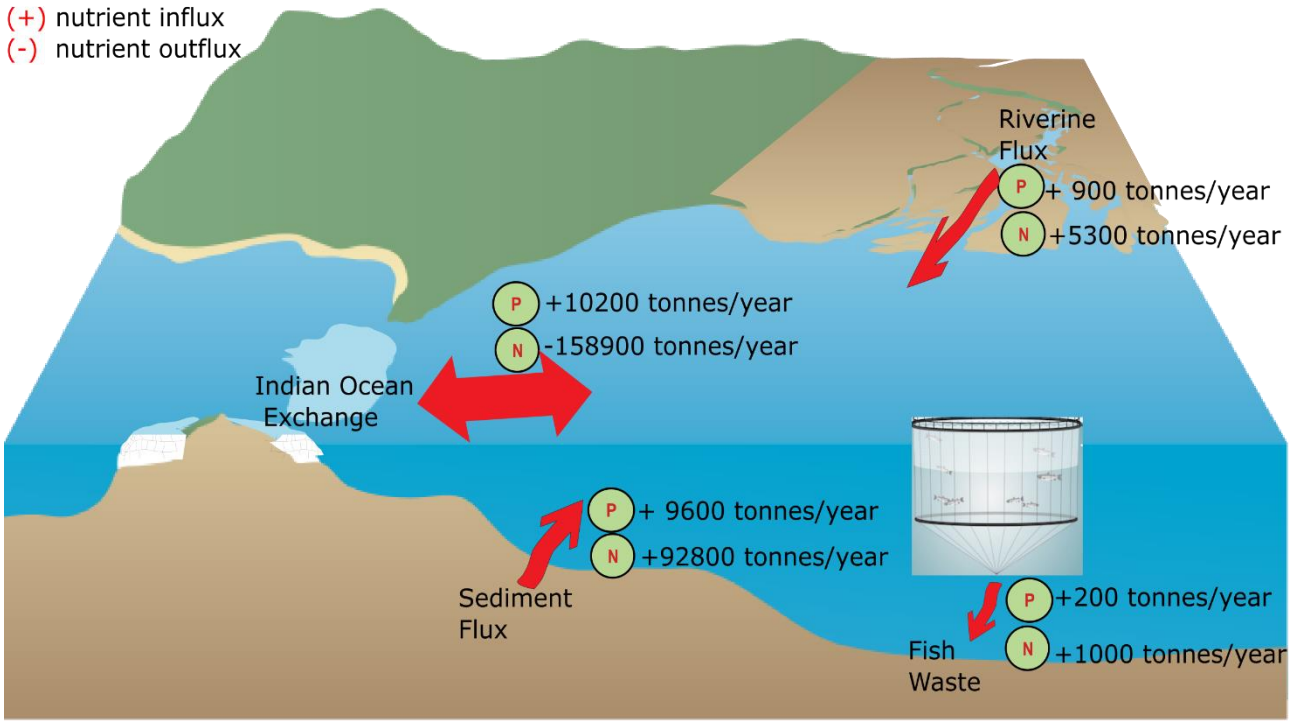

Figure 4.1 Conceptual diagram of sources and sinks for the nutrient budget under the standing biomass of 4510 tonnes/year as depicted in Scenario 1.

4.3 Hydrodynamics

Figure 4.2 and Figure 4.3 present the comparison of the net annual surface and bottom circulation around the leased areas for the baseline condition. Water circulation varied throughout the model domain impacted by wind, tide and density-driven flows, as well as interaction with shoreline topography. Annual mean surface velocity magnitude through the leases varied from 0.2 – 0.5 m/s. Current velocities recorded at depth were somewhat lower than this at 0.1 – 0.3 m/s. In general, the currents in the leases were mostly influenced by the bathymetric features and eddies shedding-off the islands, notably in the regions adjacent to the islands of the Archipelago.

Wu et al. (2014) predicted a potential increase in velocity under sea-pens near the seabed of 20%. It is not expected that this will substantially affect the erosion of sediments under the sea-pens for the proposed leases. Sediment erosion and deposition is driven by bottom shear stress, and the hydrodynamic model simulation indicated that bottom shear stress was dominated by wave action rather than current velocities within the proposed leases.

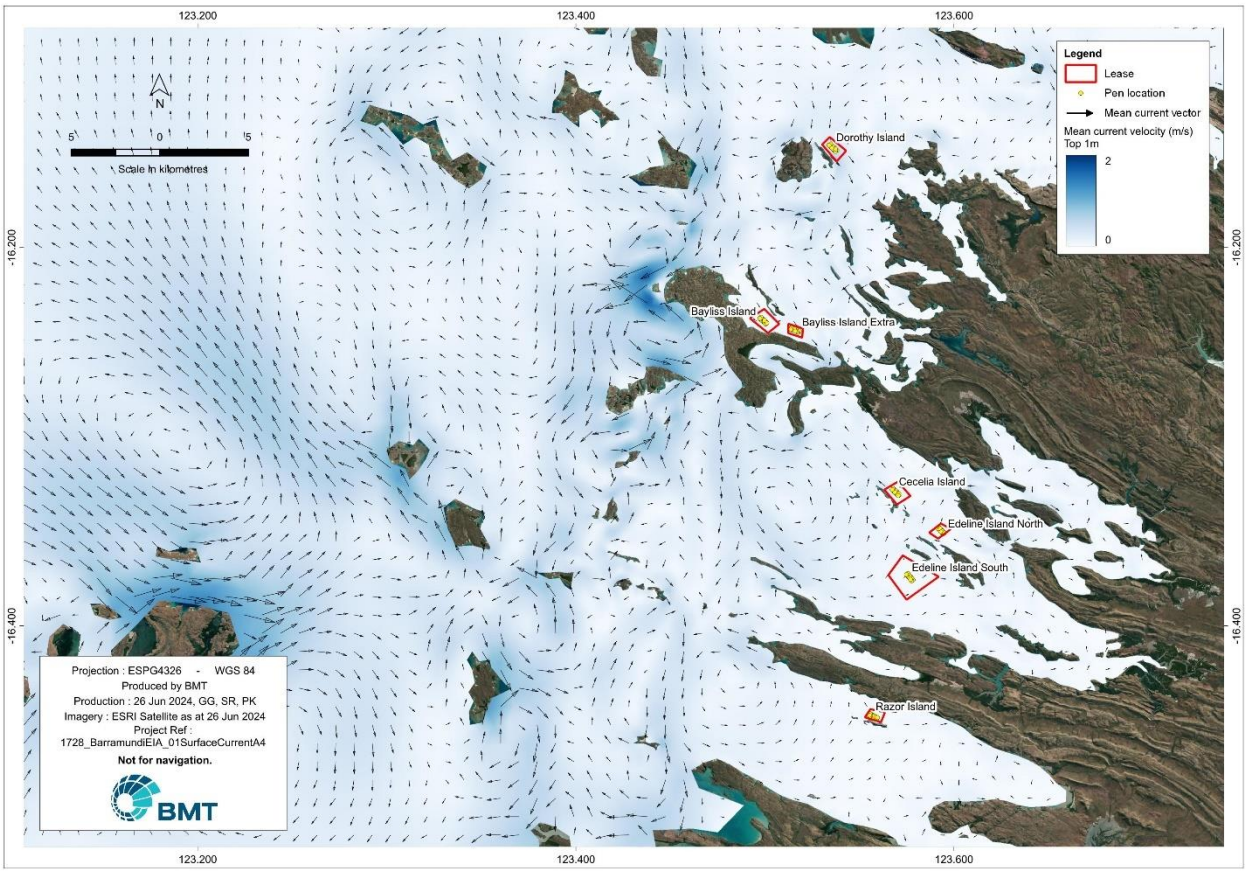

Figure 4.2 Annual median surface velocities showing circulation patterns around the leases

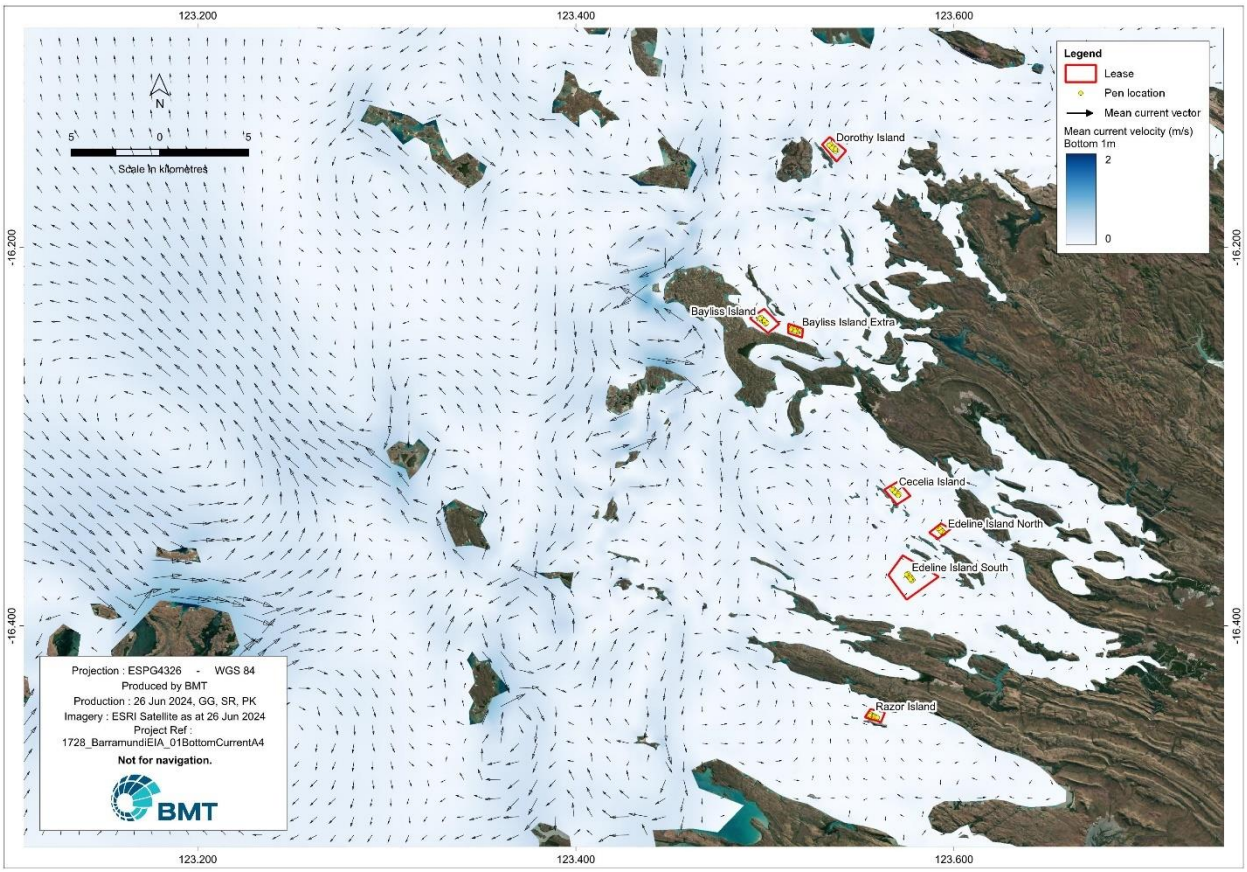

Figure 4.3 Annual median bottom velocities showing circulation patterns around the leases

4.4 Water quality

The potential effects of aquaculture on regional water quality were examined by comparing the water quality predicted under the proposed farming scenarios with the verified baseline predictions. Inputs of nitrogen, orthophosphate and their subsequent effects on regional phytoplankton and dissolved oxygen were examined over time, and in the different strata of the water column. The results are presented in the form of spatial and temporal patterns for each of the key water quality variables as:

1. Spatial variations in median concentrations of water quality variables for the baseline and scenario model output:
    a. Percentile maps of median concentrations of the surface (top 2m), bottom (last 2m) and depth average of dissolved inorganic nitrogen (DIN), dissolved oxygen (DO) and chlorophyll-a (chl-a) and the light irradiance at the sea-bed to represent impact on benthic habitats.
    b. Depth profiles at multiple instances in time
2. Temporal variation (timeseries) comparing concentrations of water quality variables for the baseline and scenario runs.

Comparisons are made using 50th percentile concentrations, representing the concentrations expected to be achieved 50% of the time over the 12-month simulation period. Time series and depth profiles plots are presented to emphasise differences in water quality over time (between seasons) and between the surface and the bottom of the water column.

4.4.1 Dissolved Inorganic Nitrogen (DIN)

Concentrations of DIN beneath and down-current of the sea-pens were analysed for each of the two farming scenarios.

4.5.1.1 Spatial pattern

- Spatial distribution of simulated median DIN concentration at Razor Island site and other three sites for Scenario 1 (FCR 1.5) are presented in Figure 4.4 and Figure 4.5.
- Spatial distribution of simulated median DIN concentration at Razor Island site and other three sites for Scenario 2 (FCR 2.3) are presented in Figure 4.6 and Figure 4.7.
- The model projected potential elevations of DIN immediately near the sea-pens, particularly under Scenario 2.
- Modelling projected that the highest DIN footprint would be associated with the pens at Razor Island.
- For both scenarios, Edeline Island South and Dorothy Island are projected to have insignificant elevations in DIN concentrations.

Figure 4.4 Predicted dissolved inorganic nitrogen concentrations in the water column under Scenario 1 – Strickland Bay, Bayliss Islands, Dorothy Island

Figure 4.5 Predicted dissolved inorganic nitrogen concentrations in the water column under Scenario 1 – Razor Island

Figure 4.6 Predicted dissolved inorganic nitrogen concentrations in the water column under Scenario 2 – Strickland Bay, Bayliss Islands, Dorothy Island

Figure 4.7 Predicted dissolved inorganic nitrogen concentrations in the water column under Scenario 2 – Razor Island

4.5.1.2 Depth profiles

Figure 4.8 through to Figure 4.13 present projected depth profiles of DIN concentrations at the corners of the proposed leases for the baseline and operational farming scenarios. The depth profiles were extracted at the beginning of each of the six months (June, August, October, December, February and April). The following points are noted:

- DIN concentrations were predicted to increase with an increase in FCR.
- The model predicted a discernible depth gradient of DIN with concentrations dictated by the magnitude of the pen nutrient excretions and sediment nutrient releases relative to ambient concentrations.

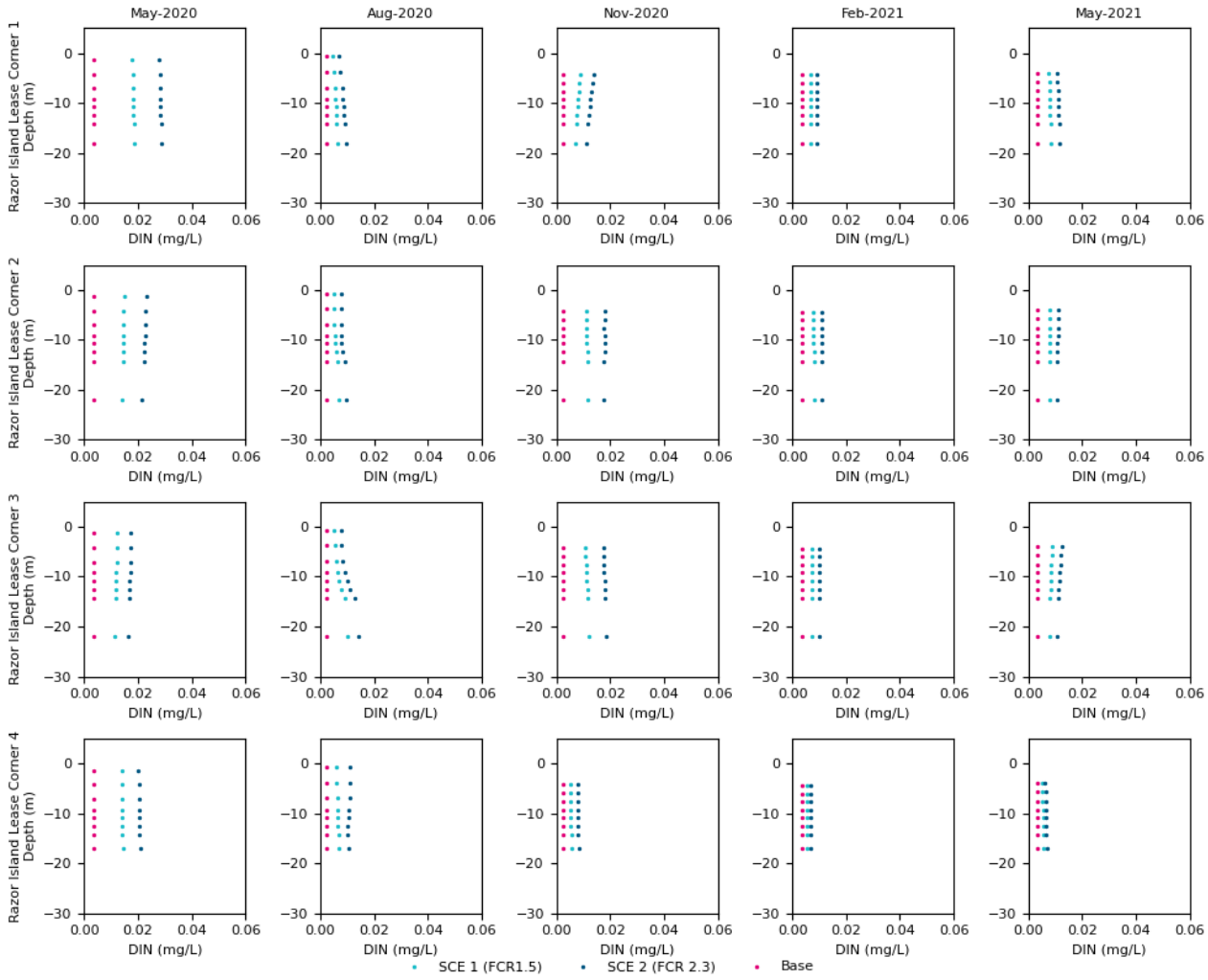

Figure 4.8 Depth profiles of simulated DIN at corners of Razor Island site at the beginning of selected months

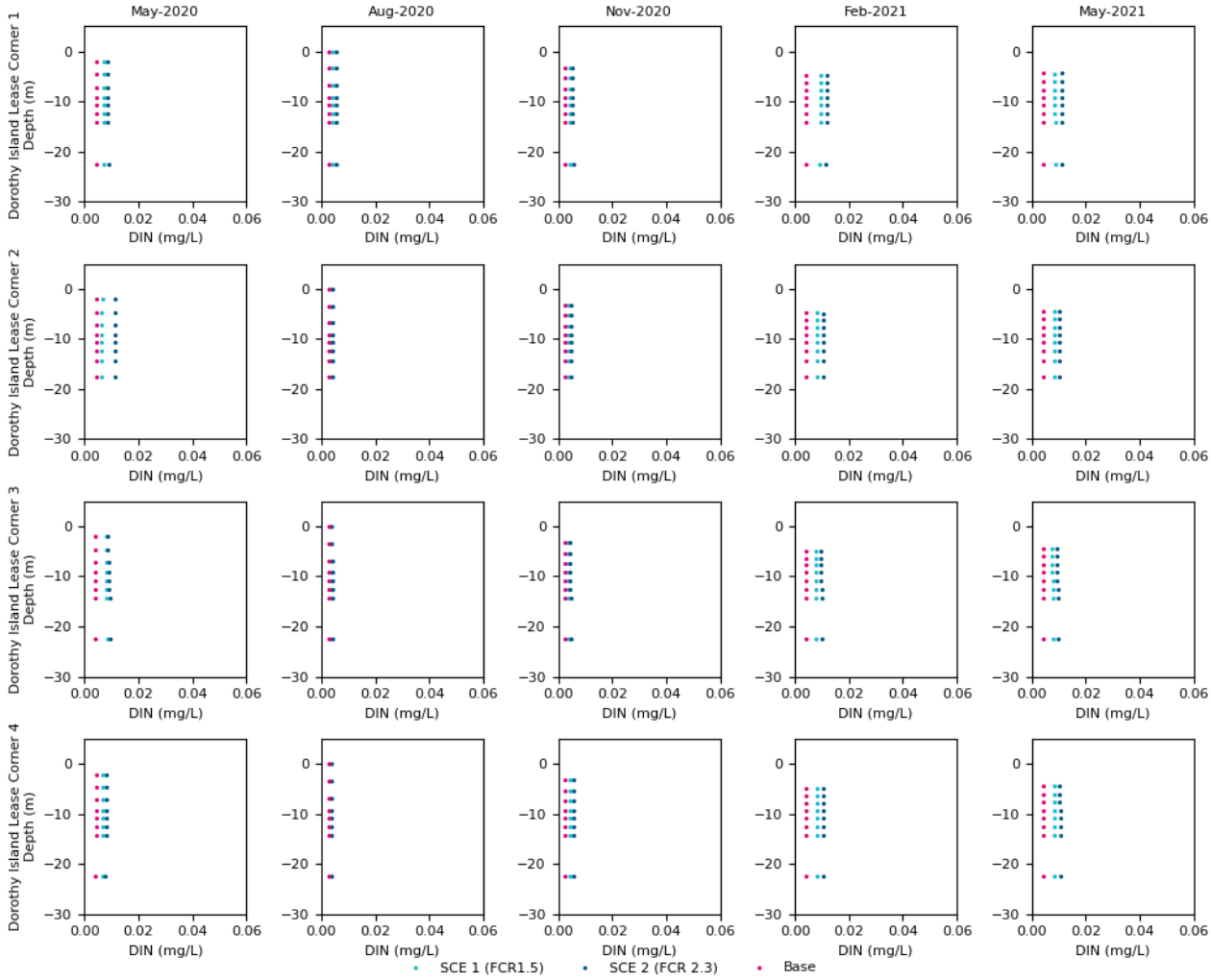

Figure 4.9 Depth profiles of simulated DIN at corners of Dorothy Island site at the beginning of selected months

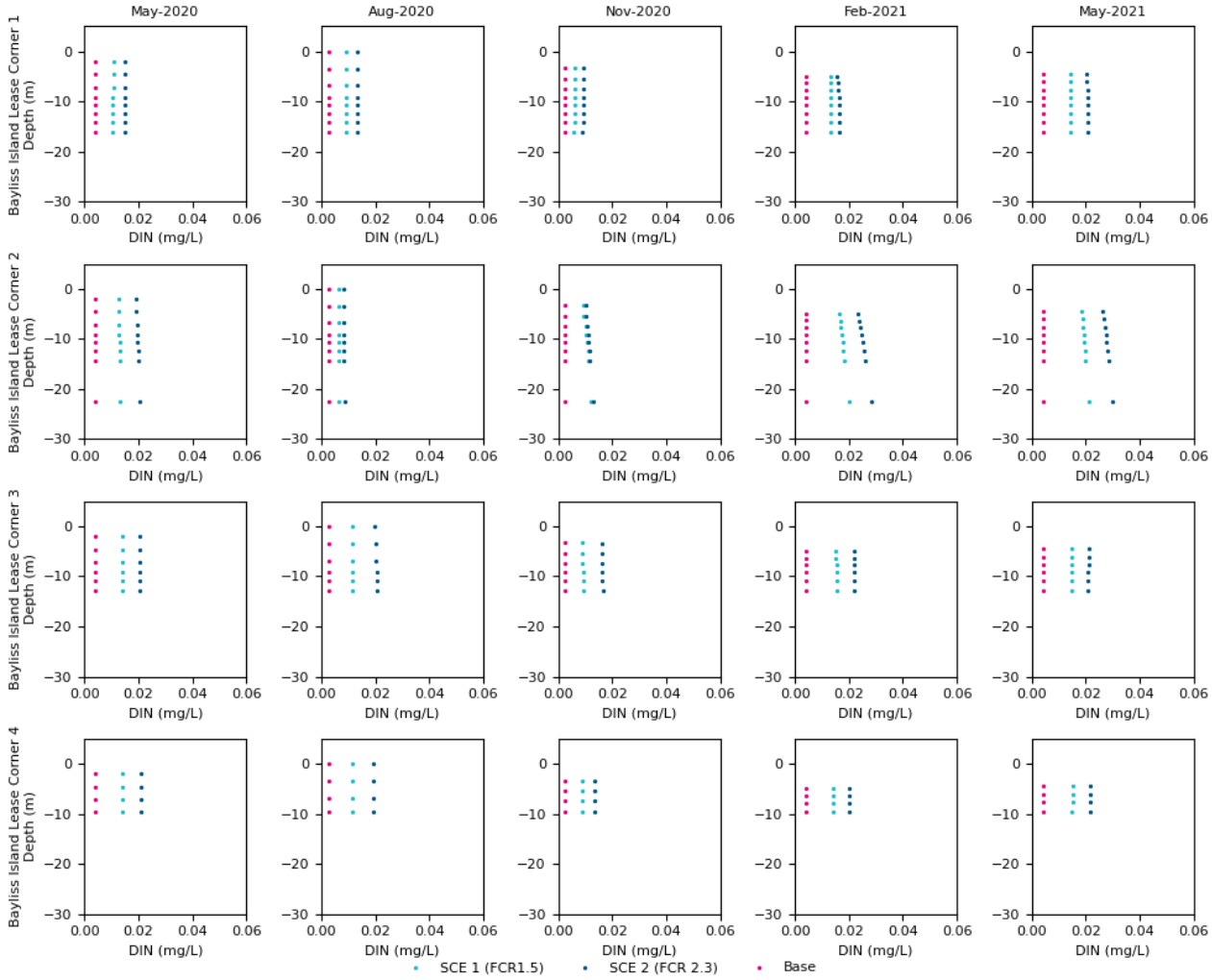

Figure 4.10 Depth profiles of simulated DIN at corners of Bayliss Island site at the beginning of selected months

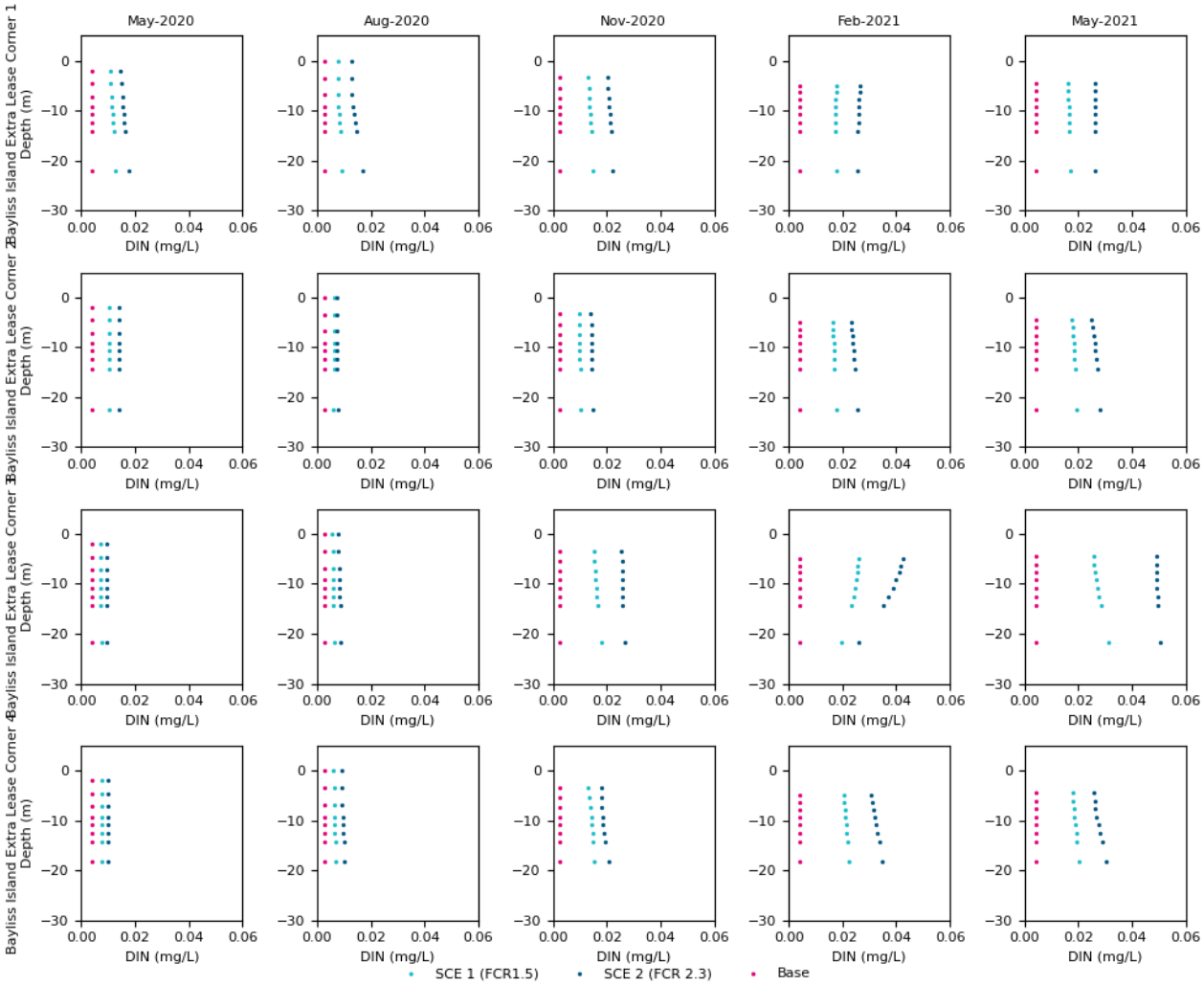

Figure 4.11 Depth profiles of simulated DIN at corners of Bayliss Extra site at the beginning of selected months

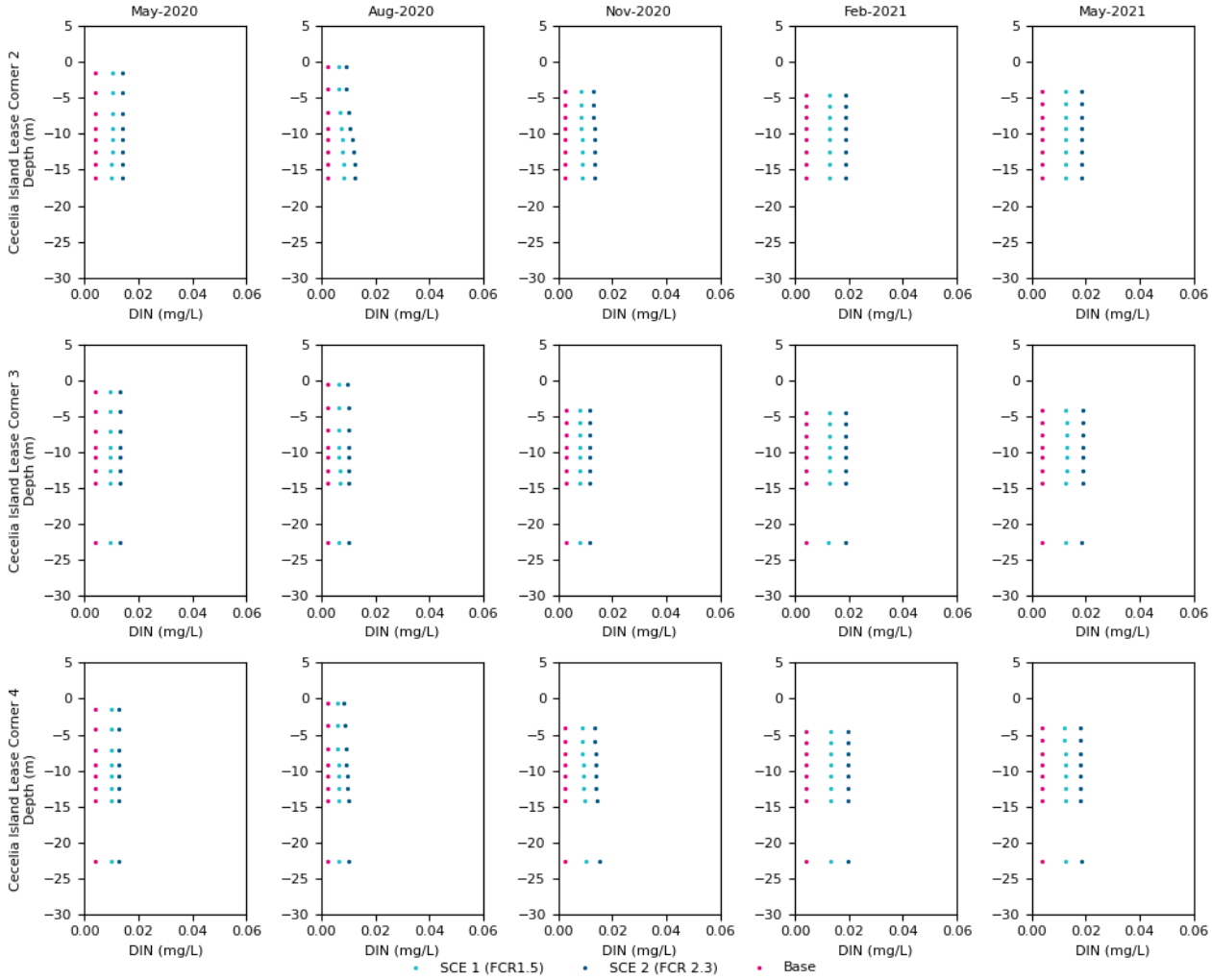

Figure 4.12 Depth profiles of simulated DIN at corners of Cecelia Island site at the beginning of selected months

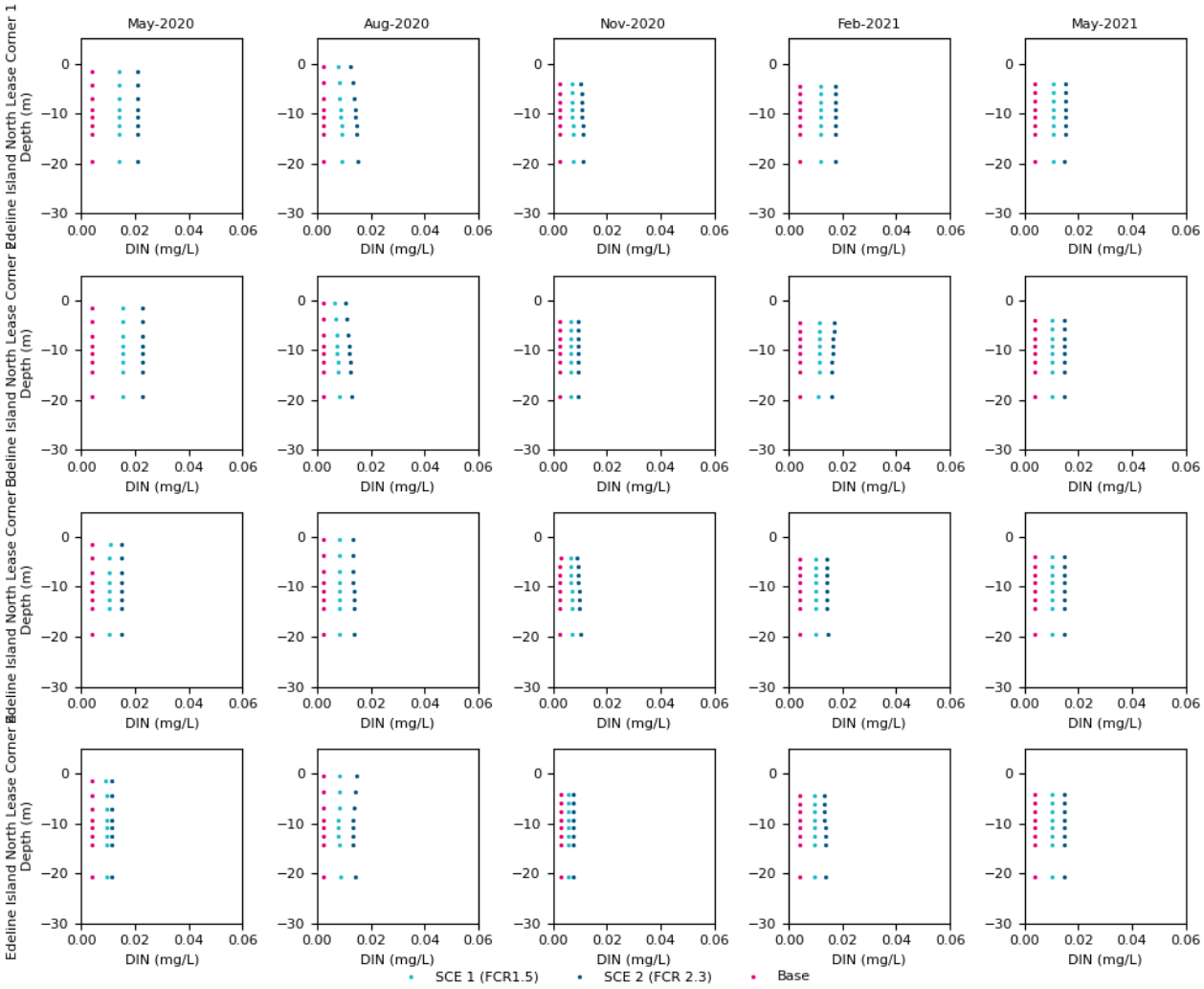

Figure 4.13 Depth profiles of simulated DIN at corners of Edeline Island North site at the beginning of selected months

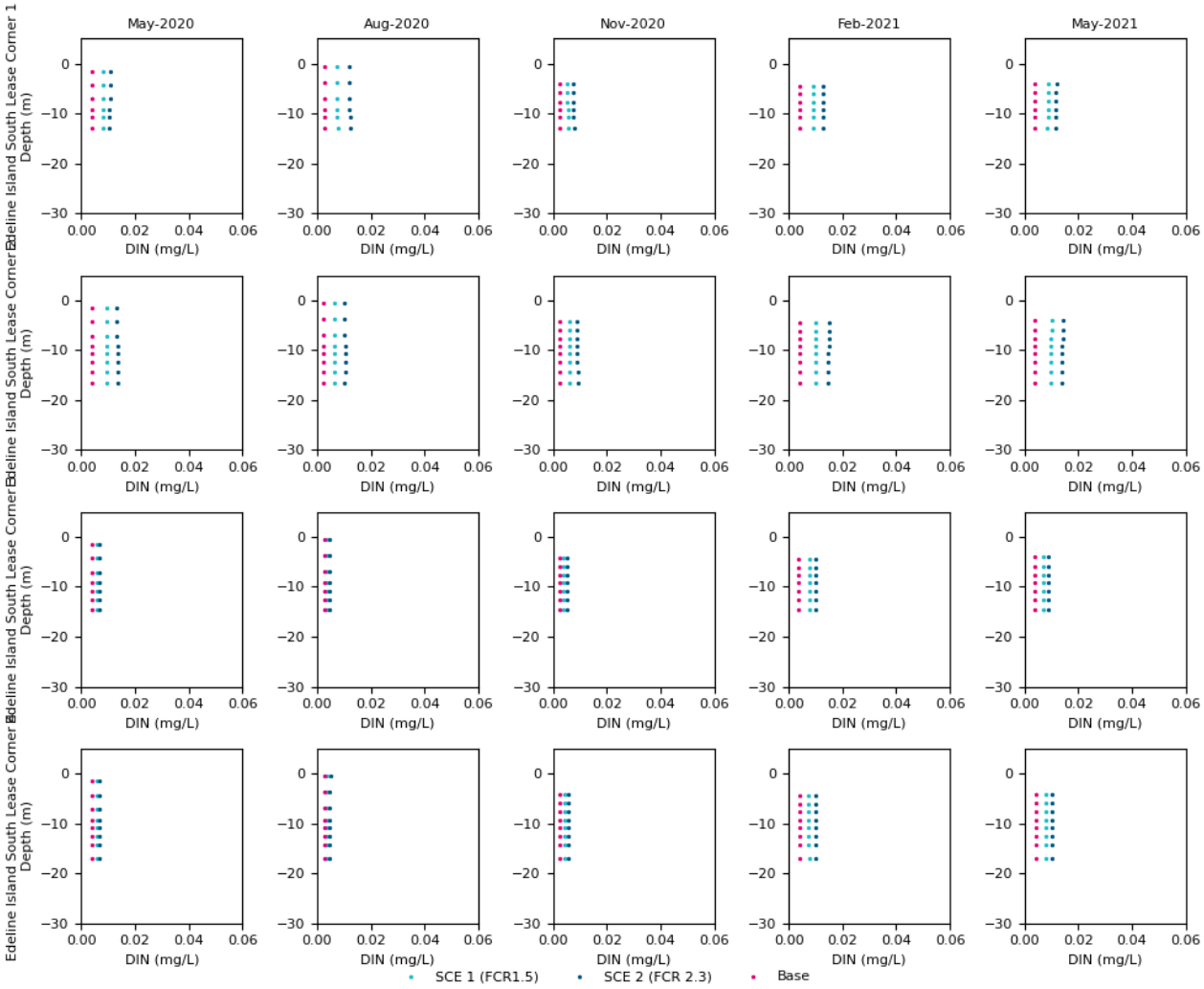

Figure 4.14 Depth profiles of simulated DIN at corners of Edeline Island South site at the beginning of selected months

4.4.2 Orthophosphate

Orthophosphate is the biologically available fraction of phosphorus in the water column, and a major constituent of fish feeds (Section 2.4). Orthophosphate is released to the water column through the mineralisation of waste fish feed and faeces after it settles to the sea floor.

Concentrations of orthophosphate (FRP) beneath and down-current of the sea-pens were analysed for each of the two farming scenarios.

4.5.2.2 Depth profiles

Figure 4.15 through to Figure 4.21 present the depth profiles of FRP concentration at the corners of the proposed leases for the baseline and operational farming scenarios. The following points are noted:

- Predicted FRP concentrations increased with an increase in FCR.
- The model predicted a clear depth gradient of FRP with concentrations dictated by the magnitude of the pen nutrient and sediment nutrient releases relative to the ambient concentrations.

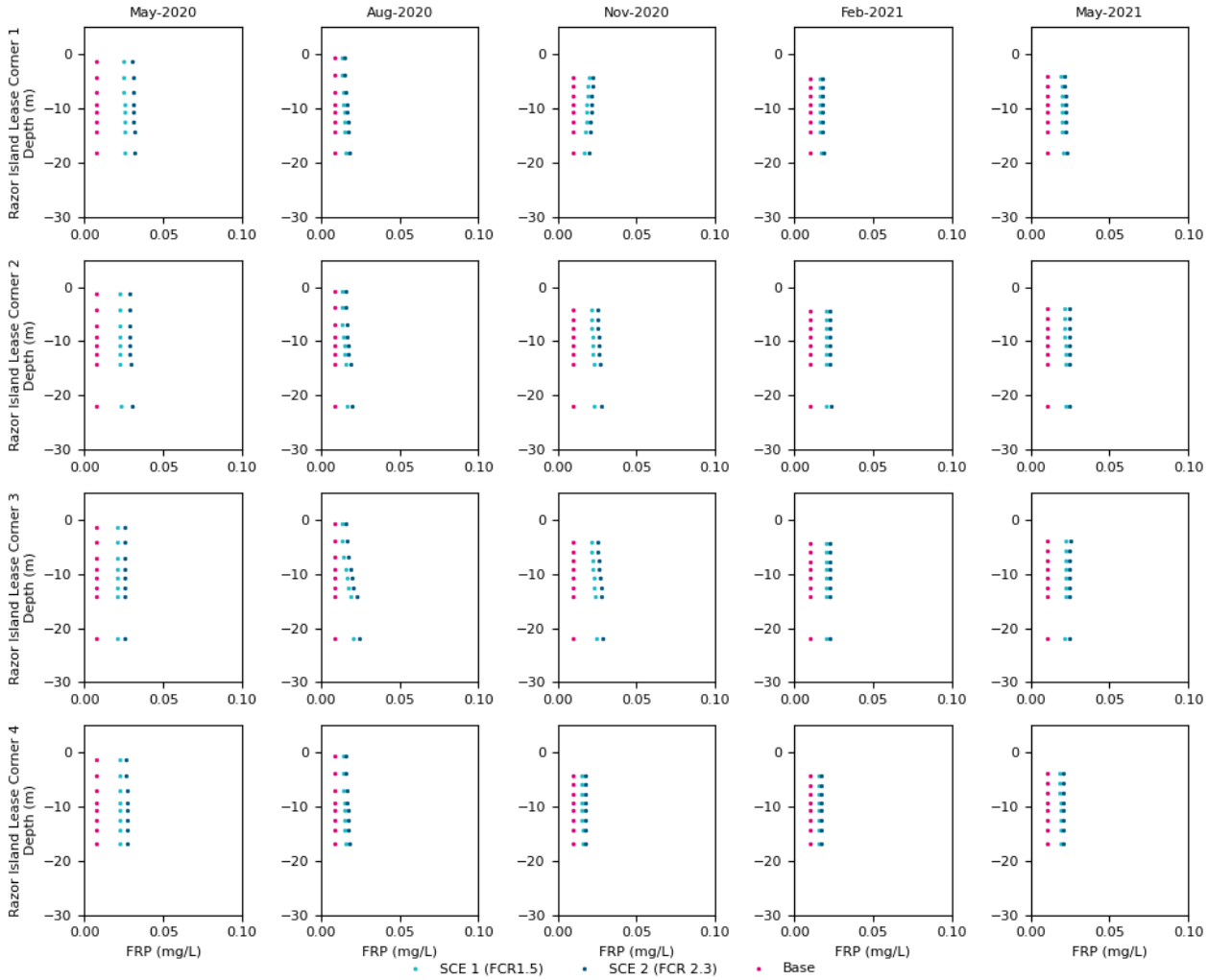

Figure 4.15 Depth profiles of simulated FRP at corners of Razor Island site at the beginning of selected months

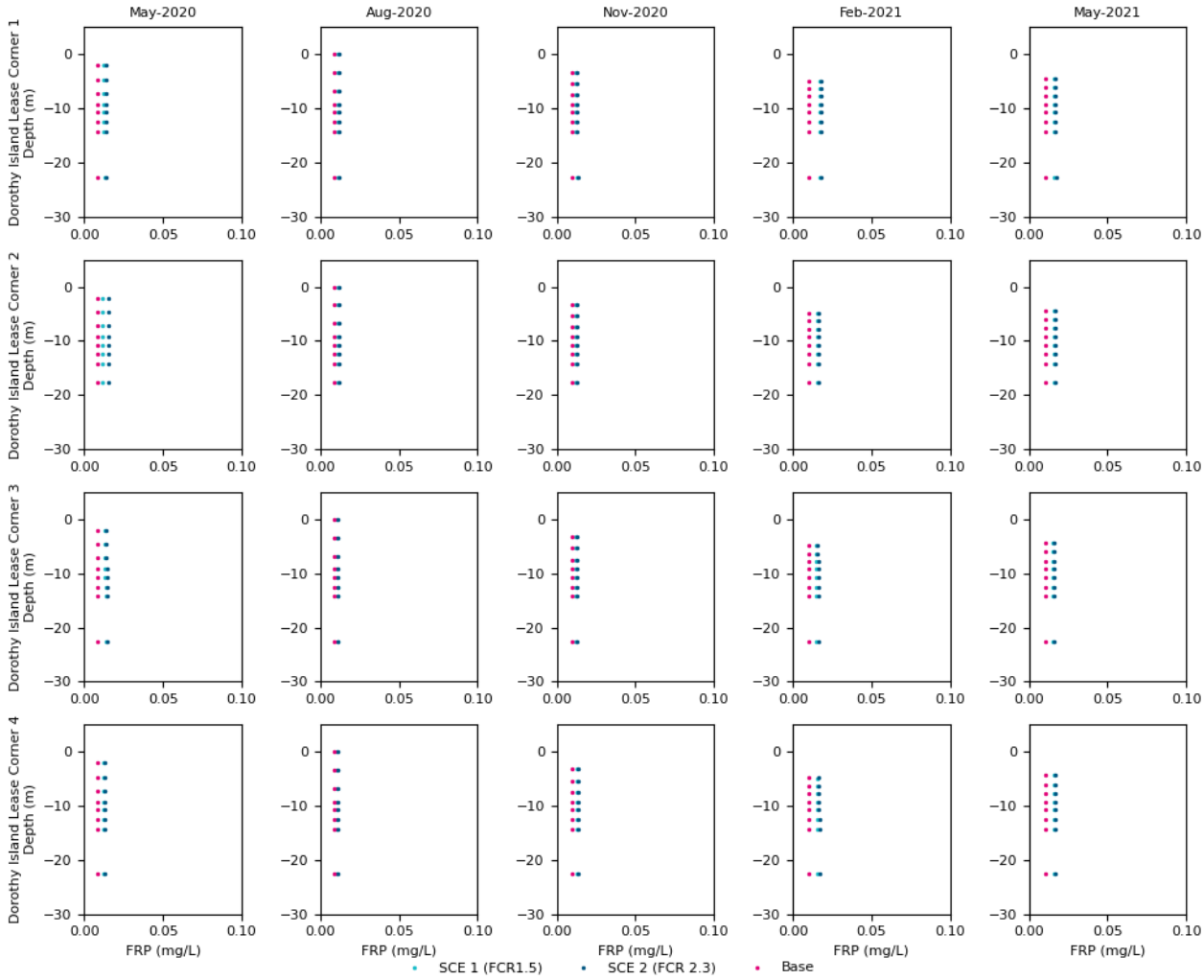

Figure 4.16 Depth profiles of simulated FRP at corners of Dorothy Island site at the beginning of selected months

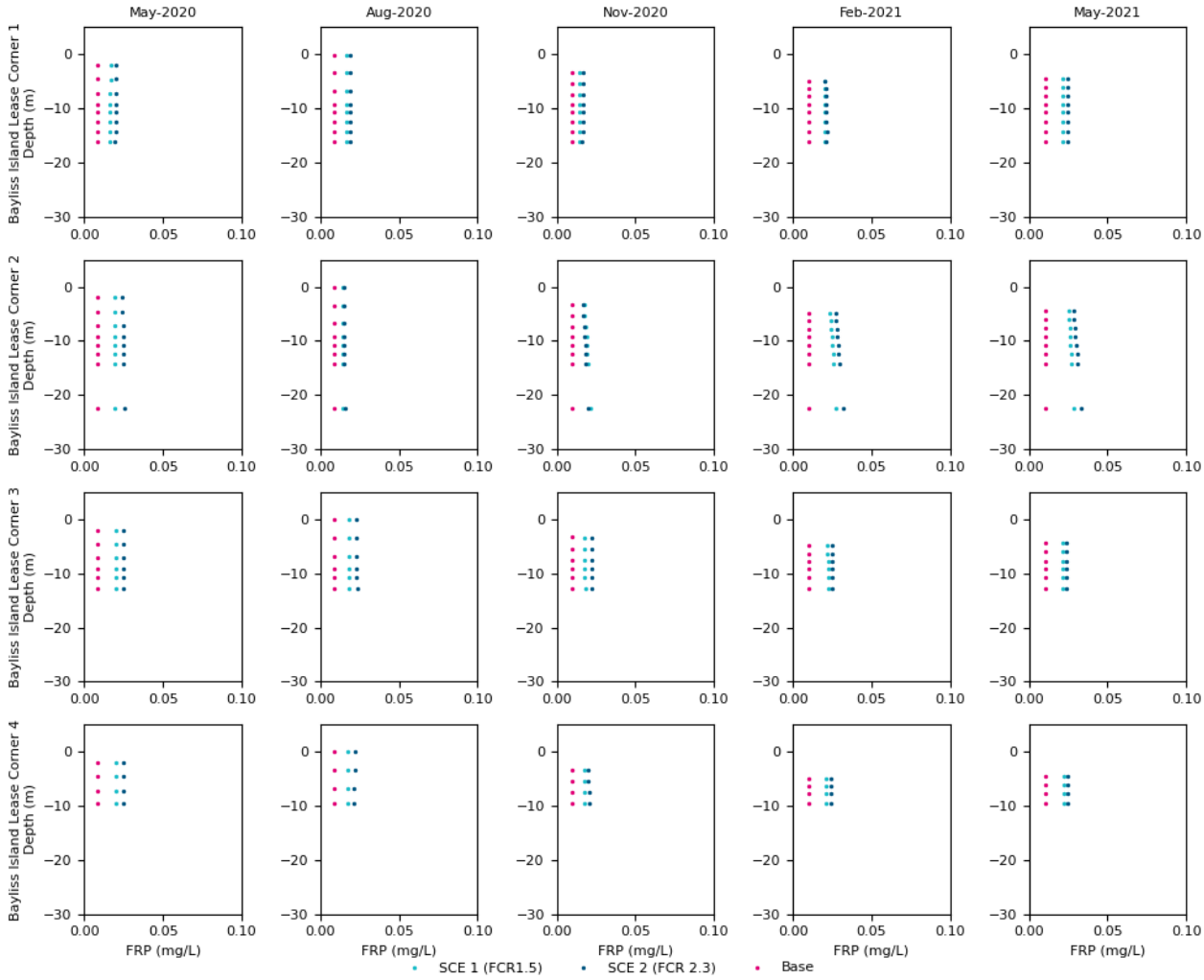

Figure 4.17 Depth profiles of simulated FRP at corners of Bayliss Island site at the beginning of selected months

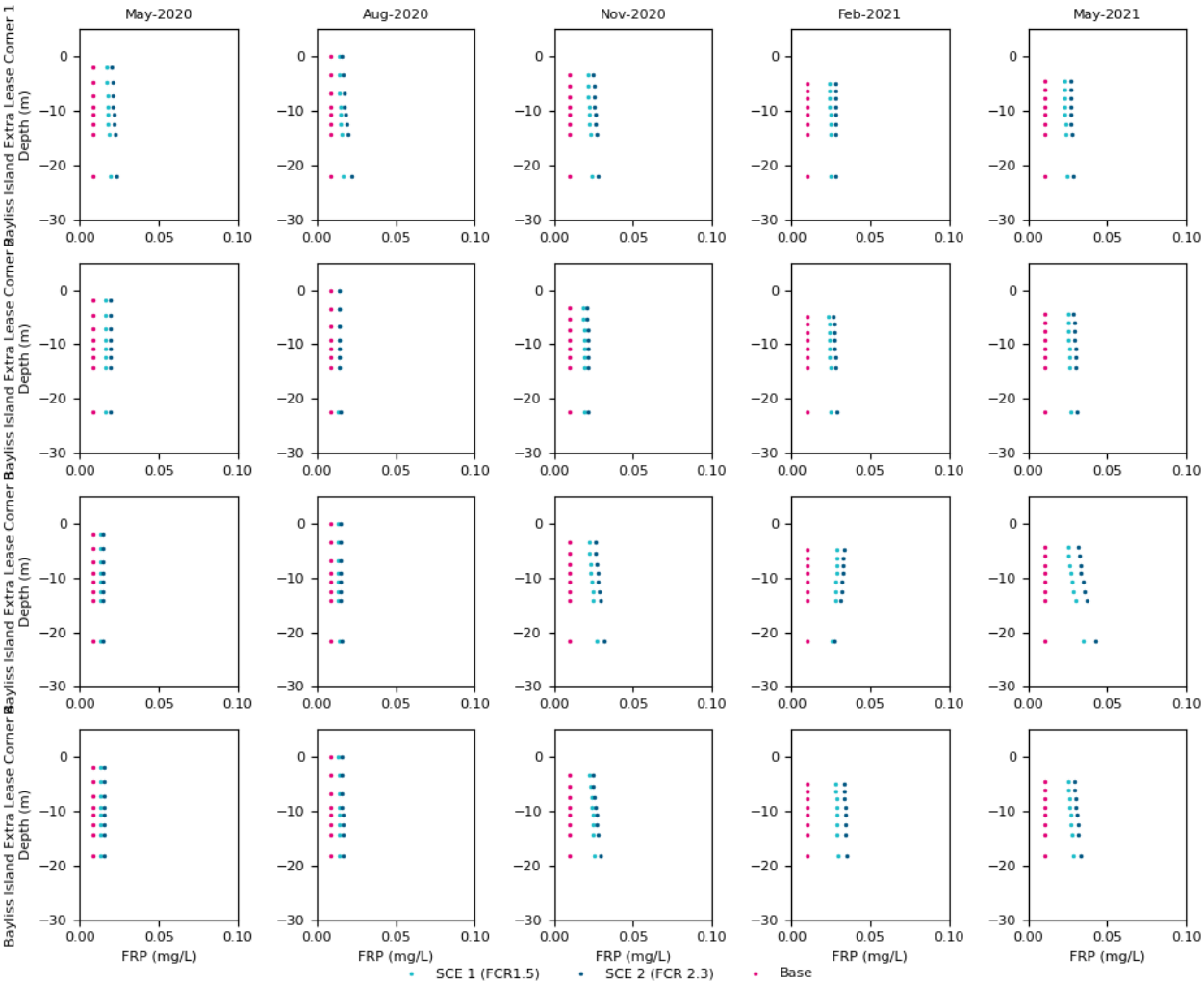

Figure 4.18 Depth profiles of simulated FRP at corners of Bayliss Extra site at the beginning of selected months

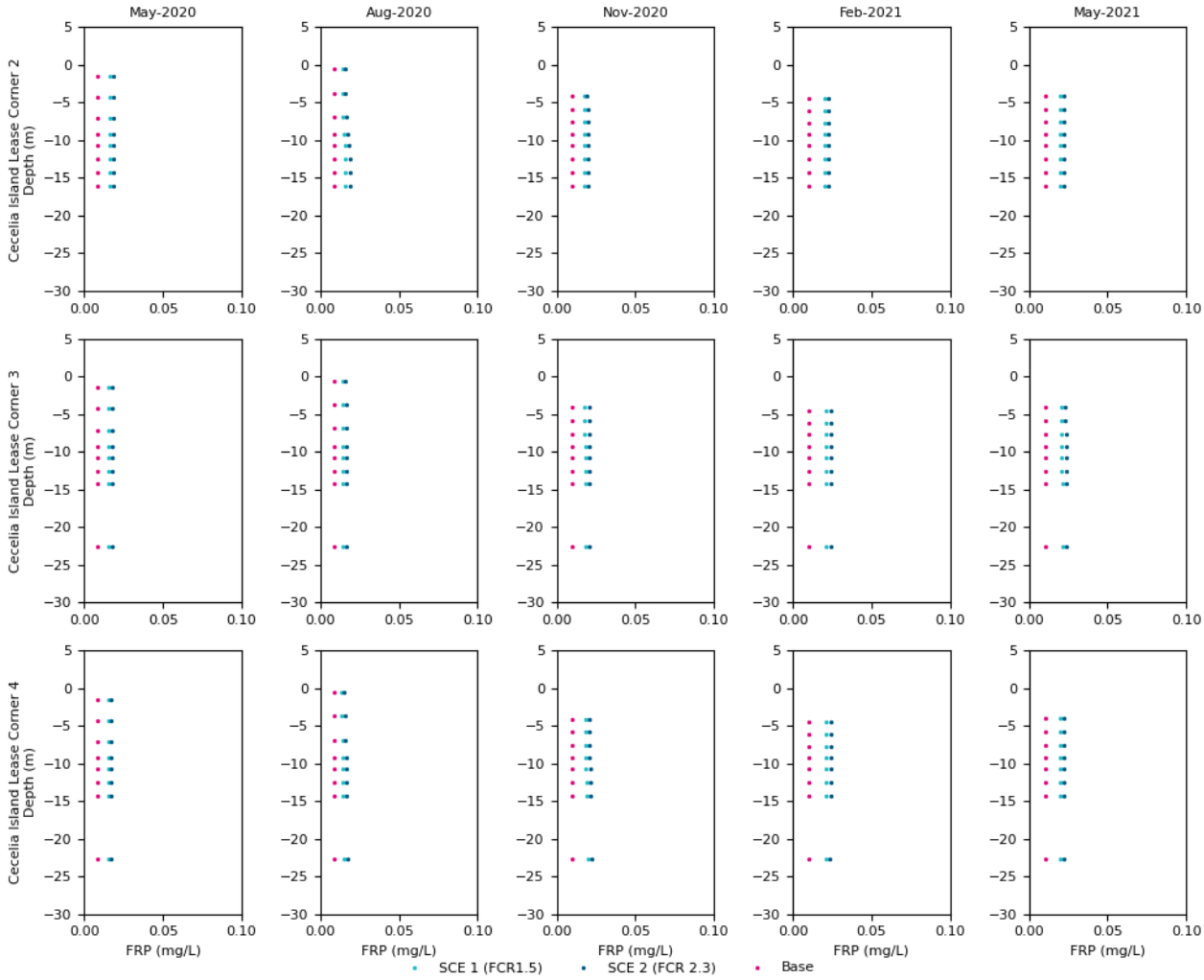

Figure 4.19 Depth profiles of simulated FRP at corners of Cecelia Island site at the beginning of selected months

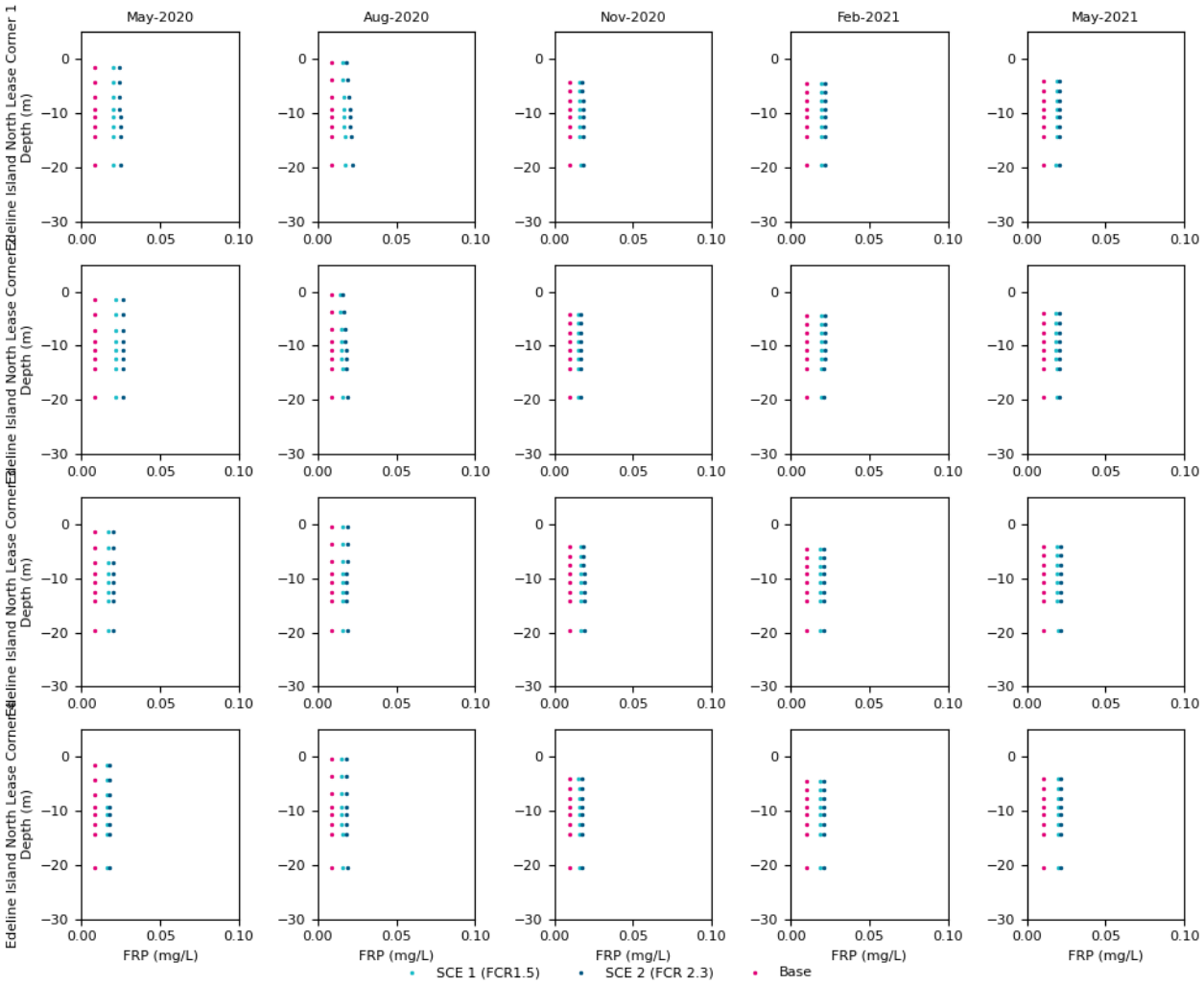

Figure 4.20 Depth profiles of simulated FRP at corners of Edeline Island North site at the beginning of selected months

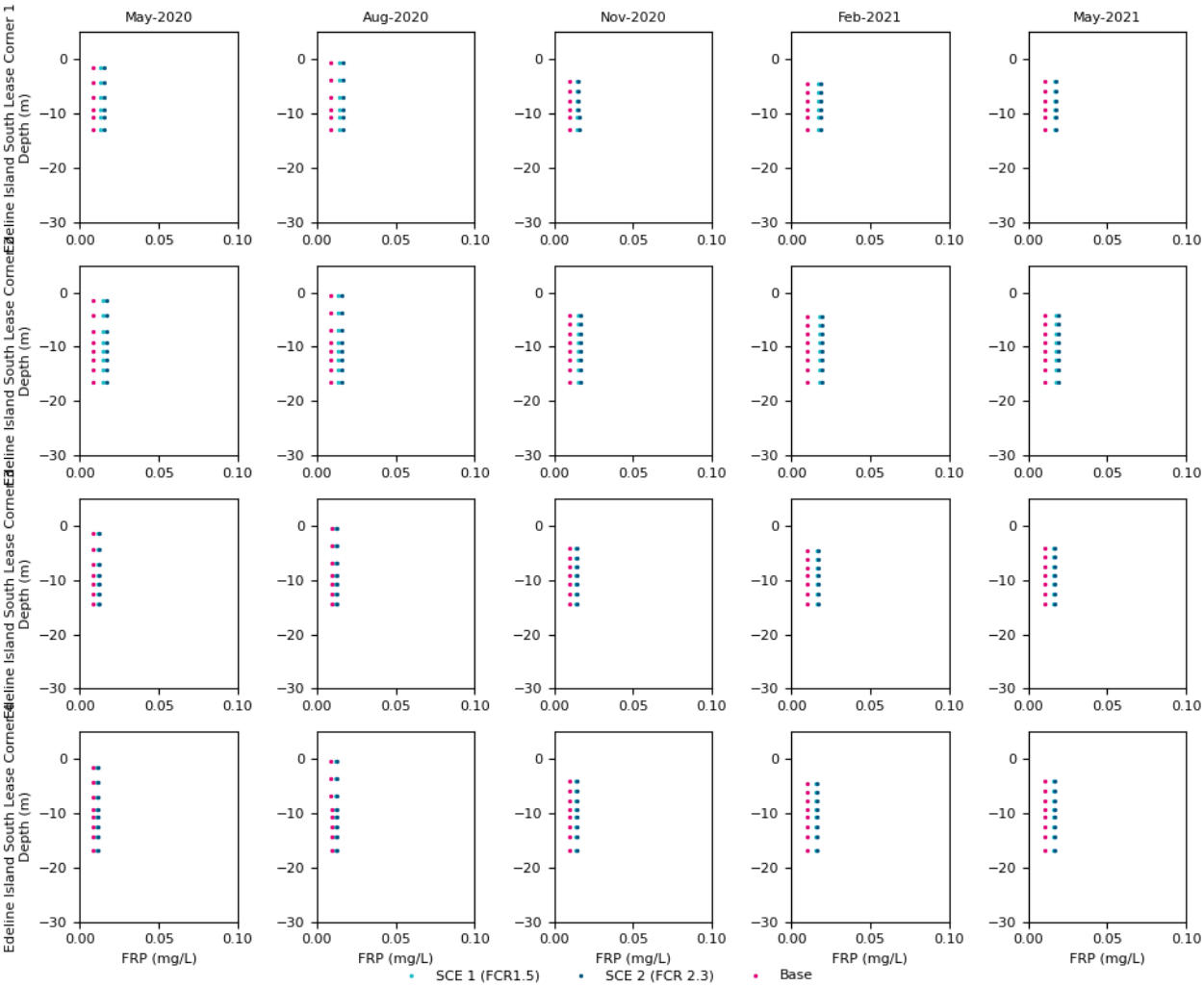

Figure 4.21 Depth profiles of simulated FRP at corners of Edeline Island South site at the beginning of selected months

4.4.3 Phytoplankton biomass

The potential for an increased risk of phytoplankton blooms resulting from proposed farming operations was modelled for the two scenarios. Natural phytoplankton populations may grow or change their species composition in response to changes in biologically available nitrogen. In contrast to simulated nutrients, the increases in simulated phytoplankton biomass downstream of sea-pens was not immediate, following a lag period between nutrient uptake and growth (processes which vary in speed depending on species composition and water temperature).

4.5.3.1 Spatial pattern

- Spatial distribution of simulated median Chl-*a* concentration at Razor Island site and other three sites for Scenario 1 (FCR 1.5) are presented in Figure 4.22 and Figure 4.23.
- Spatial distribution of simulated median Chl-*a* concentration at Razor Island site and other three sites for Scenario 2 (FCR 2.3) are presented in Figure 4.24 and Figure 4.25.
- Well flushed areas such as Bayliss, Dororthy and Edeline Islands farm sites, are projected to have median Chl-*a* concentration below the 0.8 µg/L threshold in all the modelled scenarios while

semi-enclosed areas such as Razor Bayliss Island are predicted to have median Chl-*a* concentrations above this threshold except in Scenario 1.

- Razor Island site exhibits the highest Chl-*a* footprint, likely primarily because of its proximity to river inlets compared to other leases.

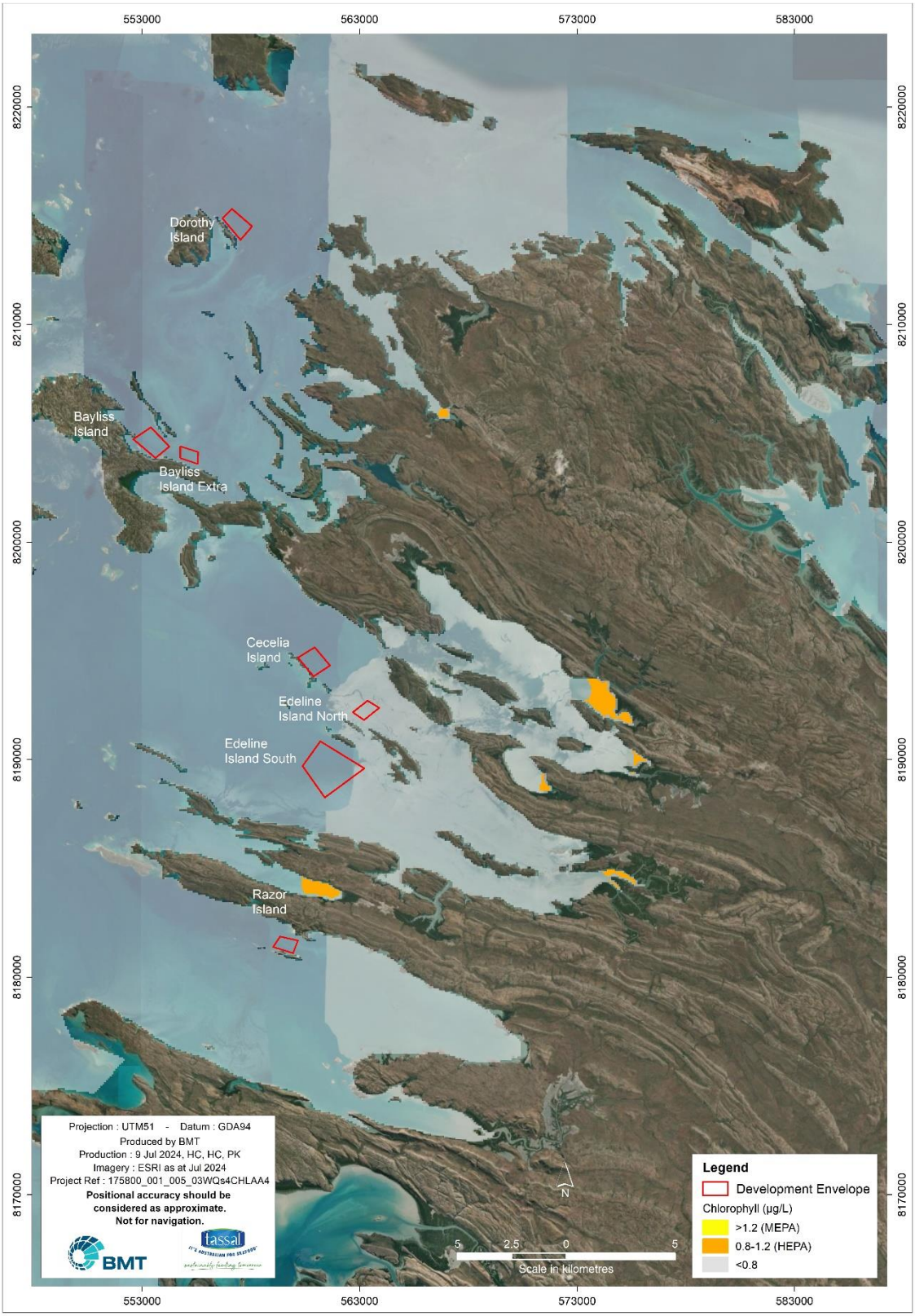

Figure 4.22 Predicted chlorophyll-a concentrations under Scenario 1 – Strickland Bay, Bayliss Islands, Dorothy Island

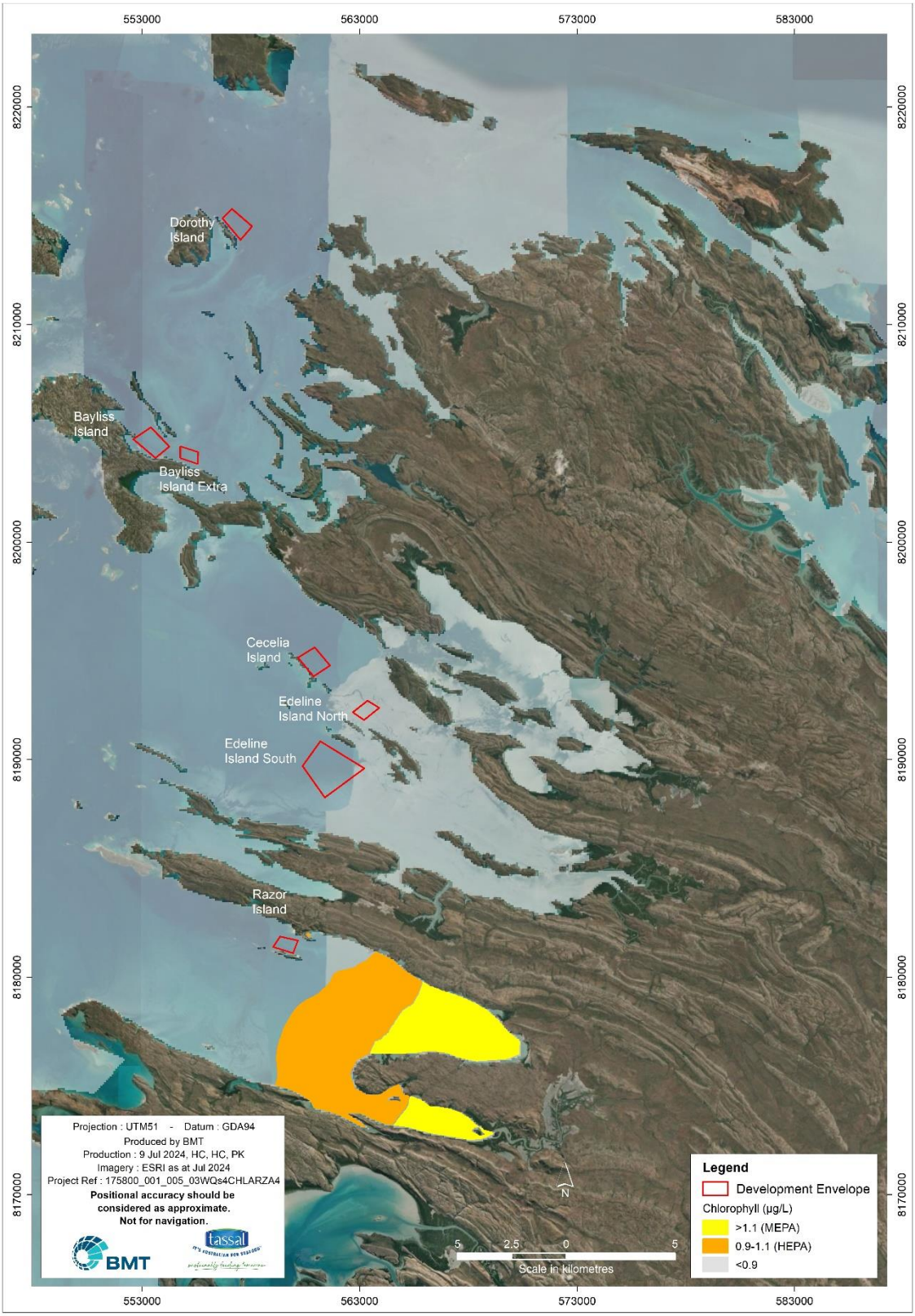

Figure 4.23 Predicted chlorophyll-a concentrations under Scenario 1 – Razor Island

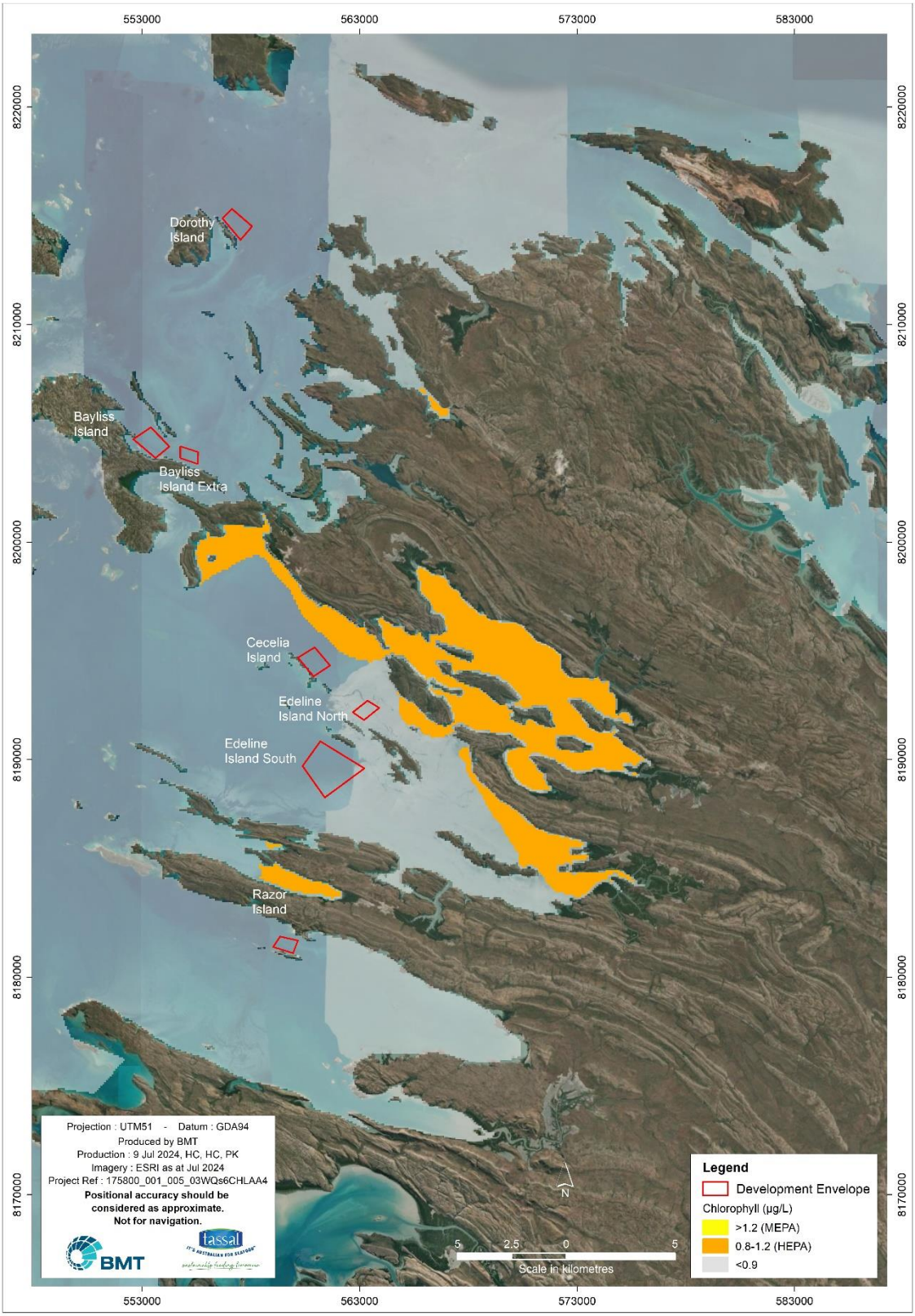

Figure 4.24 Predicted chlorophyll-a concentrations under Scenario 2 – Strickland Bay, Bayliss Islands and Dorothy Island

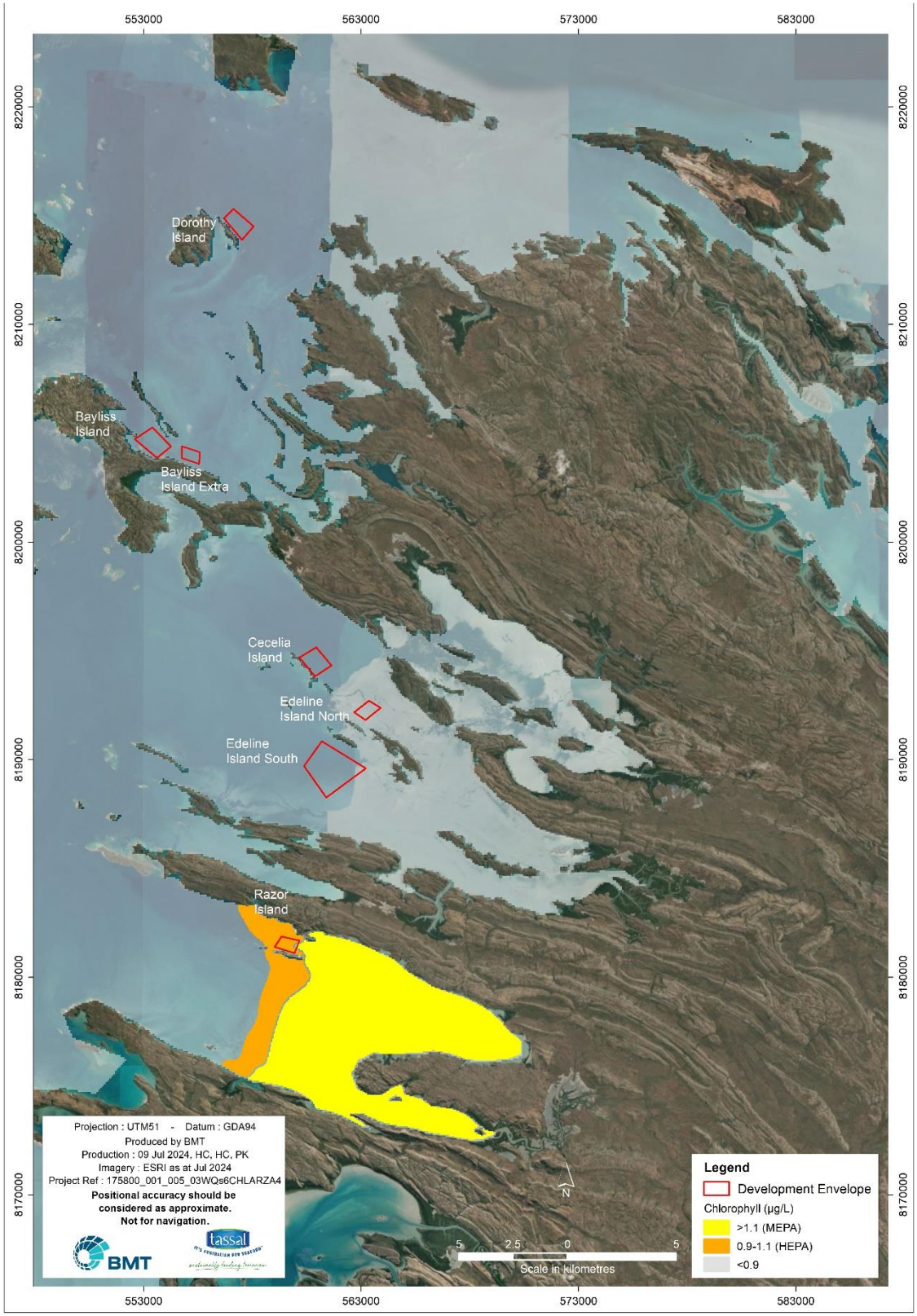

Figure 4.25 Predicted chlorophyll-a concentrations under Scenario 2 – Razor Island

4.5.3.2 Depth profiles

Figure 4.26 through to Figure 4.32 present the depth profiles of Chl-*a* concentrations around the corners of the leased areas for the baseline and operational farming scenarios. The following points are noted:

- The projected Chl-*a* concentrations increased with increased FCR.
- The model projected well-mixed Chl-*a* concentrations in periods of low primary productivity while the near-surface concentrations were slightly higher than at depths during periods of high primary productivity.

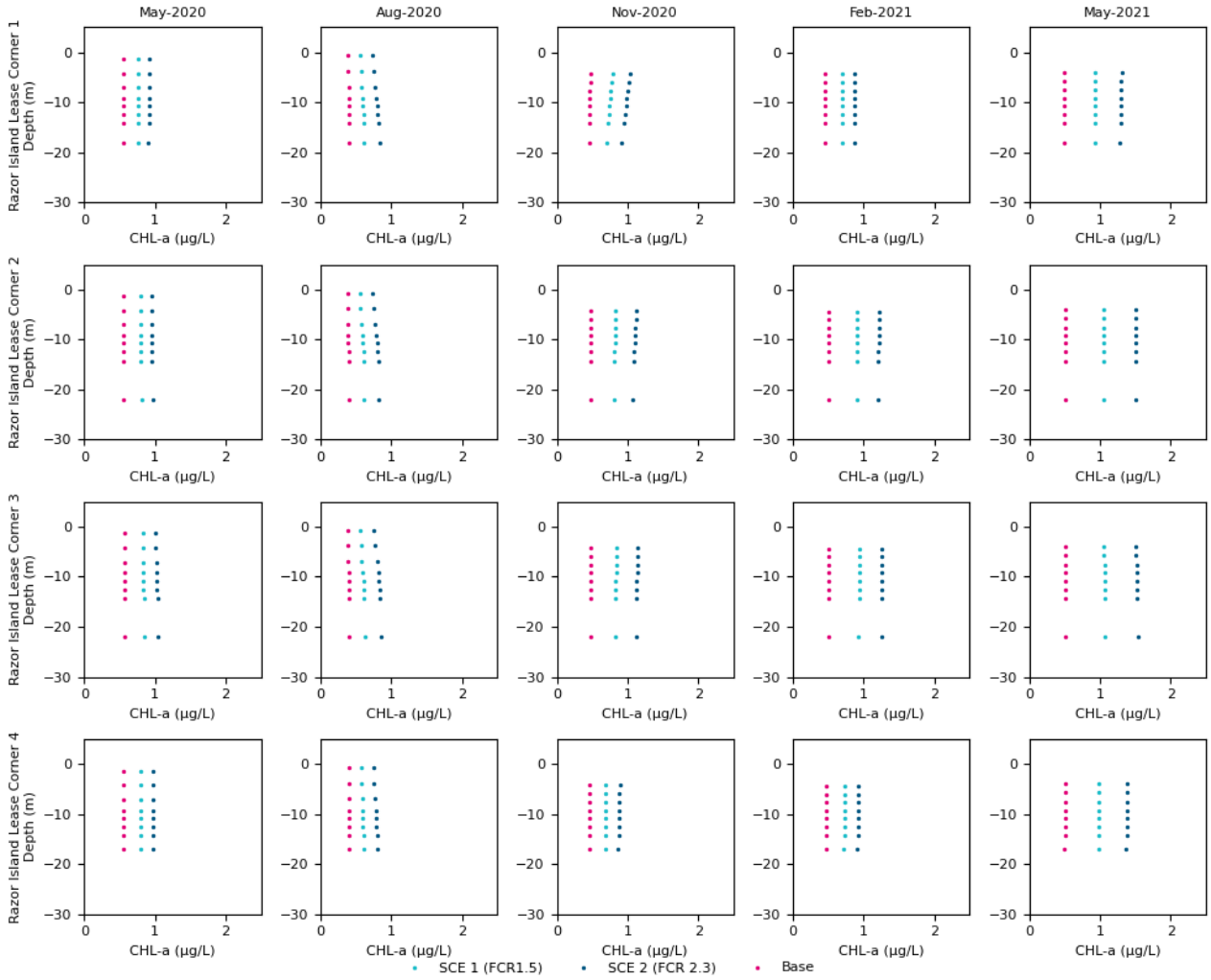

Figure 4.26 Depth profiles of simulated Chl-*a* at corners of Razor Island site at the beginning of selected months

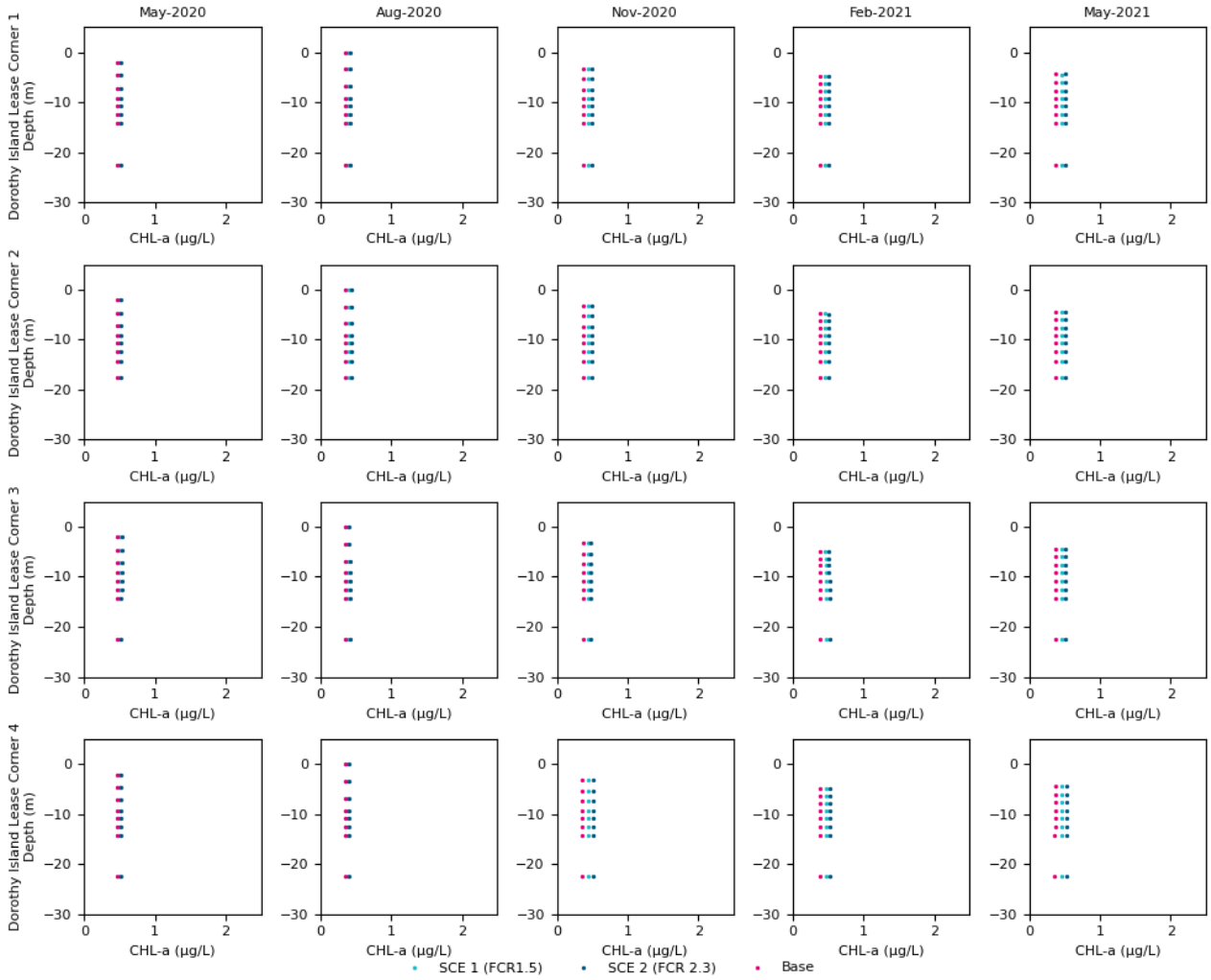

Figure 4.27 Depth profiles of simulated Chl-*a* at corners of Dorothy Island site at the beginning of selected months

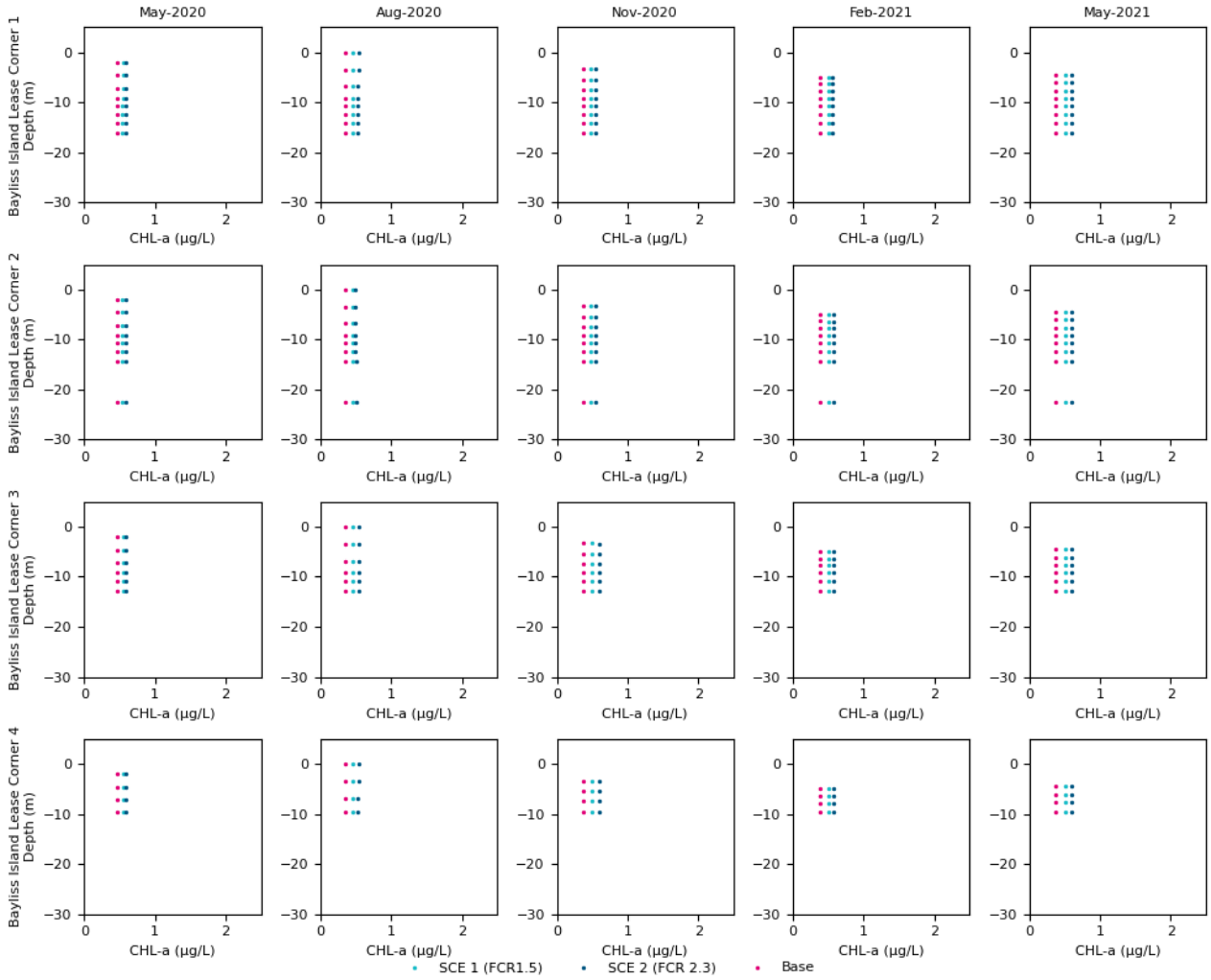

Figure 4.28 Depth profiles of simulated Chl-*a* at corners of Bayliss Island site at the beginning of selected months

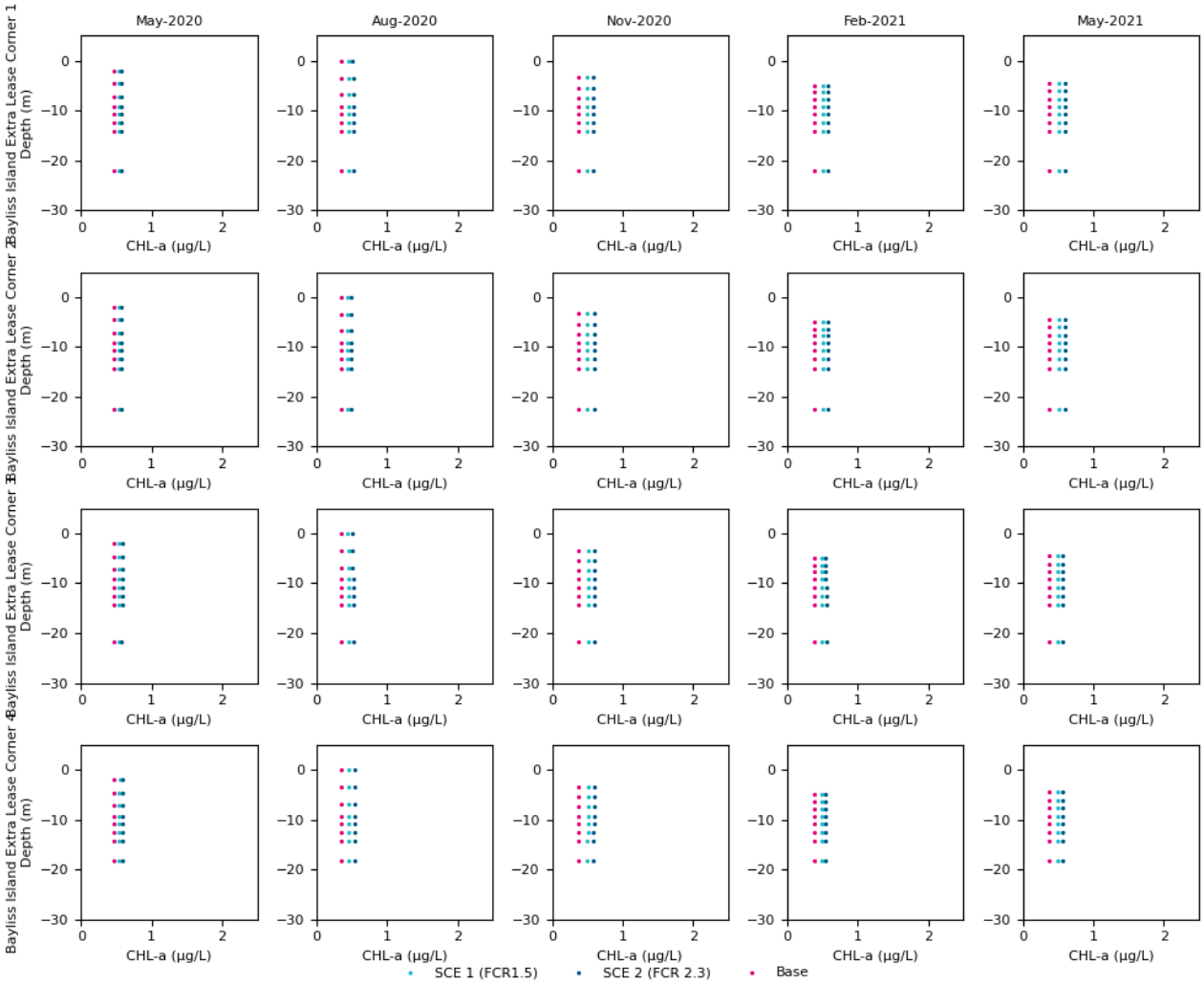

Figure 4.29 Depth profiles of simulated Chl-*a* at corners of Bayliss Extra site at the beginning of selected months

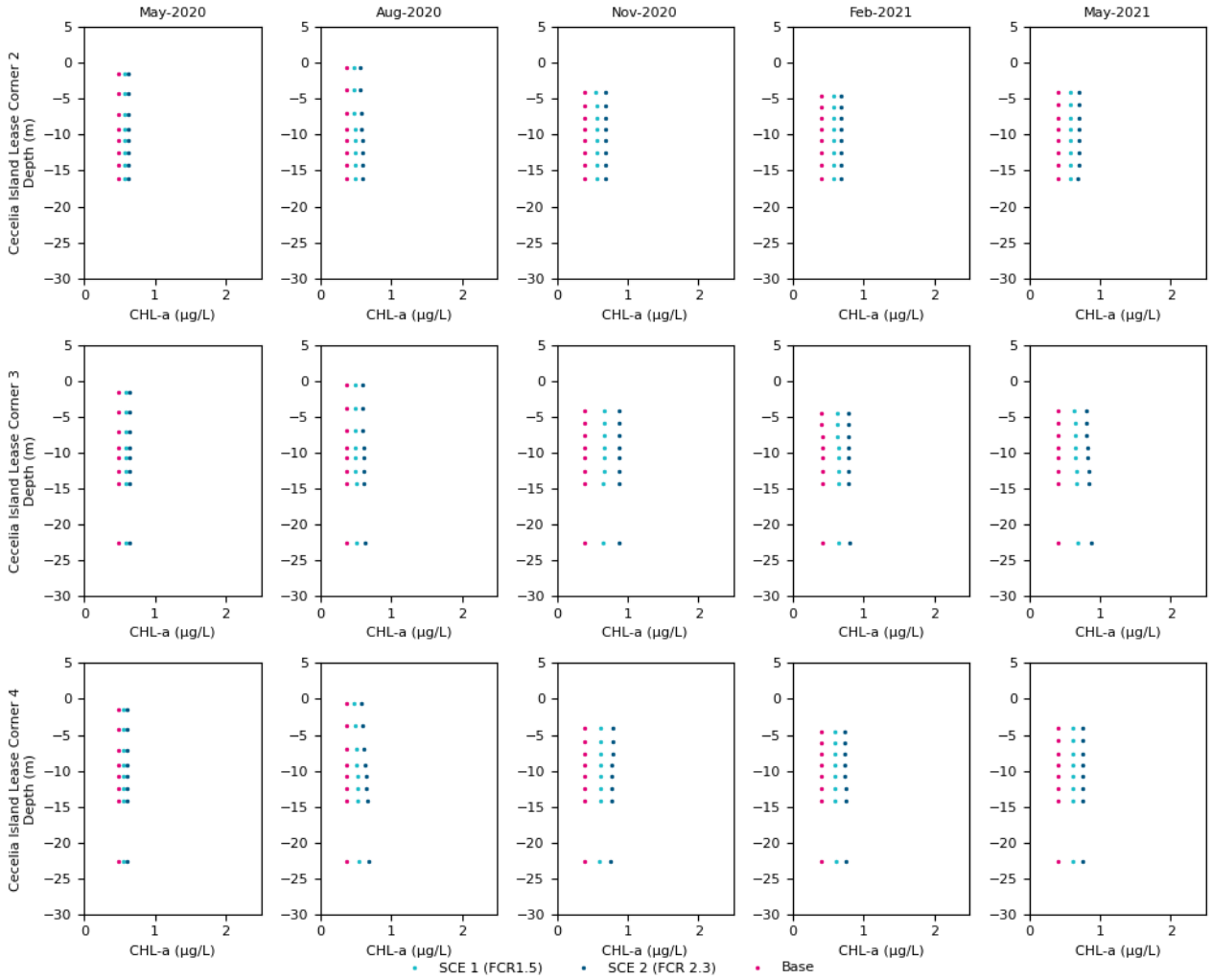

Figure 4.30 Depth profiles of simulated Chl-*a* at corners of Cecelia Island site at the beginning of selected months

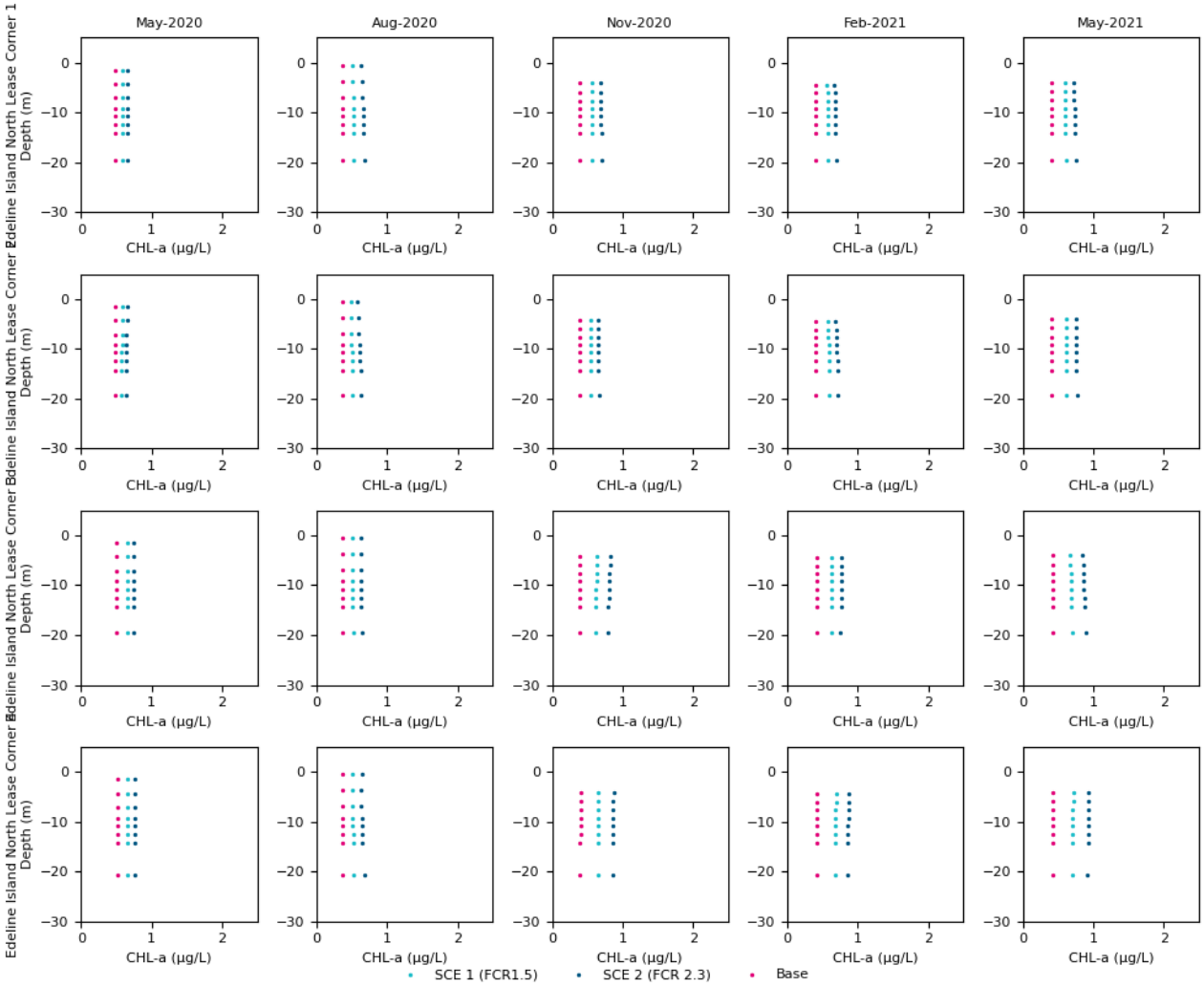

Figure 4.31 Depth profiles of simulated Chl-*a* at corners of Edeline Island North site at the beginning of selected months

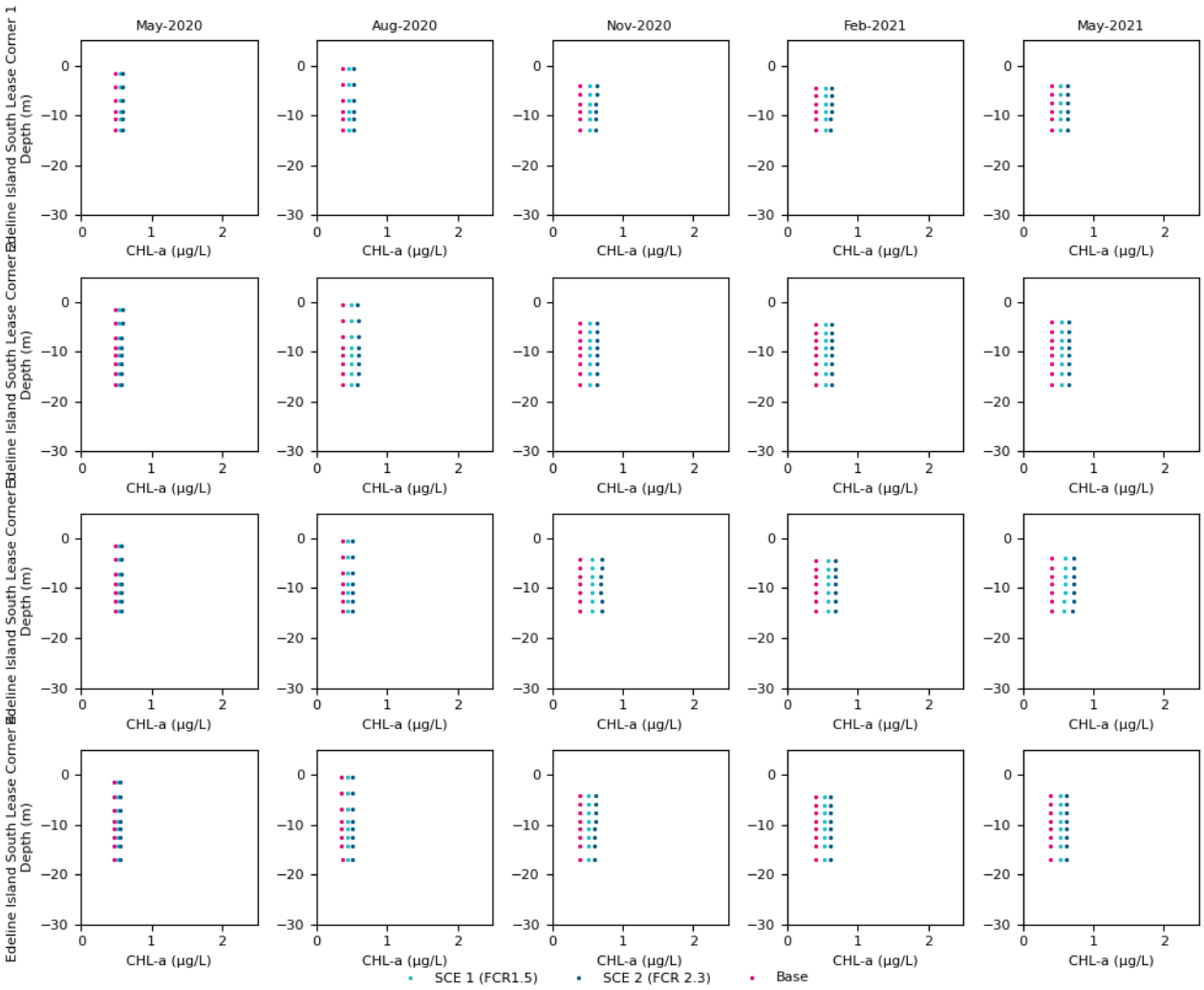

Figure 4.32 Depth profiles of simulated Chl-*a* at corners of Edeline Island South site at the beginning of selected months

4.4.4 Dissolved oxygen

The potential for deoxygenation of the water column beneath and near the sea-pens was investigated using the integrated hydrodynamic, water and sediment diagenesis model. The investigation was focussed on the bottom 1 m of the water column, which would be worst affected in the case of oxygen drawdown because of high benthic organic content and microbial community. The simulations examined the impact of organic matter on the biochemistry of the local sediments to determine whether the introduction of fish farming resulted in significant dissolved oxygen drawdown.

Despite significant inputs of organic waste from the proposed farm leases, none of the scenarios resulted in notable drawdown in the median concentration of DO concentration at the bed when compared to the base case (Refer section 4.4.6 for time series plots of DO).

Oxygen concentrations in the vicinity of the proposed farm maintained normal levels across the scenarios, with no evidence of significant oxygen drawdown even at peak FCRs. Results of the sediment diagenesis model, however, point to high levels of biological oxygen demand at the sediment water interface. Under anoxic sediment conditions, water at the sediment water interface is likely to experience some oxygen drawdown. However, the extent of water movement through the system is such that the level of drawdown is unlikely to be of any ecological consequence, as oxygen levels are quickly resupplied by new seawater inputs.

4.4.5 Timeseries plots for DIN, FRP, Chl-a, and DO

The time-series data for DIN, FRP, Chl-a, and DO are presented in Figure 4.33 to Figure 4.56 for both surface and bottom layers for Scenario 1 and Scenario 2 at corner 1 site of all leases. Plots include base case comparisons and water quality compliance thresholds.

- The time-series data for DIN concentrations show variations influenced by tidal signals, with projected concentrations generally remaining below 0.06 mg/L across all leases throughout the year for Scenario 1. In Scenario 2, the maximum simulated DIN concentration did not exceed 0.08 mg/L.
- For Scenario 1, the simulated DIN concentration at Razor Island did not exceed 0.01 mg/L more than 50% of the time and did not exceed 0.014 mg/L at other sites, meeting the High Ecological Protection Area (HEPA) criteria.
- For Scenario 1, the simulated DIN concentration at Razor Island did not exceed 0.035 mg/L more than 50% of the time and did not exceed 0.22 mg/L at other sites, meeting the Moderate Ecological Protection Area (MEPA) criteria.
- For Scenario 2, Bayliss, Bayliss Extra, Cecelia, Edeline North, and Razor Island did not meet the DIN HEPA criteria; however, all sites met the DIN MEPA criteria.
- The bottom layer exhibited slightly higher DIN concentrations compared to the surface layer during late summer and early autumn.
- The time-series for FRP concentrations also show variations with tidal signals, with projected concentrations generally remaining below 0.08 mg/L at all sites for the Scenario 1 and below 0.1 mg/L for Scenario 2. Highest simulated FRP was projected Razor Island.
- The time-series data for Chl-a concentrations show variations influenced by tidal signals, with projected concentrations generally remaining below 1.5 ug/L across all leases throughout the year for Scenario 1. In Scenario 2, the maximum simulated Chl-a concentration did not exceed 2 ug/L.

- For Scenario 1, the simulated Chl-a concentration at Razor Island did not exceed 0.9 ug/L more than 50% of the time and did not exceed 0.8 ug/L at other sites, meeting the HEPA criteria.
- For Scenario 1, the simulated Chl-a concentration at Razor Island did not exceed 1.1 ug/L more than 50% of the time and did not exceed 1.2 ug/L at other sites, meeting the MEPA criteria.
- For Scenario 2, except for Razor Island, all the other sites met the MEPA criteria; and all sites met the HEPA criteria for Chl-a.
- The highest simulated DIN, FRP and Chla-a concentrations were recorded at the Razor Island site.
- For dissolved oxygen, the potential sediment drawdown was examined using the time-series of saturated DO levels. The figures indicate that the model predicted no significant influence on oxygen levels at the corners of the sites throughout the year.

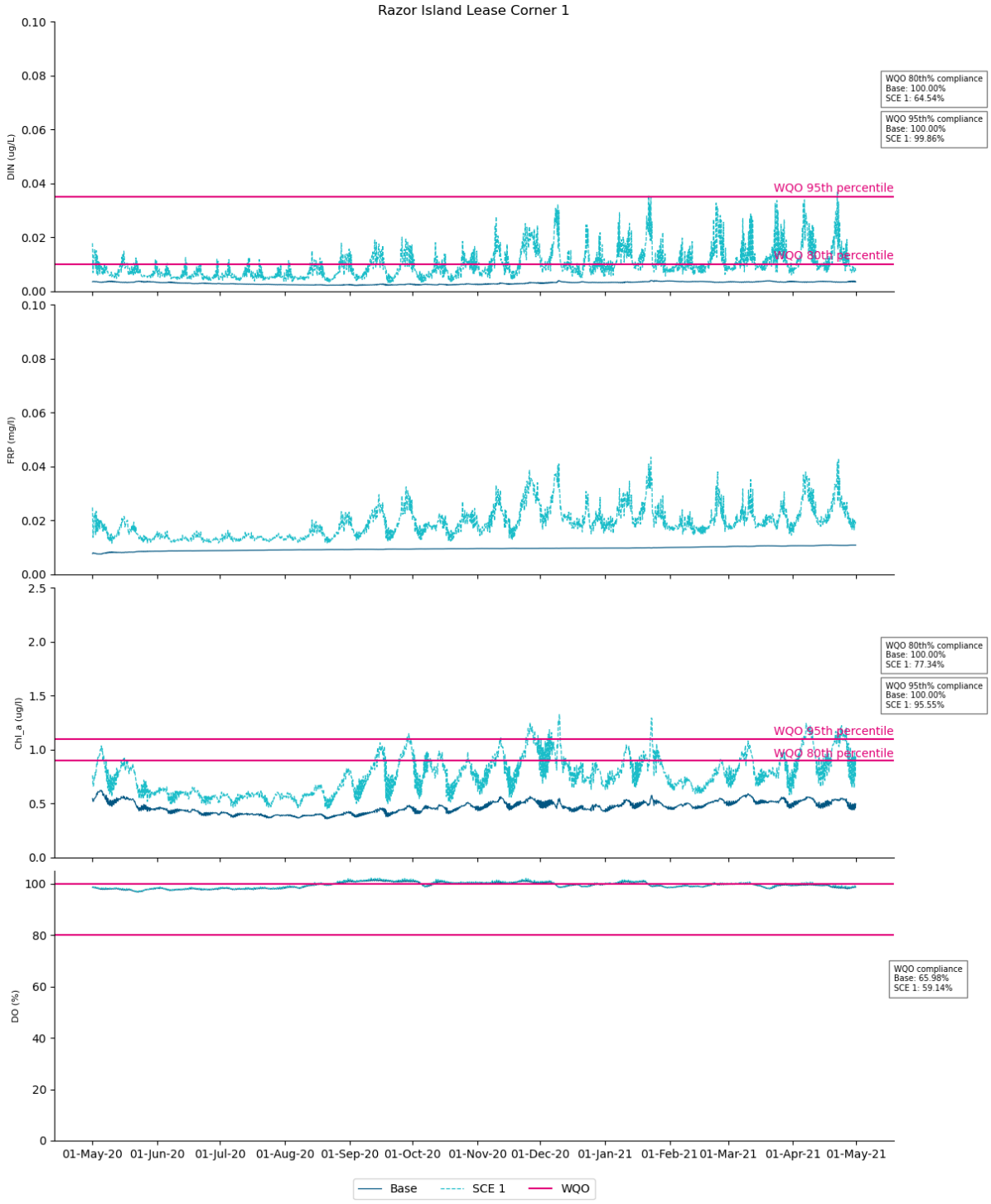

Figure 4.33 Time series of near surface concentrations of DIN, FRP, Chl-*a* and saturated DO at the edge of the site (Corner 1) around Razor Island for Scenario 1

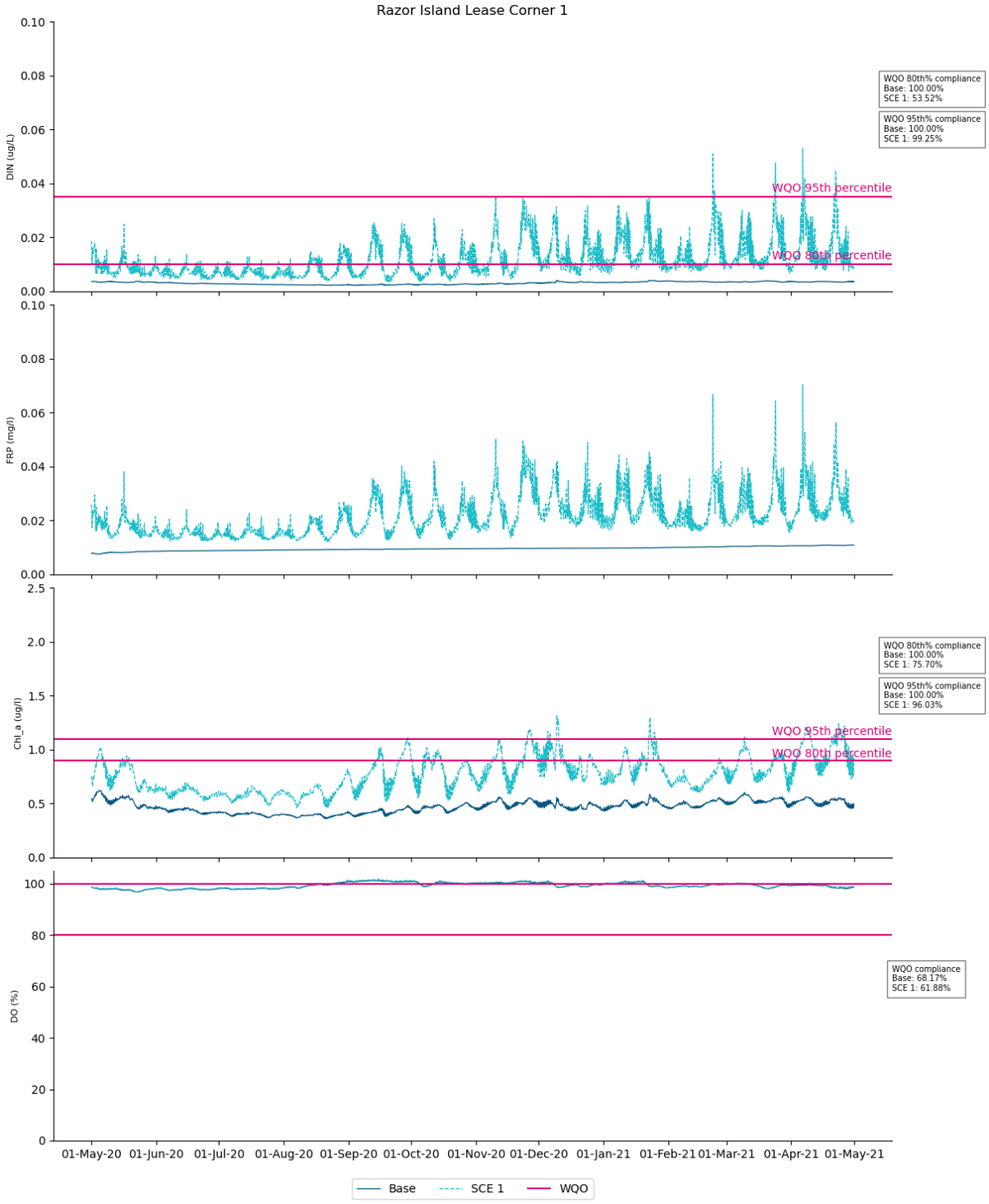

Figure 4.34 Time series of near bottom concentrations of DIN, FRP, Chl-*a* and saturated DO at the edge of the site (Corner 1) around Razor Island for Scenario 1

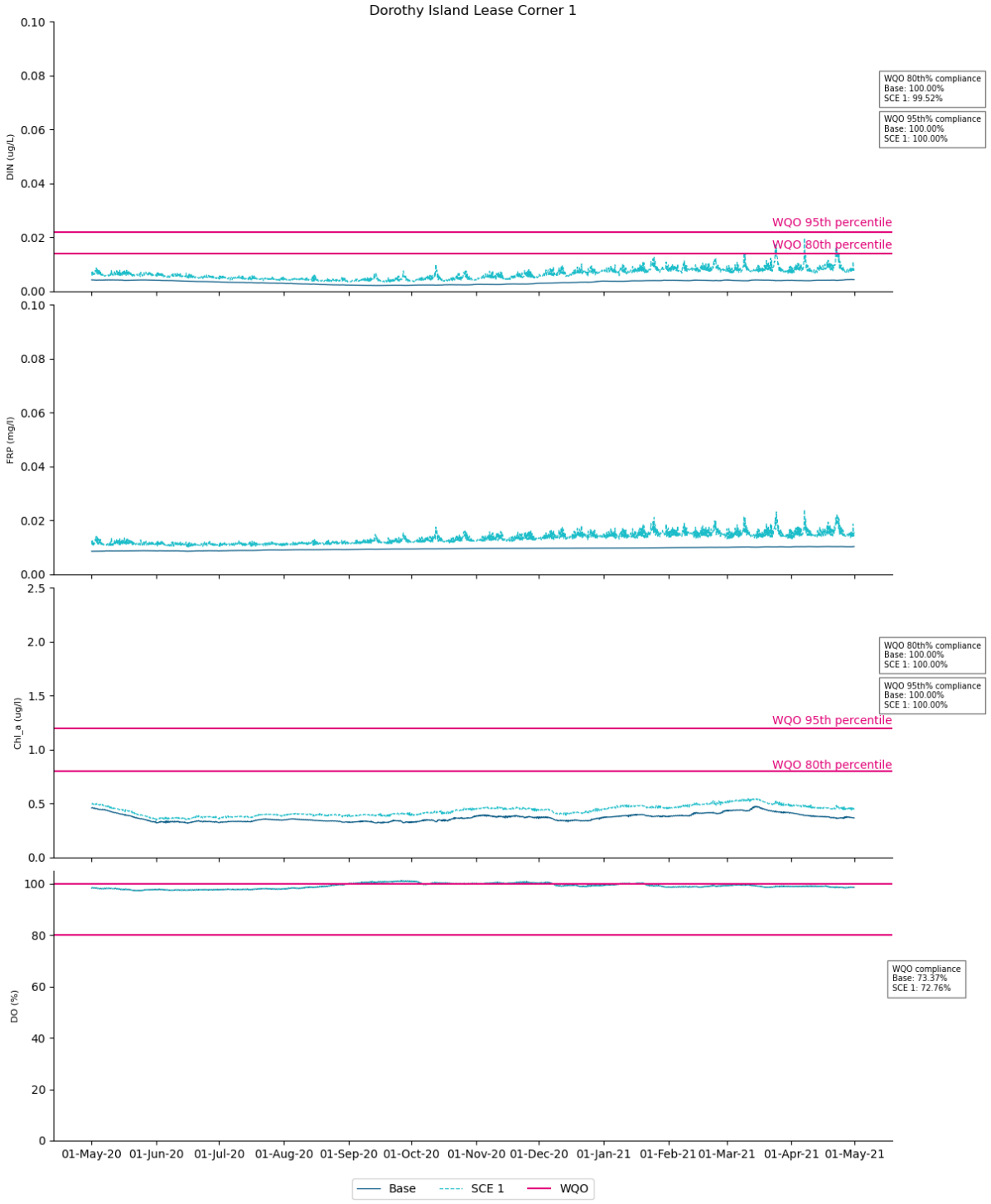

Figure 4.35 Time series of near surface concentrations of DIN, FRP, Chl-*a* and saturated DO at the edge of the site (Corner 1) around Dorothy Island for Scenario 1

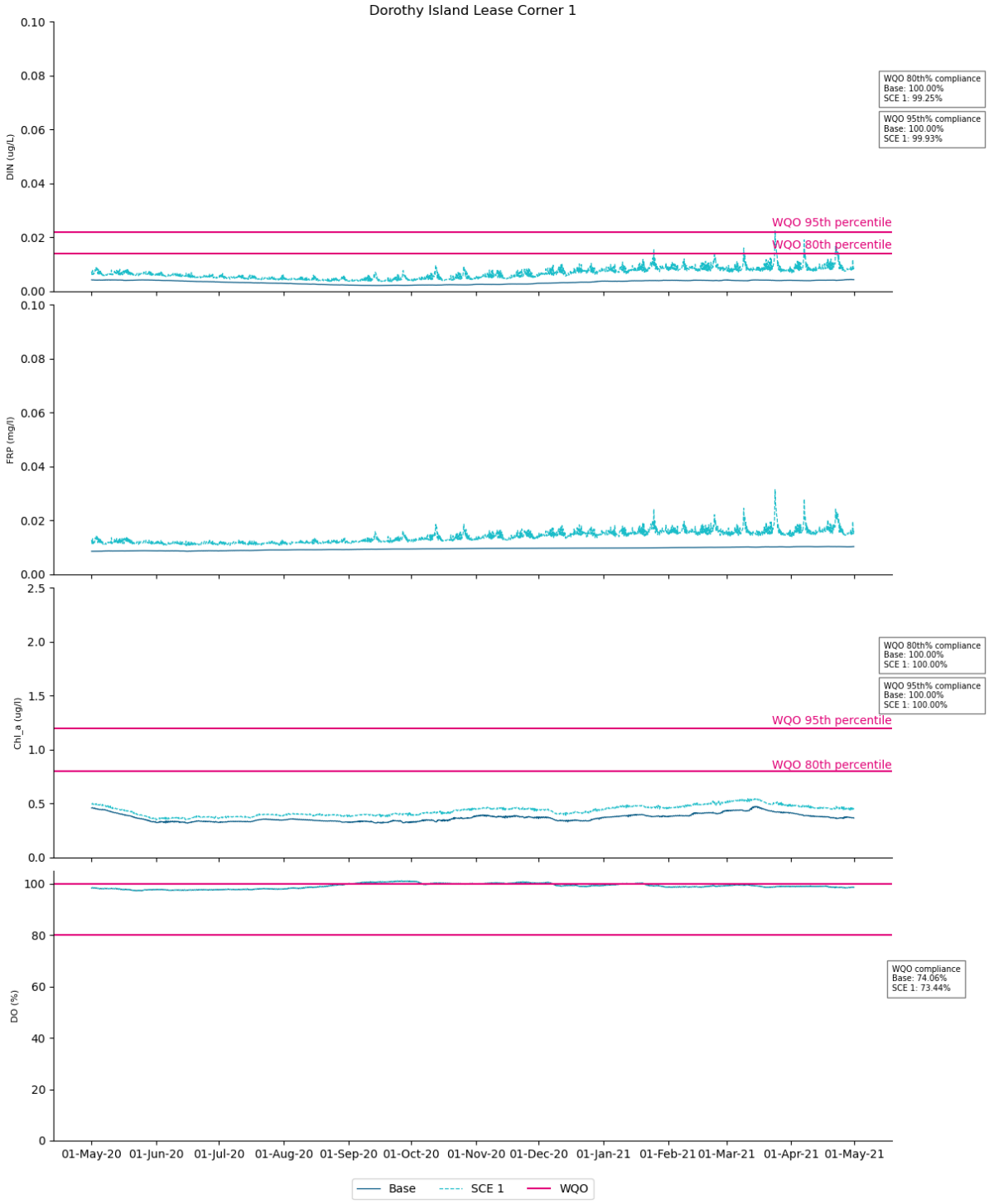

Figure 4.36 Time series of near bottom concentrations of DIN, FRP, Chl-*a* and saturated DO at the edge of the site (Corner 1) around Dorothy Island for Scenario 1

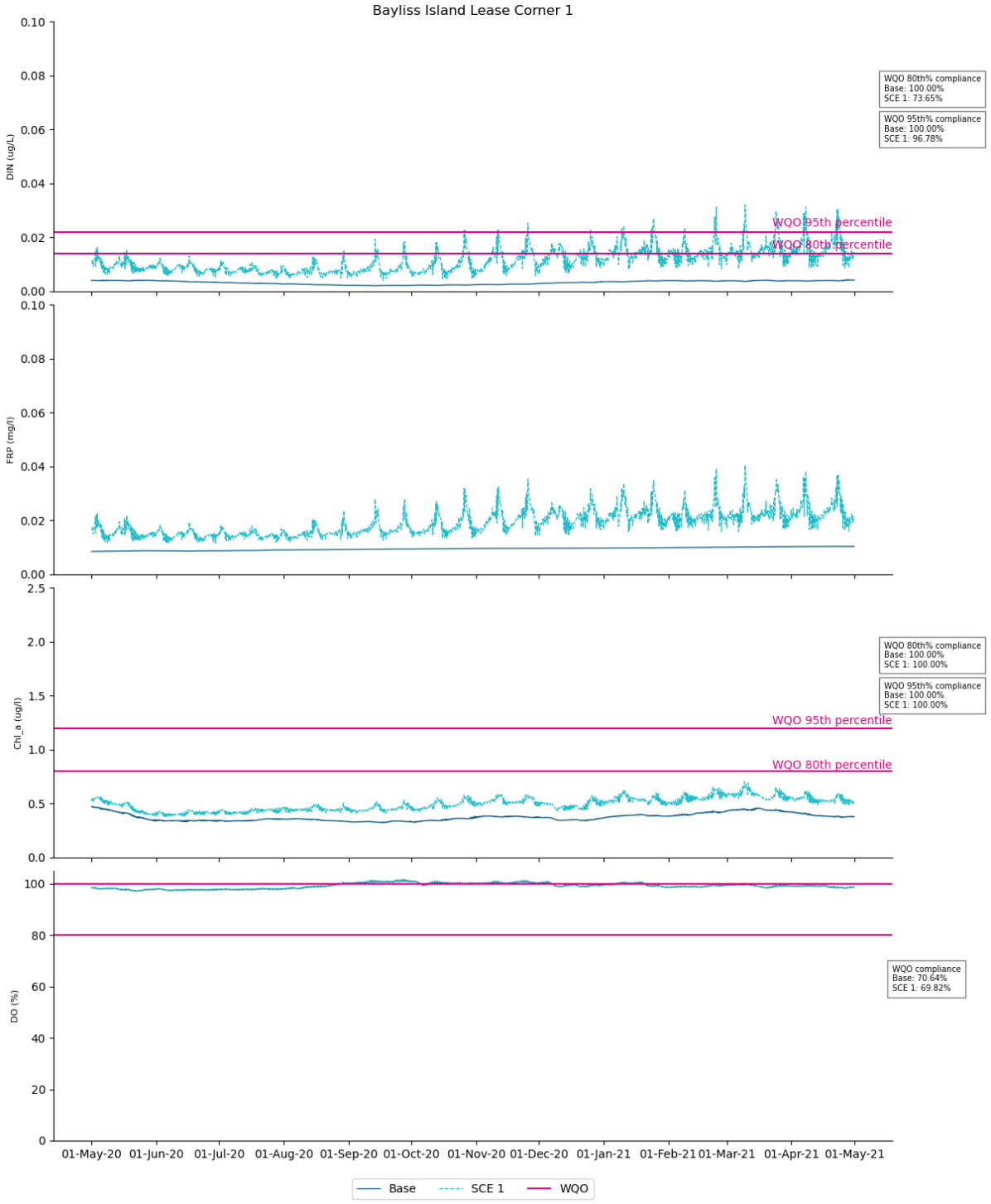

Figure 4.37 Time series of near surface concentrations of DIN, FRP, Chl-*a* and saturated DO at the edge of the site (Corner 1) around Bayliss Island for Scenario 1

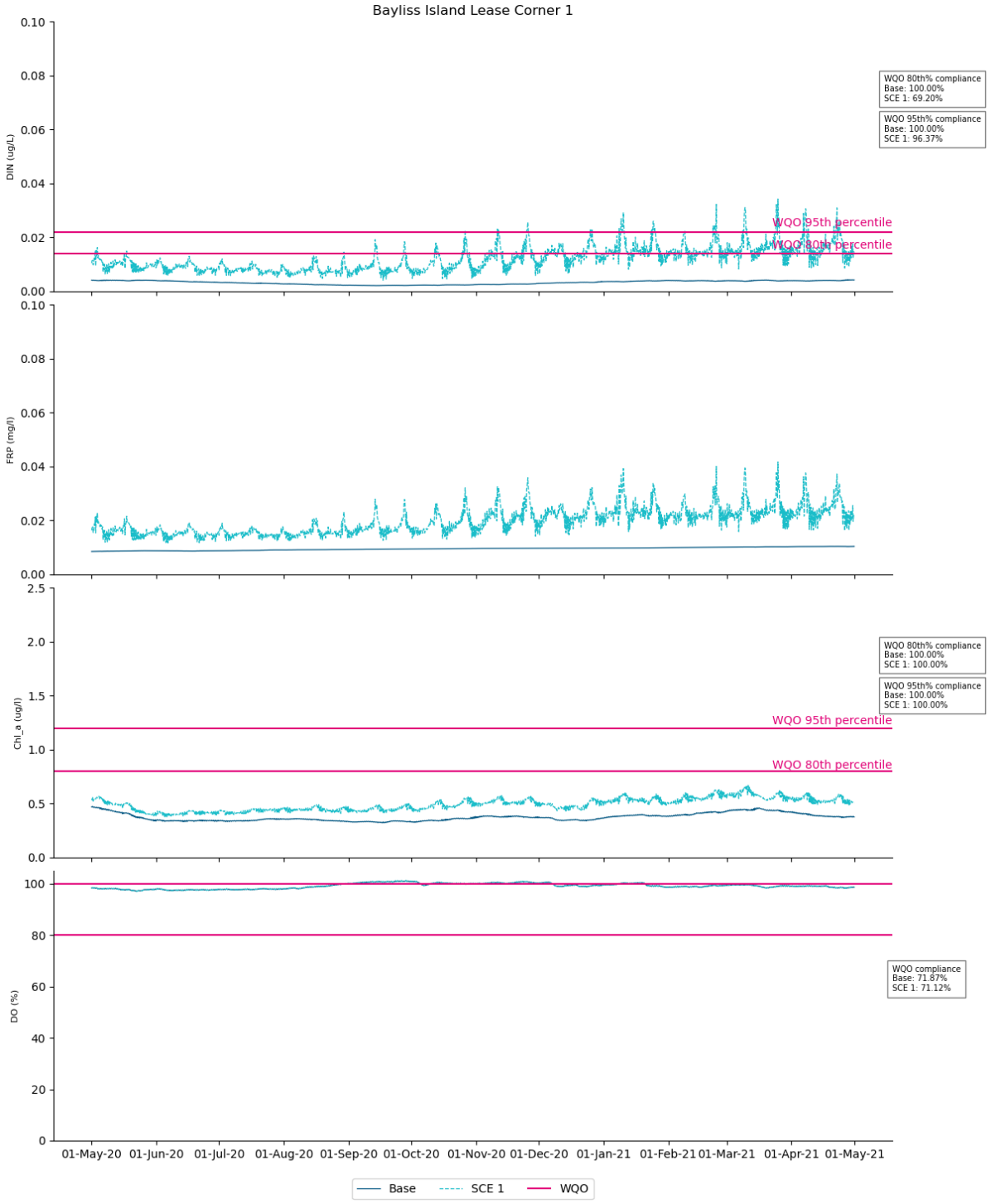

Figure 4.38 Time series of near bottom concentrations of DIN, FRP, Chl-*a* and saturated DO at the edge of the site (Corner 1) around Bayliss Island for Scenario 1

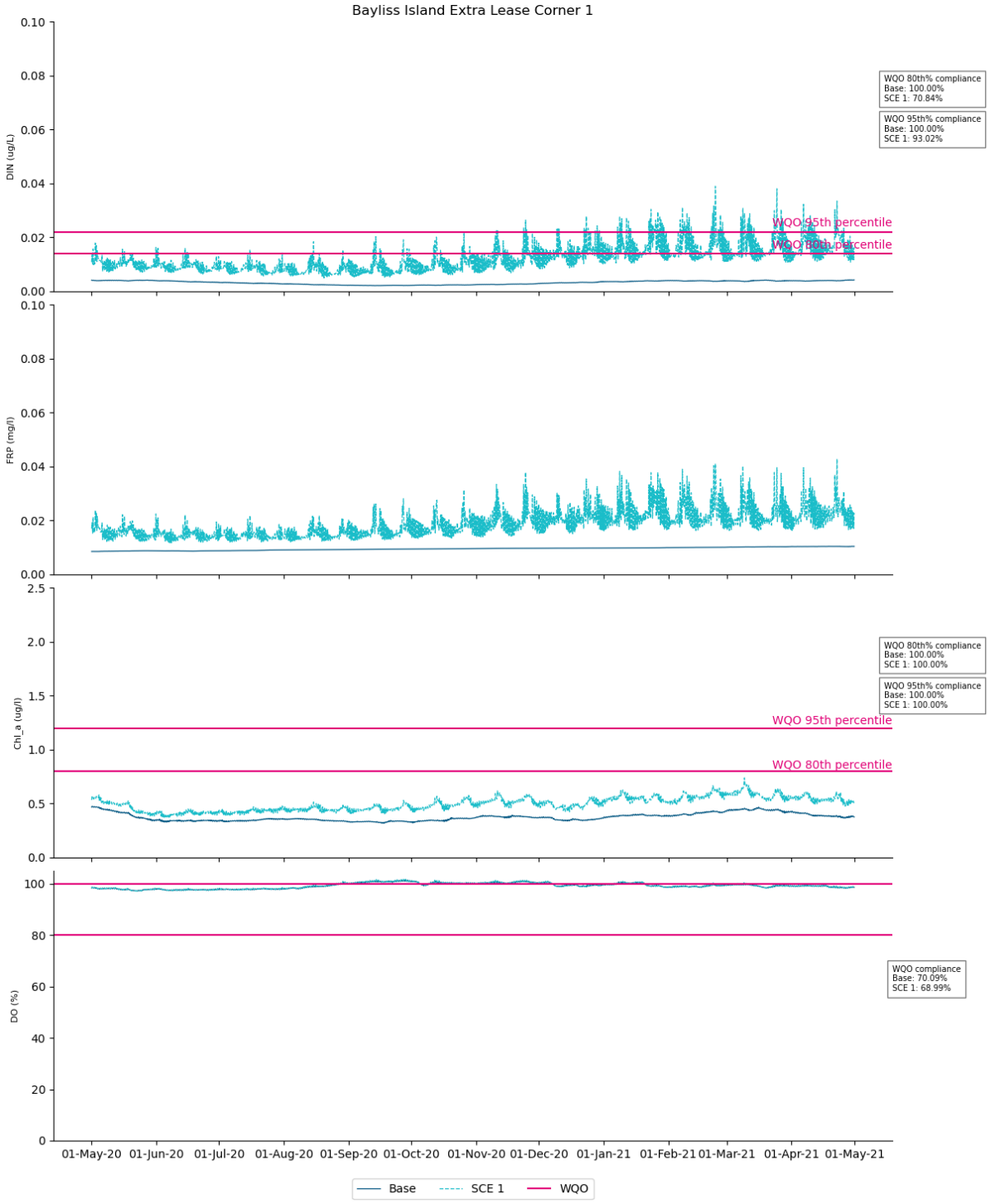

Figure 4.39 Time series of near surface concentrations of DIN, FRP, Chl-*a* and saturated DO at the edge of the site (Corner 1) around Bayliss Extra for Scenario 1

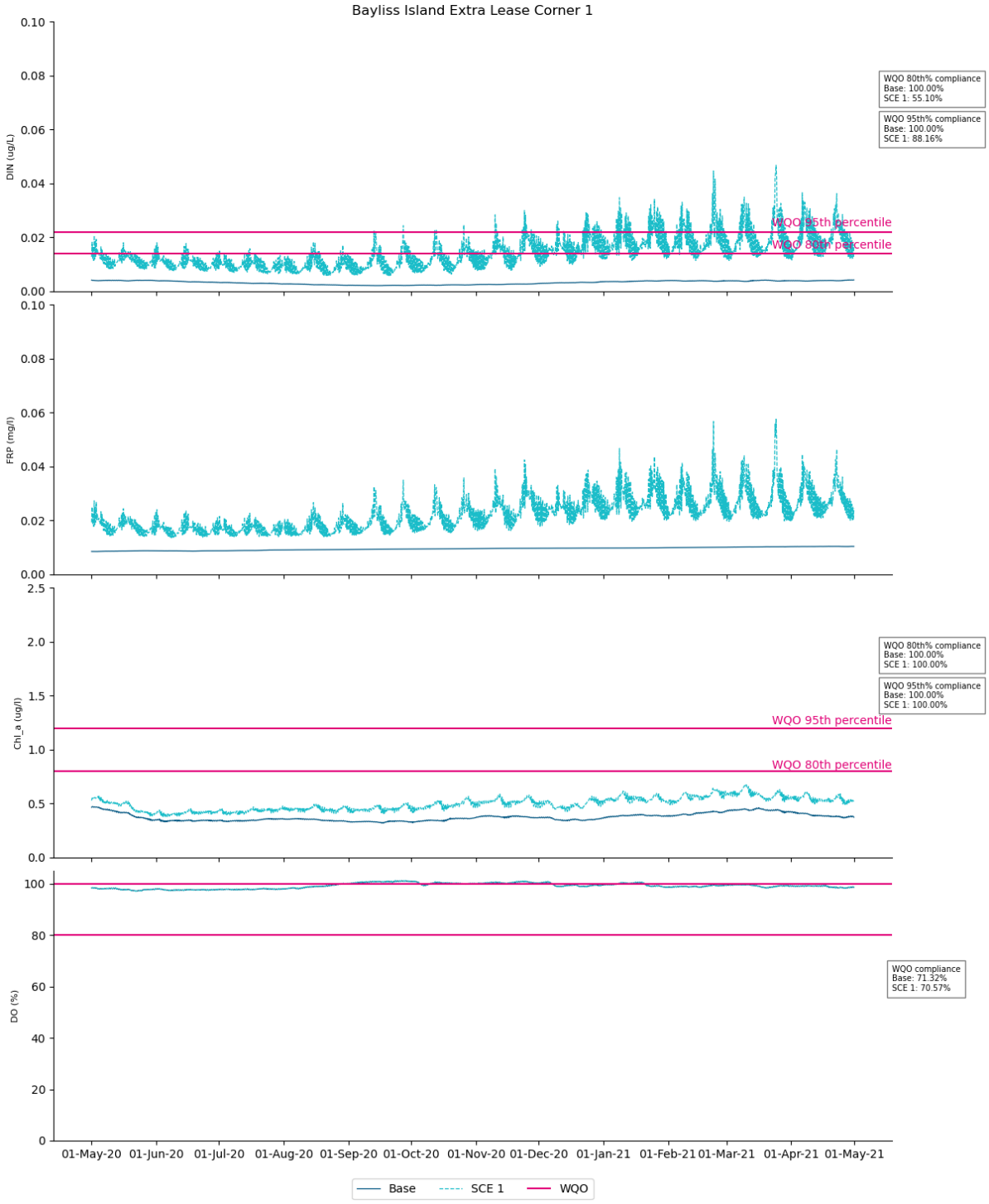

Figure 4.40 Time series of near bottom concentrations of DIN, FRP, Chl-*a* and saturated DO at the edge of the site (Corner 1) around Bayliss Extra for Scenario 1

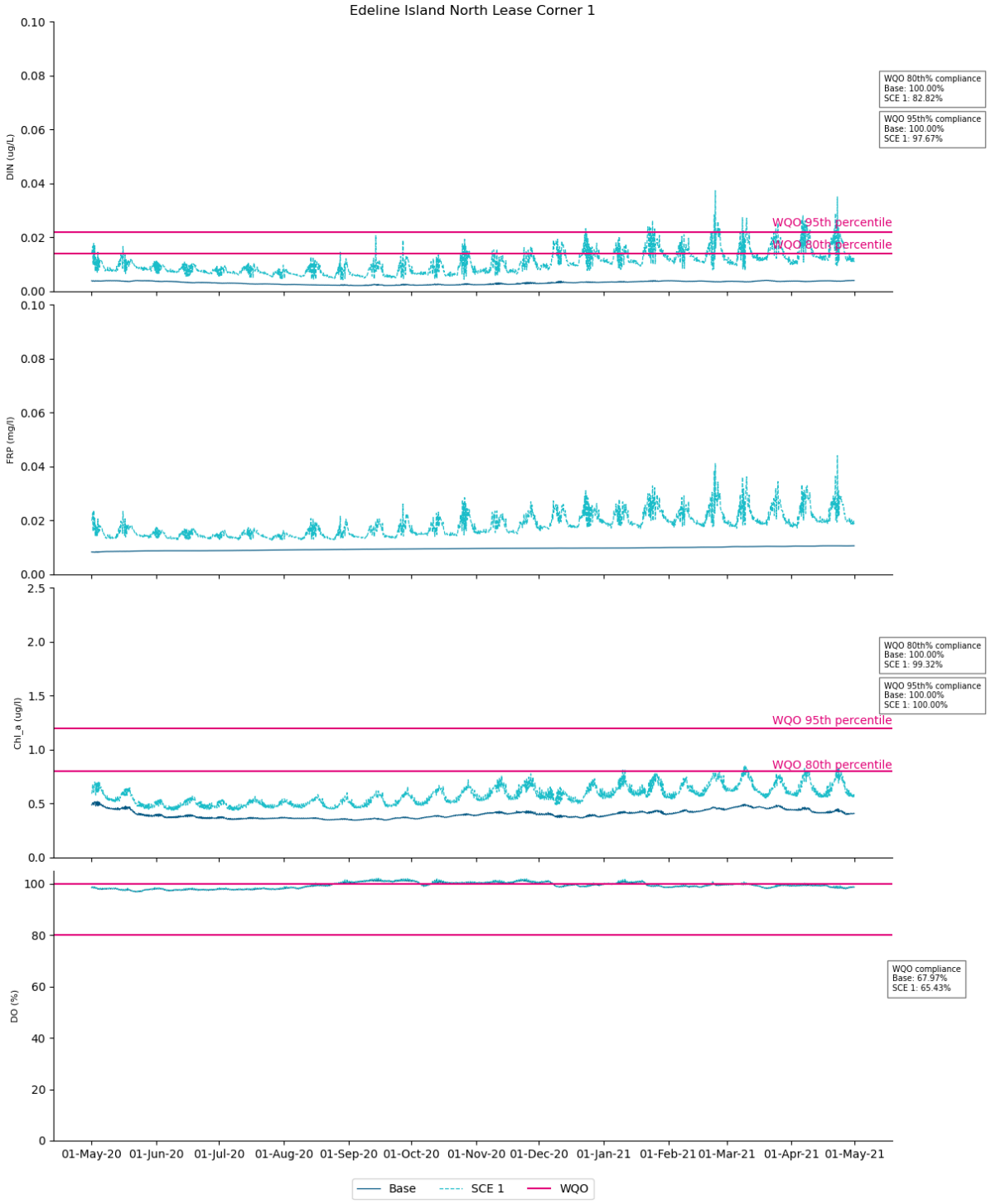

Figure 4.41 Time series of near surface concentrations of DIN, FRP, Chl-*a* and saturated DO at the edge of the site (Corner 1) around Edeline North for Scenario 1

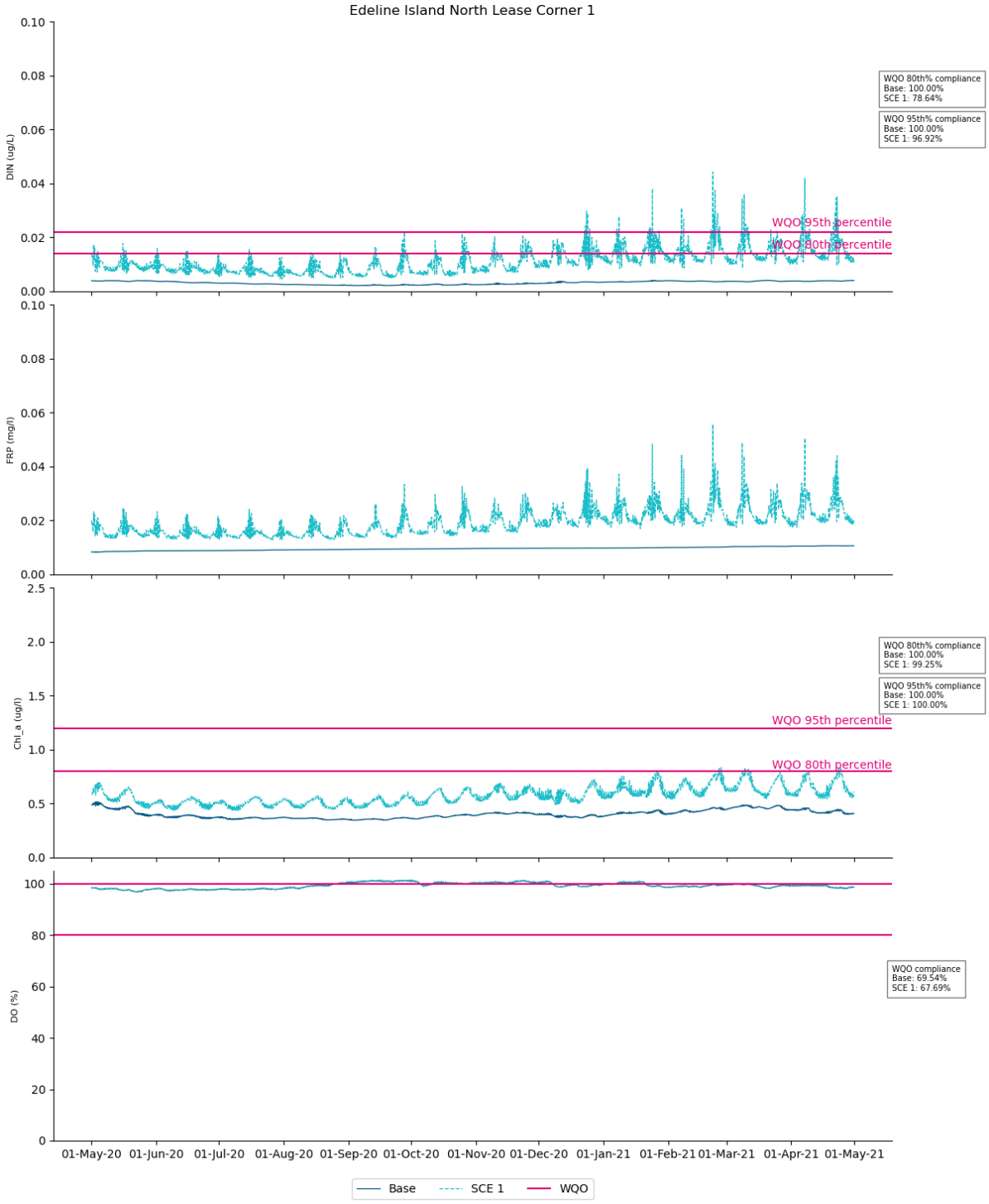

Figure 4.42 Time series of near bottom concentrations of DIN, FRP, Chl-*a* and saturated DO at the edge of the site (Corner 1) around Edeline North for Scenario 1

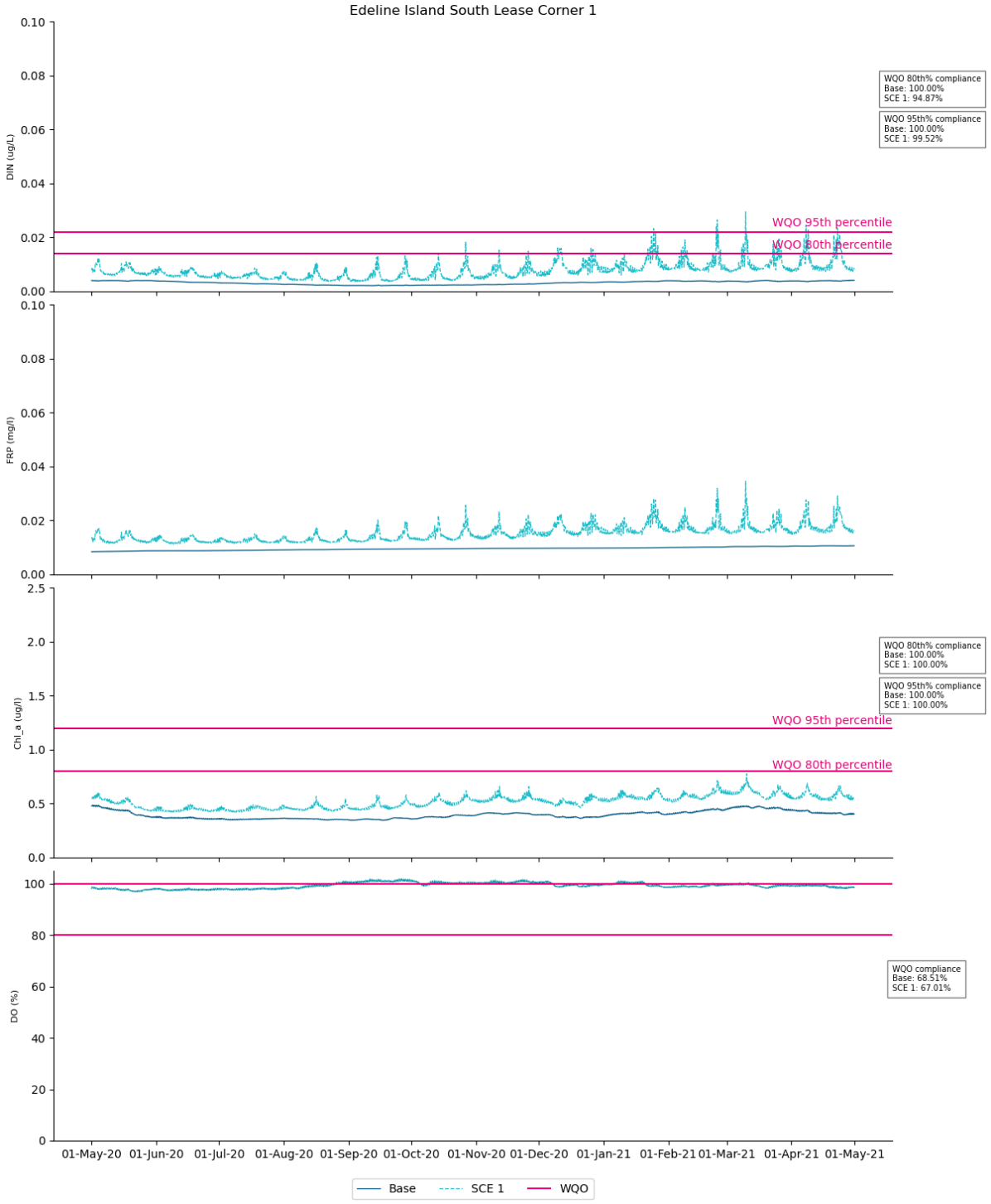

Figure 4.43 Time series of near surface concentrations of DIN, FRP, Chl-*a* and saturated DO at the edge of the site (Corner 1) around Edeline South for Scenario 1

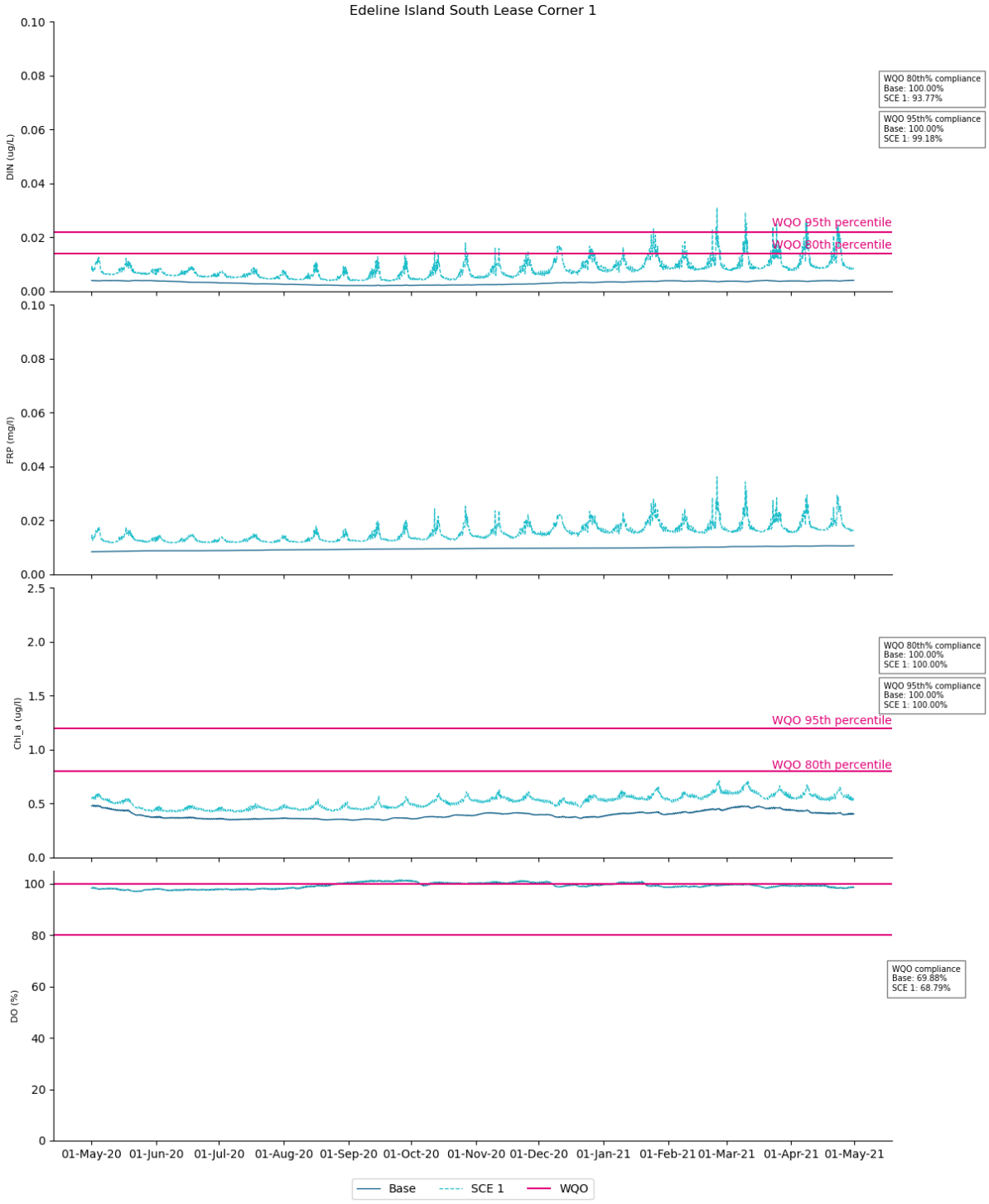

Figure 4.44 Time series of near bottom concentrations of DIN, FRP, Chl-*a* and saturated DO at the edge of the site (Corner 1) around Edeline South for Scenario 1

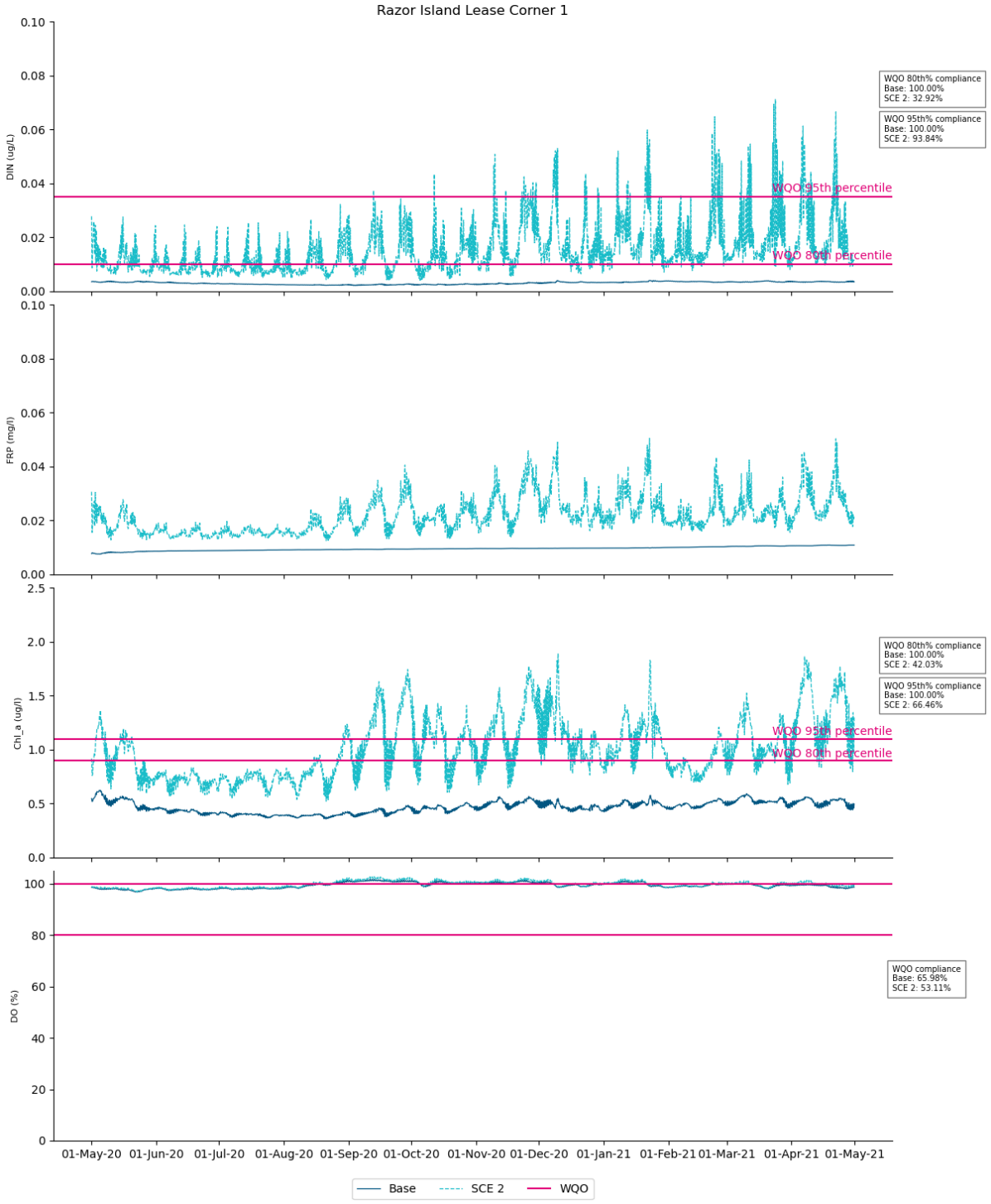

Figure 4.45 Time series of near surface concentrations of DIN, FRP, Chl-*a* and saturated DO at the edge of the site (Corner 1) around Razor Island for Scenario 2

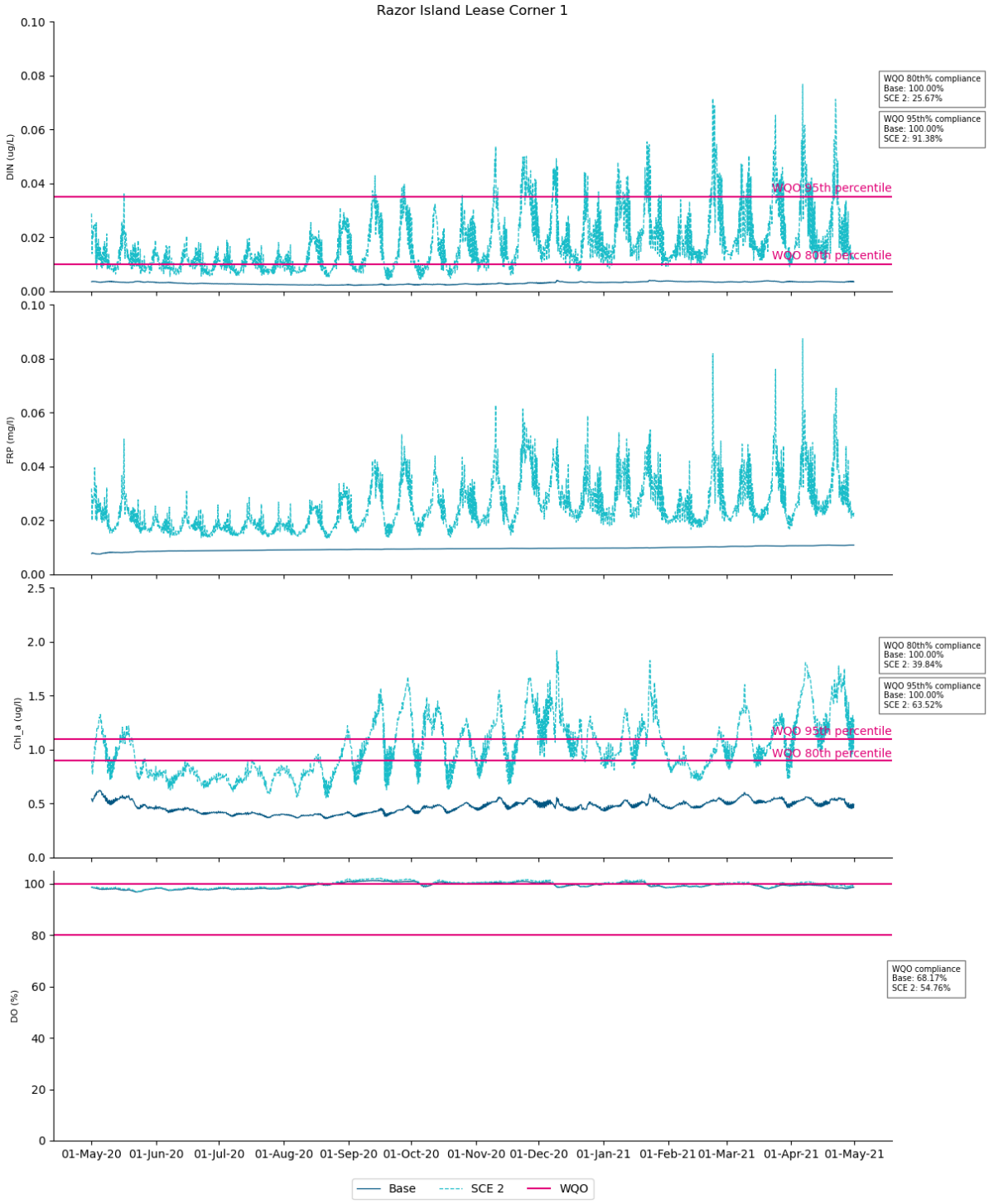

Figure 4.46 Time series of near bottom concentrations of DIN, FRP Chl-*a* and saturated DO at the edge of the site (Corner 1) around Razor Island for Scenario 2

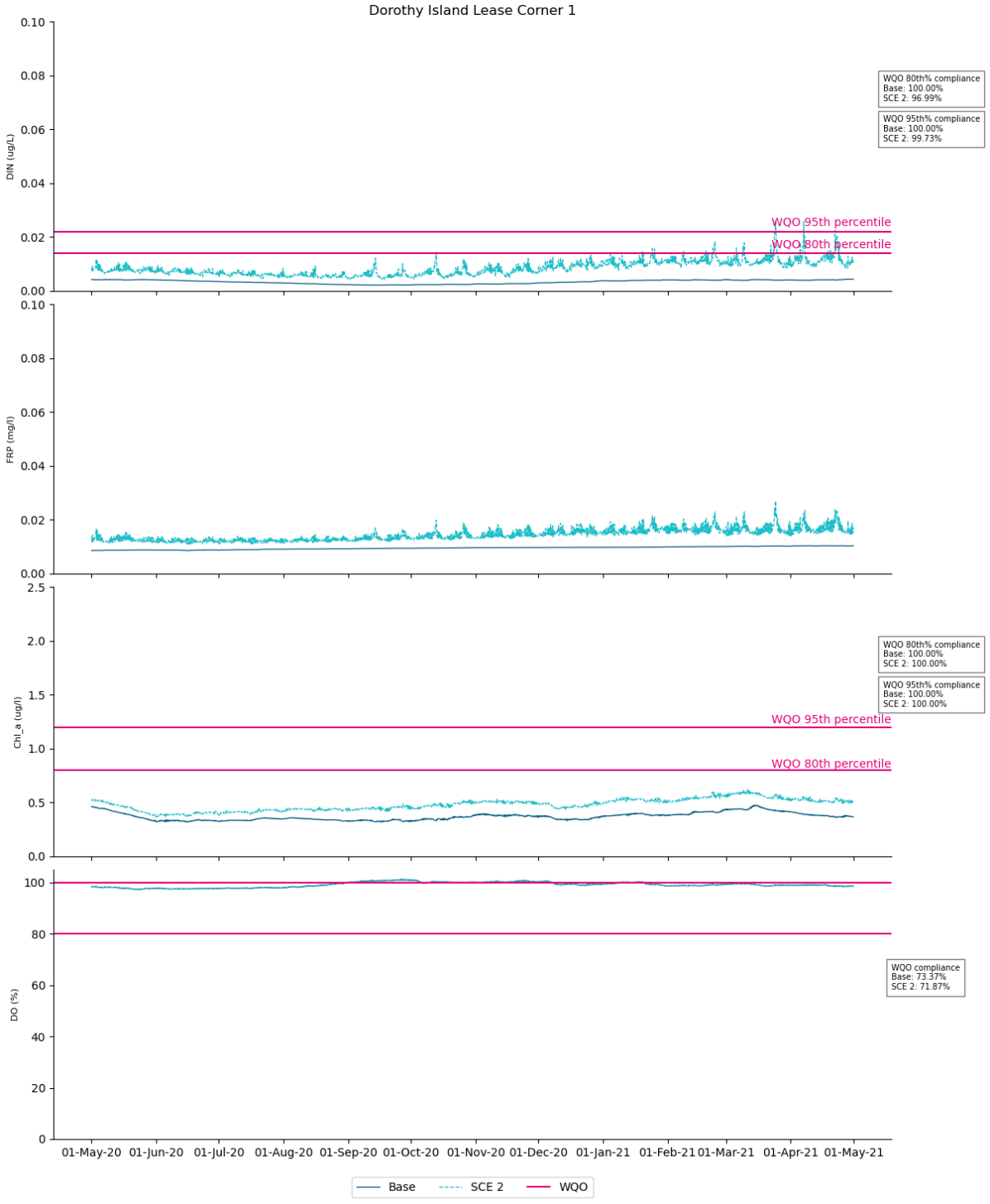

Figure 4.47 Time series of near surface concentrations of DIN, FRP Chl-*a* and saturated DO at the edge of the site (Corner 1) around Dorothy Island for Scenario 2

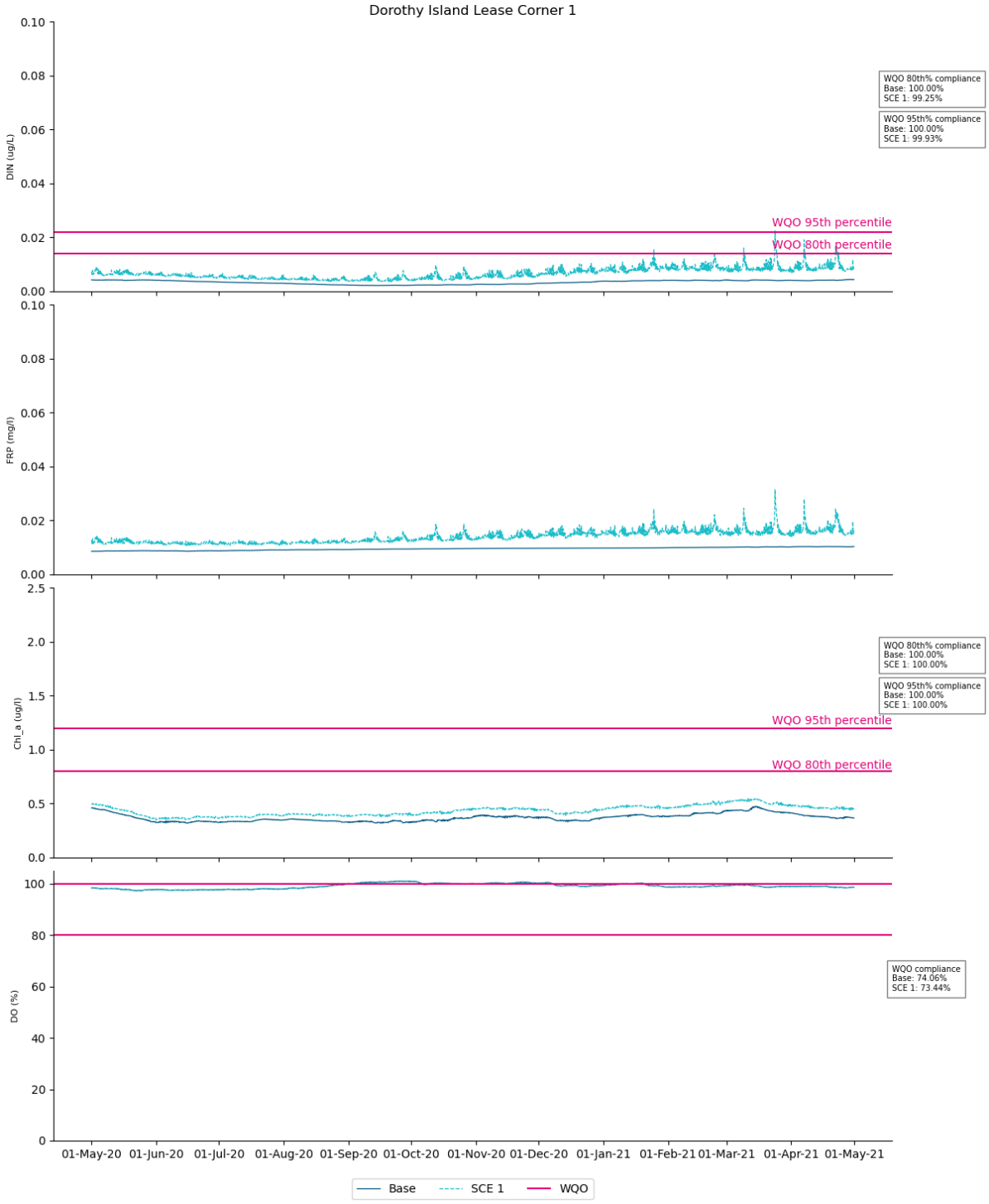

Figure 4.48 Time series of near bottom concentrations of DIN, FRP Chl-*a* and saturated DO at the edge of the site (Corner 1) around Dorothy Island for Scenario 2

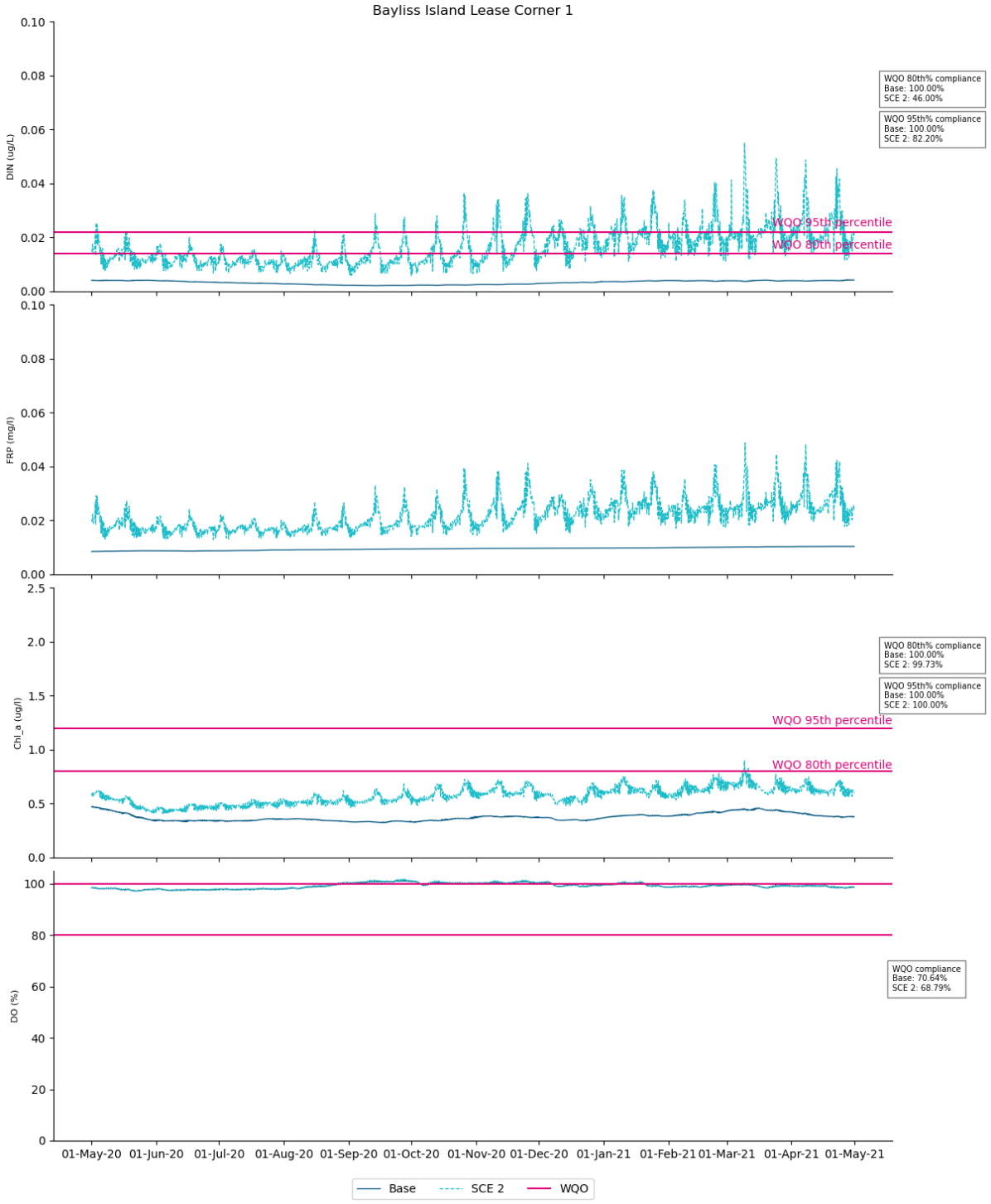

Figure 4.49 Time series of near surface concentrations of DIN, FRP Chl-*a* and saturated DO at the edge of the site (Corner 1) around Bayliss Island for Scenario 2

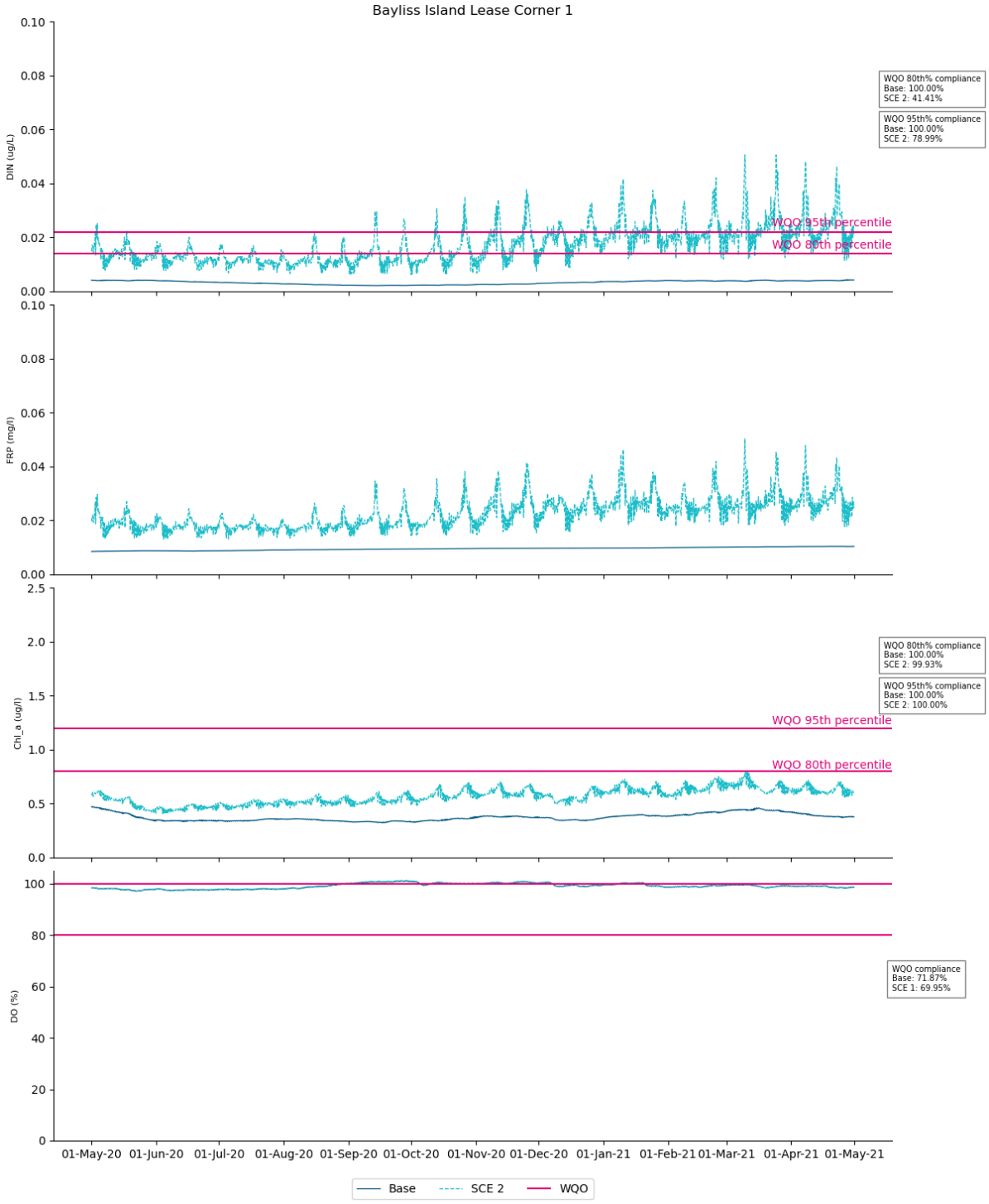

Figure 4.50 Time series of near bottom concentrations of DIN, FRP Chl-*a* and saturated DO at the edge of the site (Corner 1) around Bayliss Island for Scenario 2

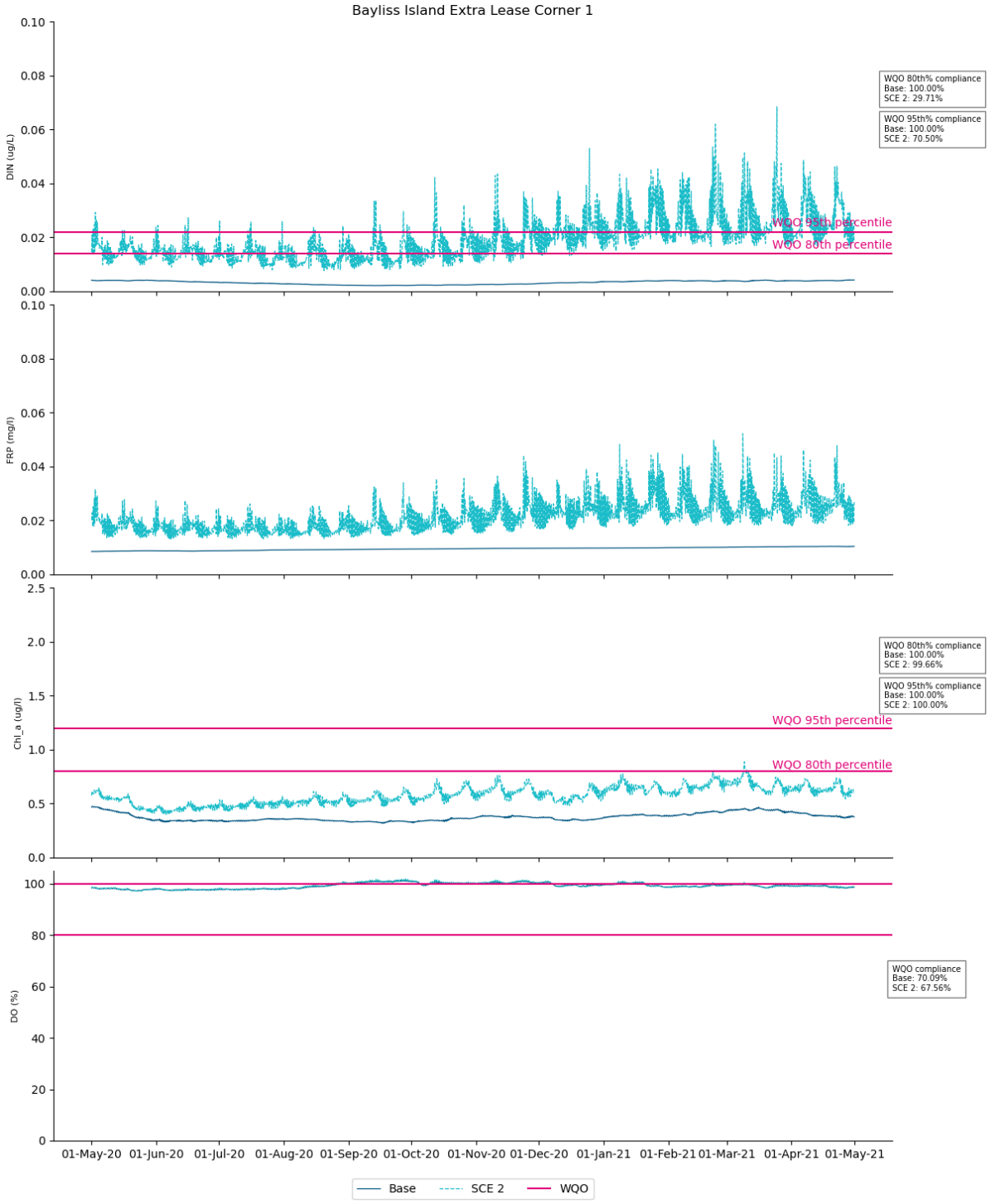

Figure 4.51 Time series of near surface concentrations of DIN, FRP Chl-*a* and saturated DO at the edge of the site (Corner 1) around Bayliss Extra for Scenario 2

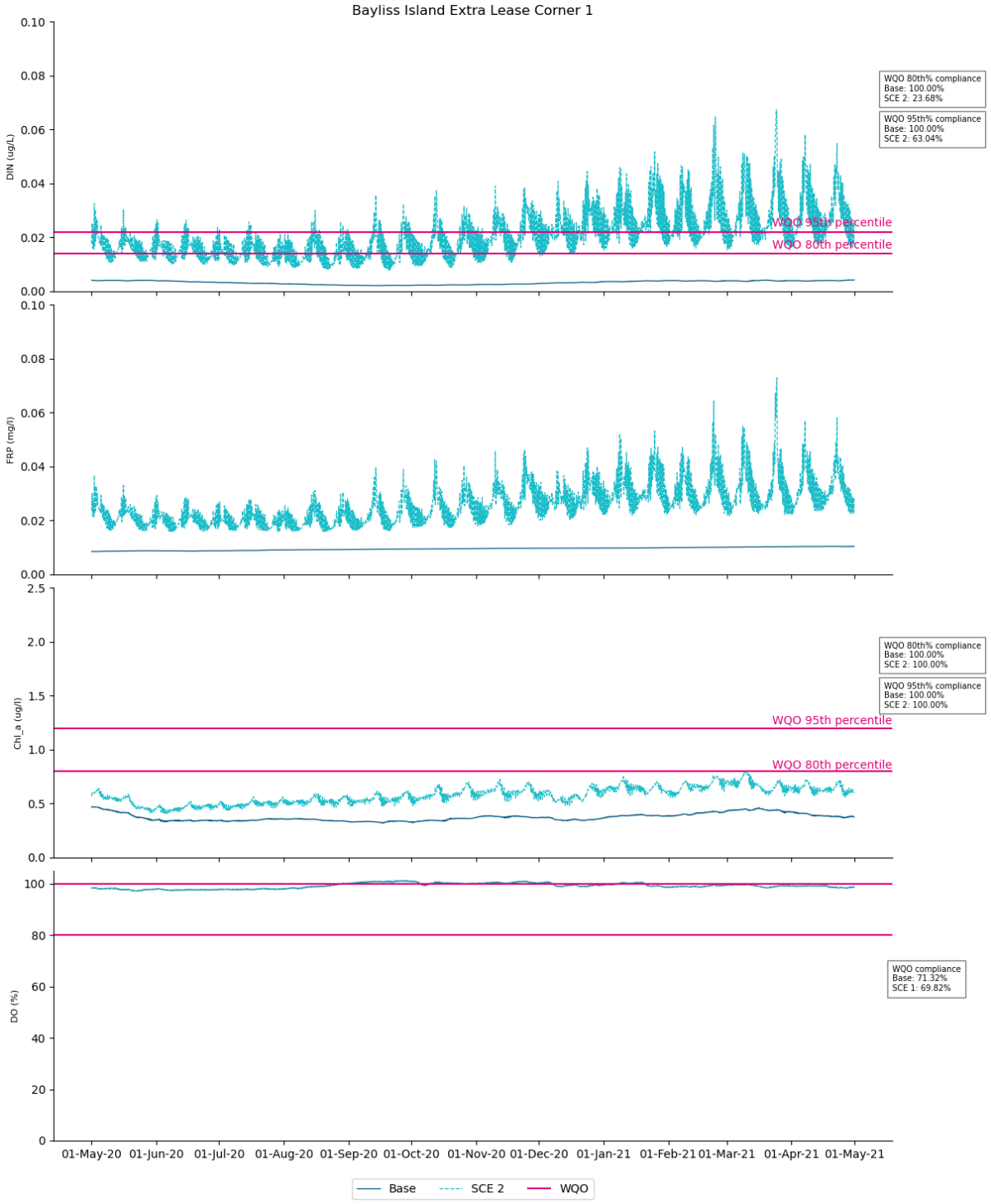

Figure 4.52 Time series of near bottom concentrations of DIN, FRP Chl-*a* and saturated DO at the edge of the site (Corner 1) around Bayliss Extra for Scenario 2

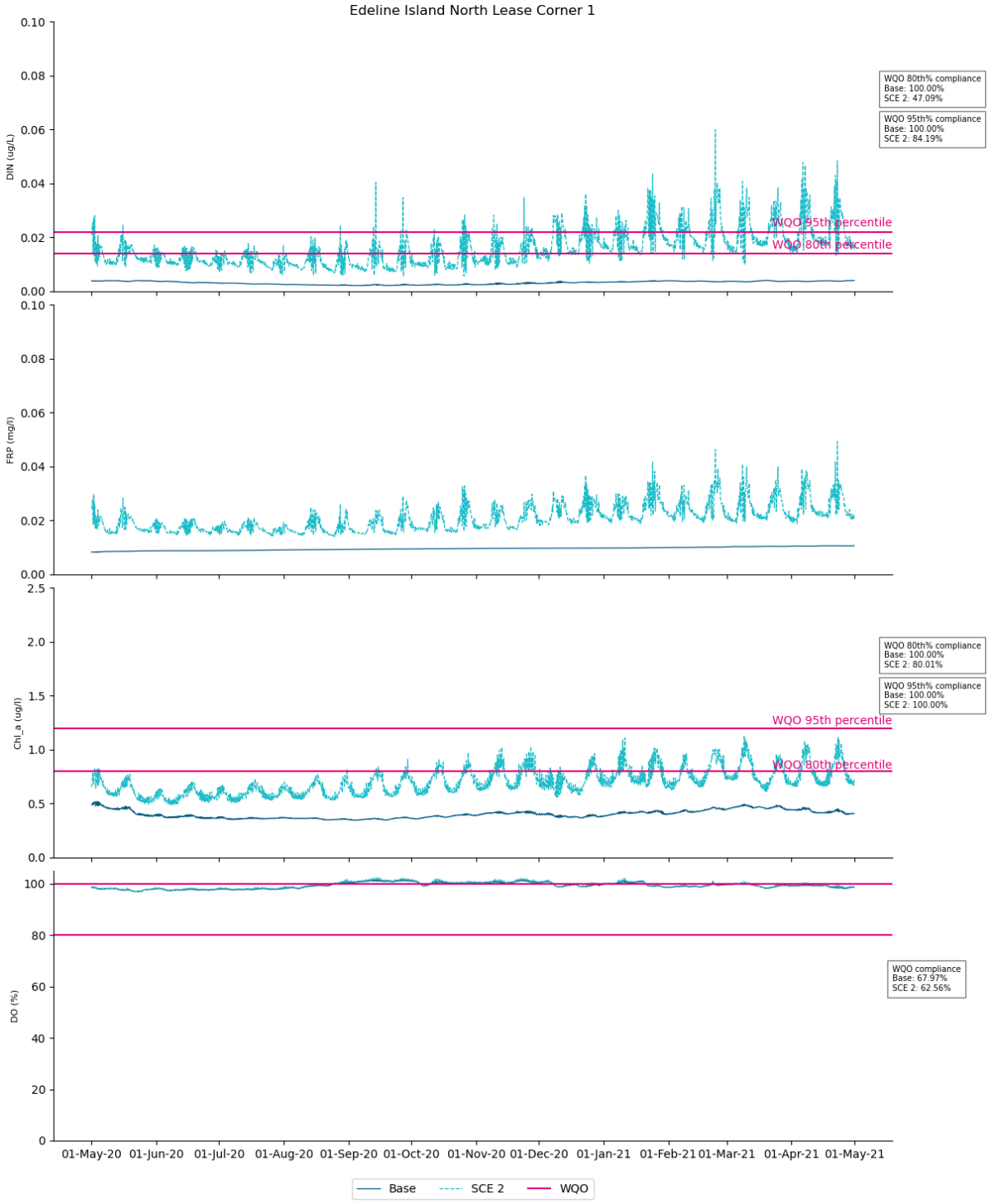

Figure 4.53 Time series of near surface concentrations of DIN, FRP Chl-*a* and saturated DO at the edge of the site (Corner 1) around Edeline North for Scenario 2

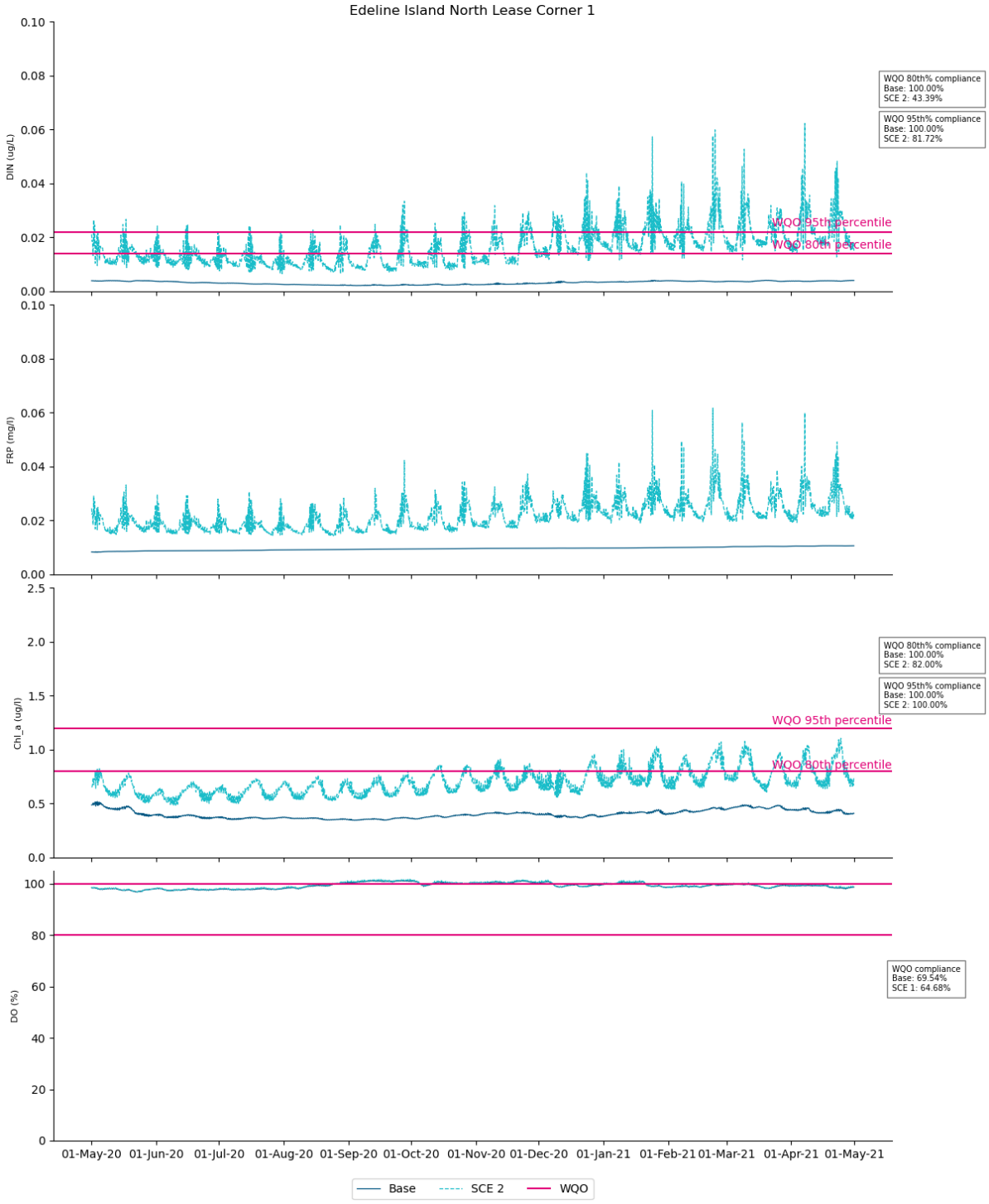

Figure 4.54 Time series of near bottom concentrations of DIN, FRP Chl-*a* and saturated DO at the edge of the site (Corner 1) around Edeline North for Scenario 2

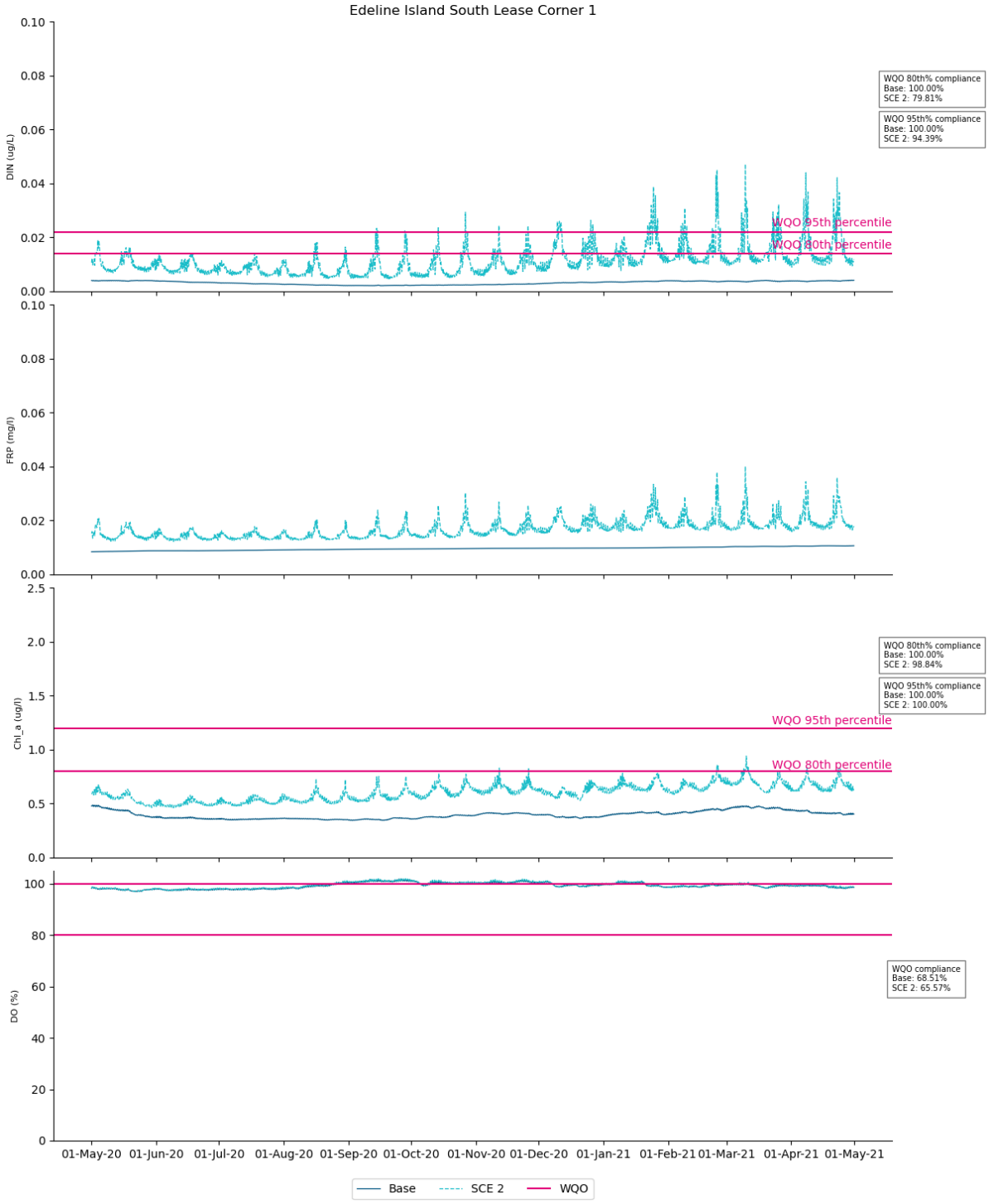

Figure 4.55 Time series of near surface concentrations of DIN, FRP Chl-*a* and saturated DO at the edge of the site (Corner 1) around Edeline South for Scenario 2

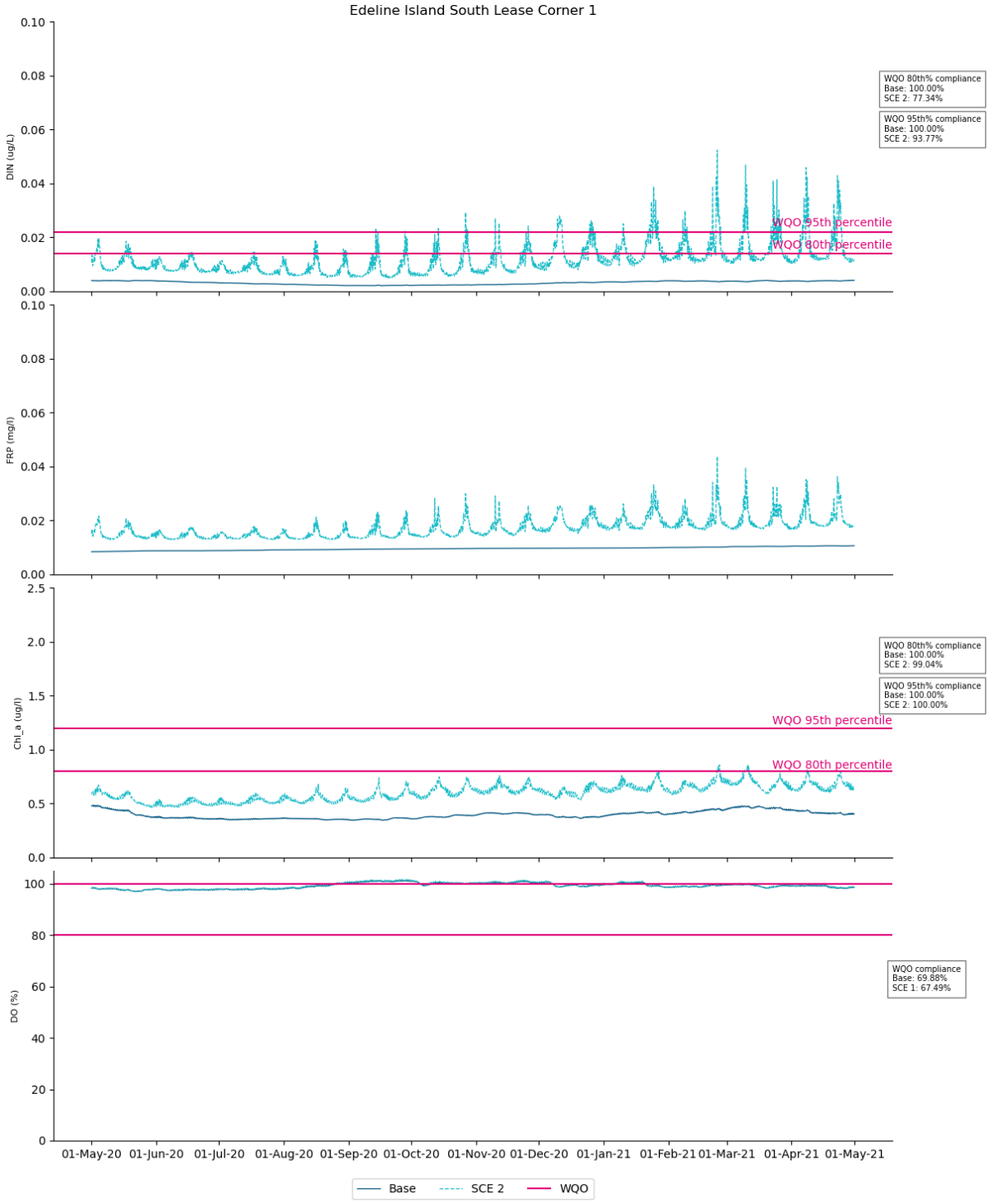

Figure 4.56 Time series of near bottom concentrations of DIN, FRP Chl-*a* and saturated DO at the edge of the site (Corner 1) around Edeline South for Scenario 2.

4.4.6 Total suspended solids, photosynthetically active radiation and daily light integrals

Modelled time series plots for total suspended solids (TSS), photosynthetically active radiation (PAR), and daily light integral (DLI) were produced for January 2021 (representing the wet season) and August 2021 (representing the dry season) at selected corner sites (Corner 1 and Corner 2) across all sites for Scenario 1. The top plot shows TSS in mg/L, the middle plot shows PAR in W/m², and the bottom plot shows DLI in mol-photons/m²/day. Refer to Figure 4.57 to Figure 4.63 for plots of TSS, PAR, and DLI for Scenario 1 compared to the base model during the wet season, and Figure 4.70 to Figure 4.64 for Scenario 1 during the dry season in August.

- In January, TSS values range from 15 to 25 mg/L, higher than the 10 to 15 mg/L observed in August. Measured data collected from February to April 2022 indicate TSS ranges from 20 to 30 mg/L across the site s. Dispersive leases such as Bayliss, Bayliss Extra and Dorothy show slightly lower TSS compared to other leases. The higher TSS during the summer wet season may be attributed to inputs from three rivers as well as resuspension dynamics.

- PAR exhibits a diurnal pattern, peaking midday. PAR levels depend on light attenuation, influenced by water depth, TSS, and local hydrodynamics. Diurnal maximum PAR can reach up to 100 W/m² at some sites (e.g., Edeline South), while others (e.g., Razor) may not exceed 50 W/m².

- DLI is calculated based on PAR values modelled at 6-hour intervals (Apogee Instruments 2016, 2024; DES 2018). DLI ranges from 2 to 4 mol-photons/m²/day, depending on PAR levels. DLI represents the total amount of photosynthetically active radiation (PAR) received over a day, and values can vary widely depending on factors such as water clarity, depth, and turbidity.

- DLI values were typically higher during the summer months compared to the winter months. In a study conducted in Onslow, Western Australia, mean surface DLI values ranged from 3.2 to 4.5 mol/m²/day in summer and from 0.8 to 1.3 mol/m²/day in winter (O2Marine, 2021). Another study reported low DLI concentrations in nearshore waters in North-western Australia, with values below the threshold of 0.9 mol/m²/day designated for *Halophila ovalis* seagrass communities (Strydom et al. 2017). Despite the sensitivity of seagrass to changes in light quality, natural and anthropogenic changes may not always have strong effects on *H. ovalis* growth. In Kimberly nearshore waters, similar DLI ranges were observed for summer in the base case model, while winter values were slightly higher than those recorded in the Onslow study. Typically, in turbid, deeper coastal waters, DLI values can range from 2 to 10 mol/m²/day (Falkowski & Raven, 2013) depending on the extent of light attenuation caused by suspended particles, water depth, and other factors.

- Given these typical ranges, DLI values of 2-4 mol/m²/day at Kimberly leases suggest relatively high light attenuation. This implies that the water may be turbid with substantial suspended particles (as indicated by the high TSS values), which reduces the amount of light that penetrates through the water column. While these DLI values are on the lower end compared to clearer coastal waters, they still provide sufficient light for photosynthetic organisms, albeit at reduced efficiency. The scenario runs didn't show any substantial difference form the base model for the selected model periods.

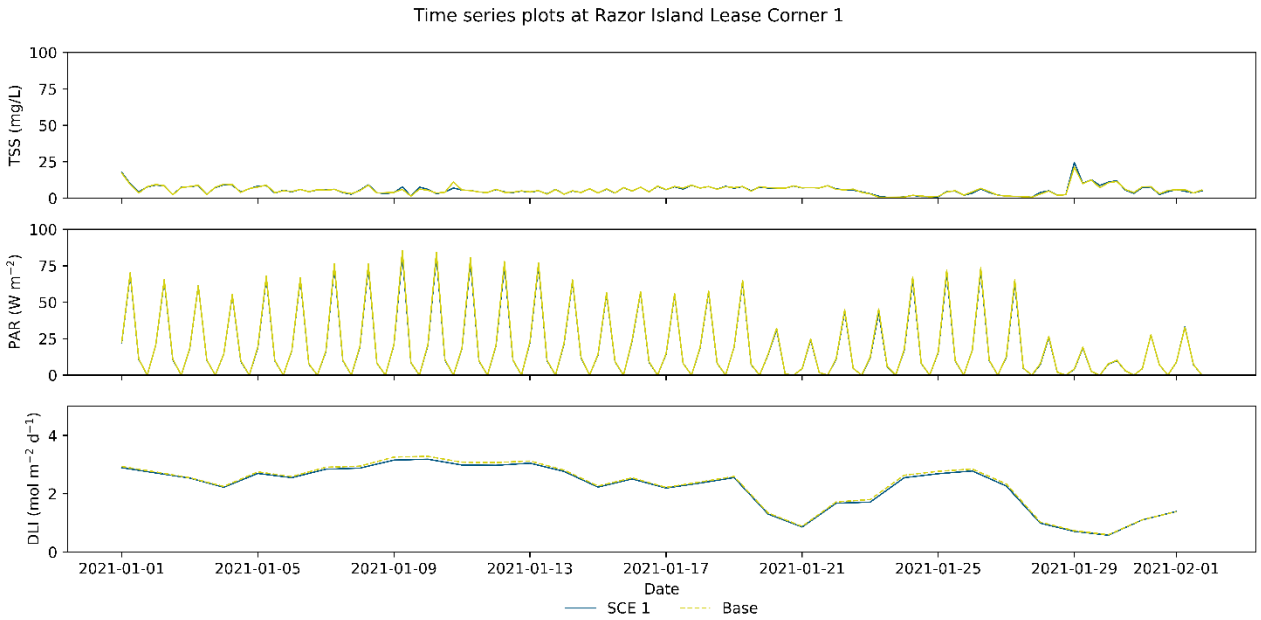

Figure 4.57 Modelled TSS (top), PAR (middle) and DLI (bottom) at Razor Island corner 1 site for the base case and Scenario 1 during January 2021 (summer)

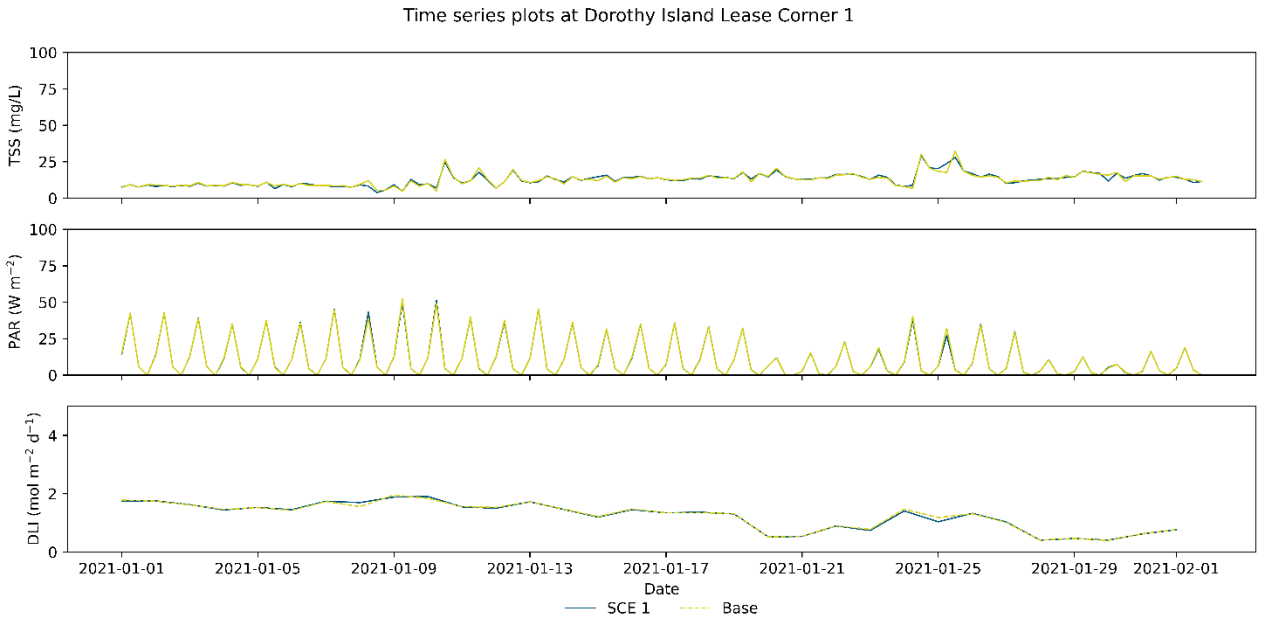

Figure 4.58 Modelled TSS (top), PAR (middle) and DLI (bottom) at Dorothy Island corner 1 site for the base case and Scenario 1 during January 2021 (summer)

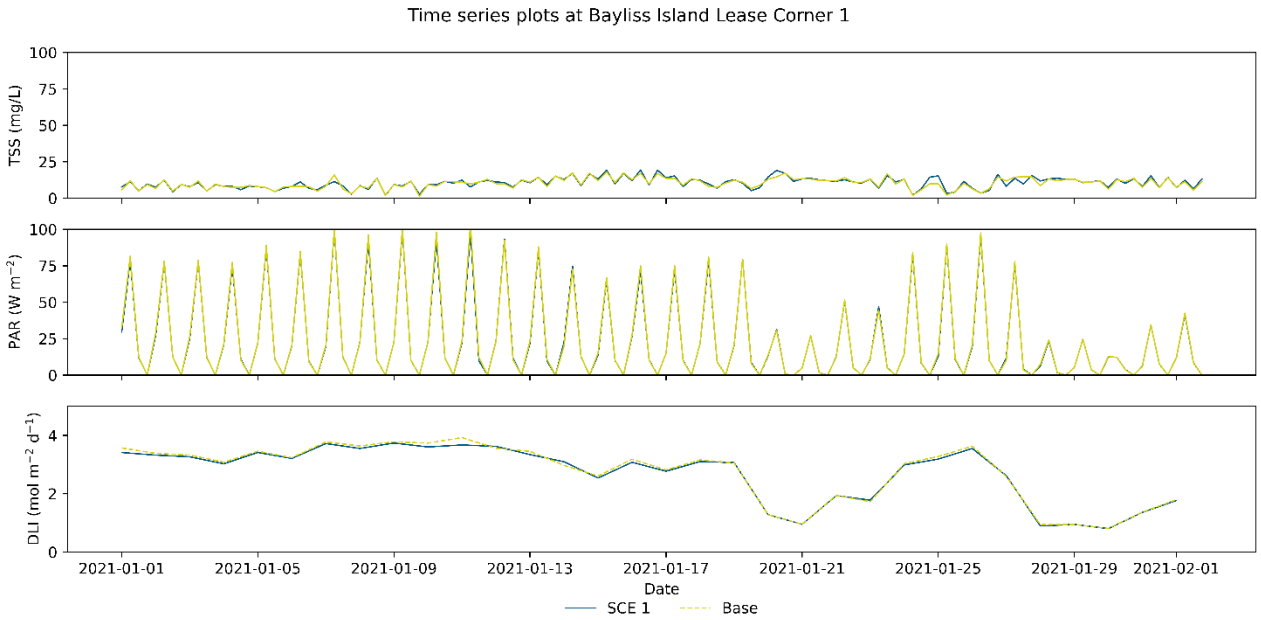

Figure 4.59 Modelled TSS (top), PAR (middle) and DLI (bottom) at Baylis Island corner 1 site for the base case and Scenario 1 during January 2021 (summer)

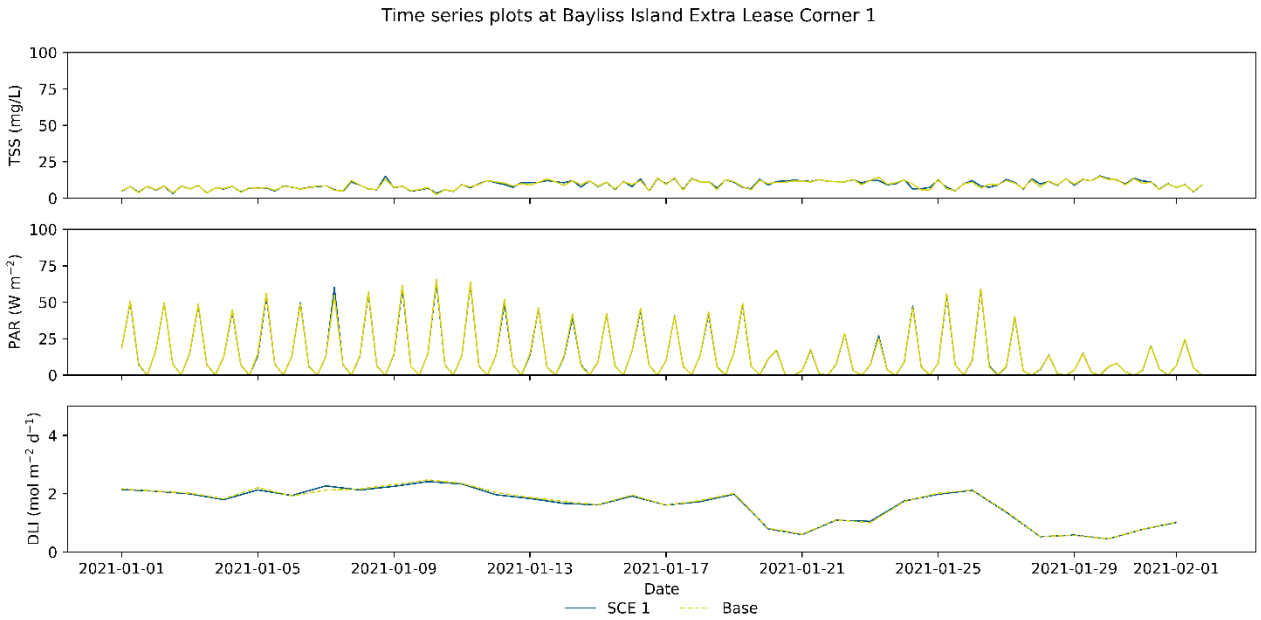

Figure 4.60 Modelled TSS (top), PAR (middle) and DLI (bottom) at Bayliss Extra corner 1 site for the base case and Scenario 1 during January 2021 (summer)

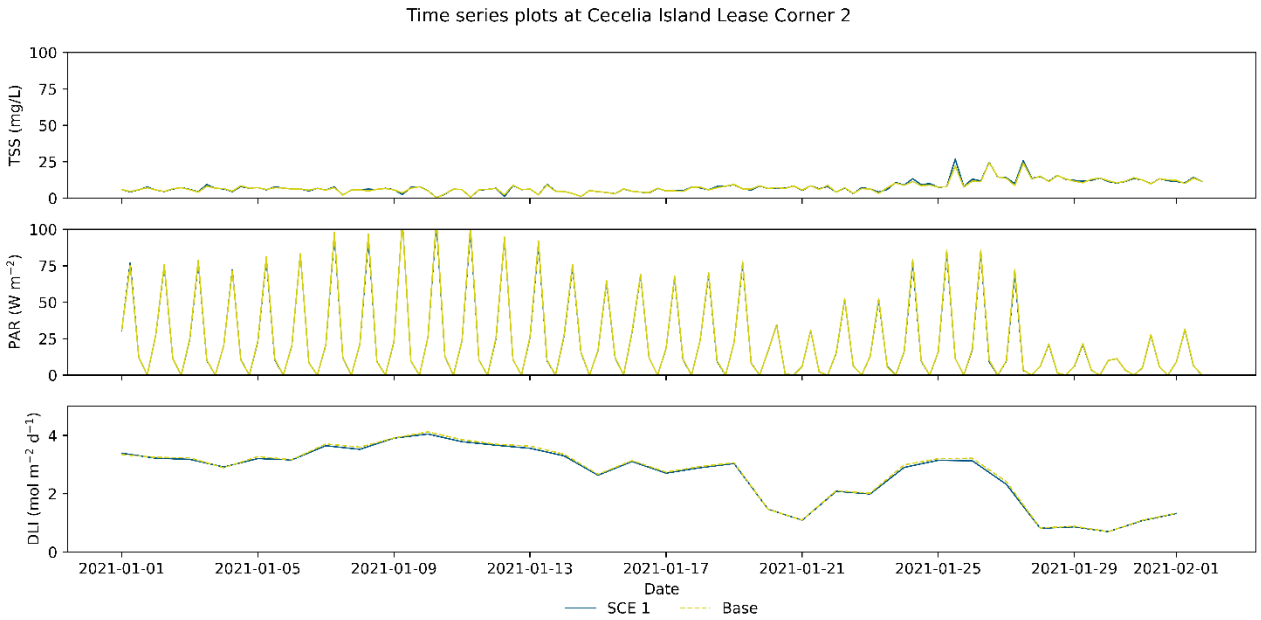

Figure 4.61 Modelled TSS (top), PAR (middle) and DLI (bottom) at Cecelia Island corner 2 site for the base case and Scenario 1 during January 2021 (summer)

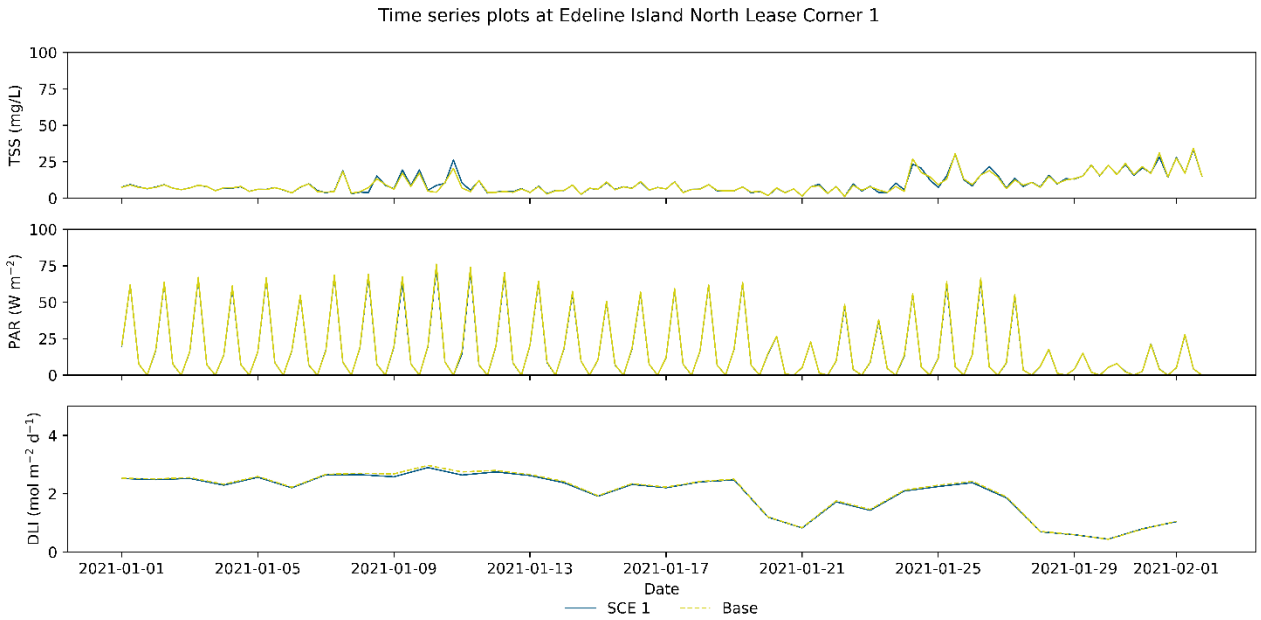

Figure 4.62 Modelled TSS (top), PAR (middle) and DLI (bottom) at Edeline North corner 1 site for the base case and Scenario 1 during January 2021 (summer)

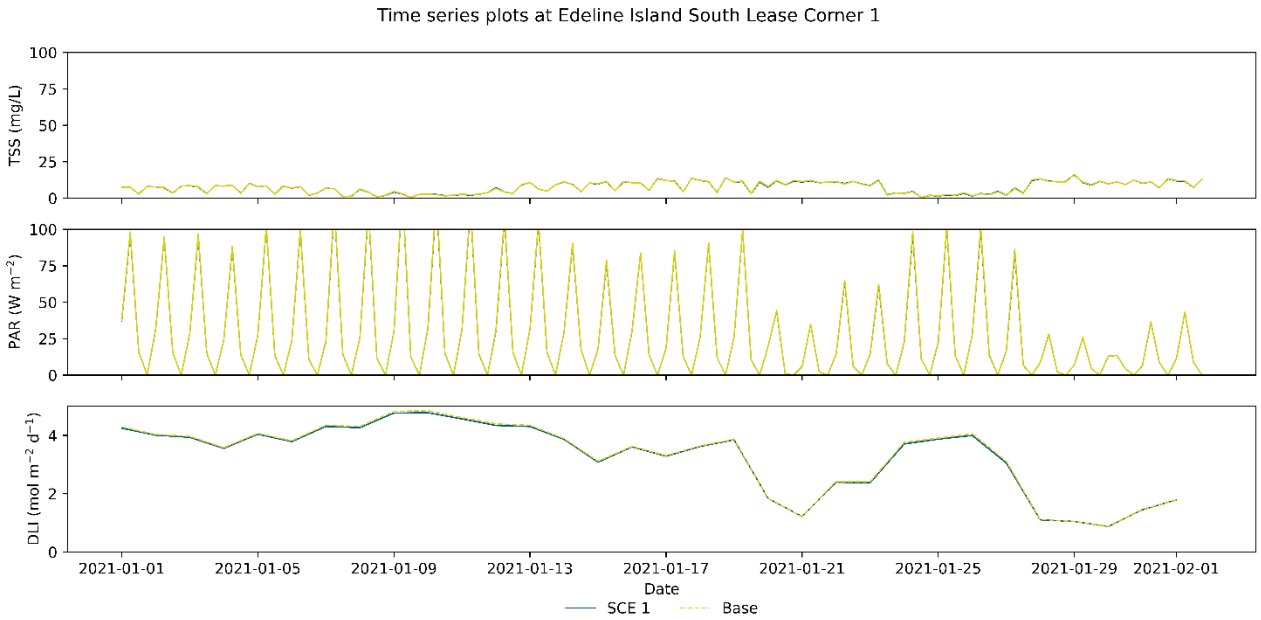

Figure 4.63 Modelled TSS (top), PAR (middle) and DLI (bottom) at Edeline South corner 1 site for the base case and Scenario 1 during January 2021 (summer)

Figure 4.64 Modelled TSS (top), PAR (middle) and DLI (bottom) at Razor Island corner 1 site for the base case and Scenario 1 during August 2021 (winter)

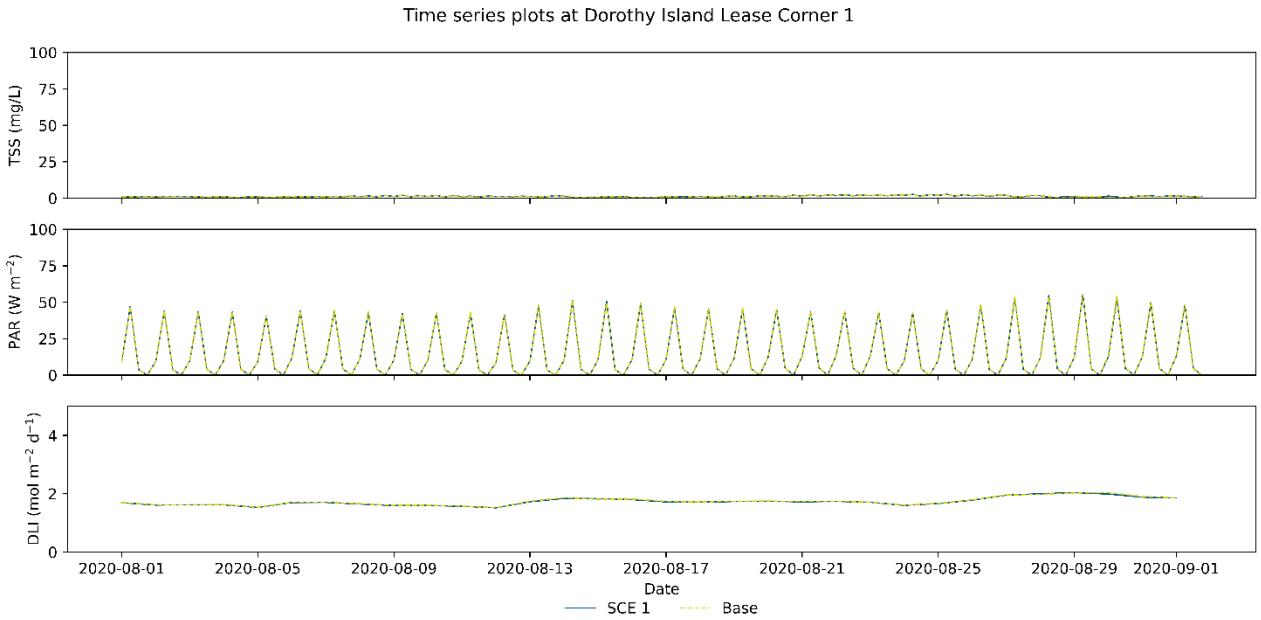

Figure 4.65 Modelled TSS (top), PAR (middle) and DLI (bottom) at Dorothy Island corner 1 site for the base case and Scenario 1 during August 2021 (winter)

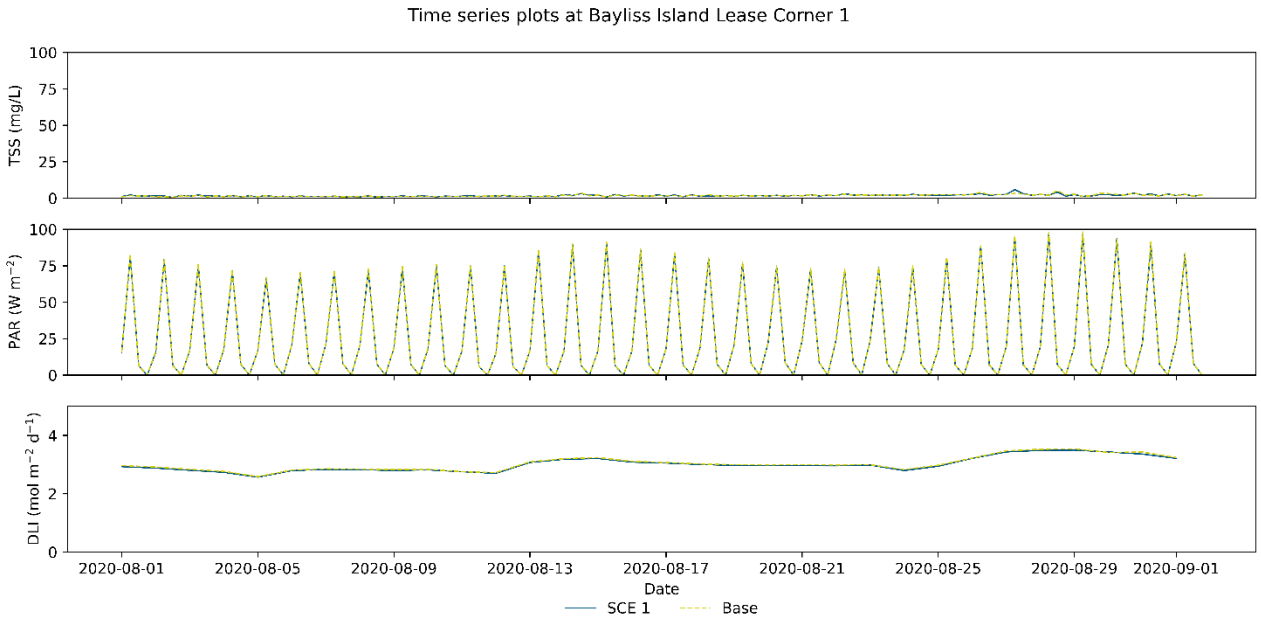

Figure 4.66 Modelled TSS (top), PAR (middle) and DLI (bottom) at Baylis Island corner 1 site for the base case and Scenario 1 during August 2021 (winter)

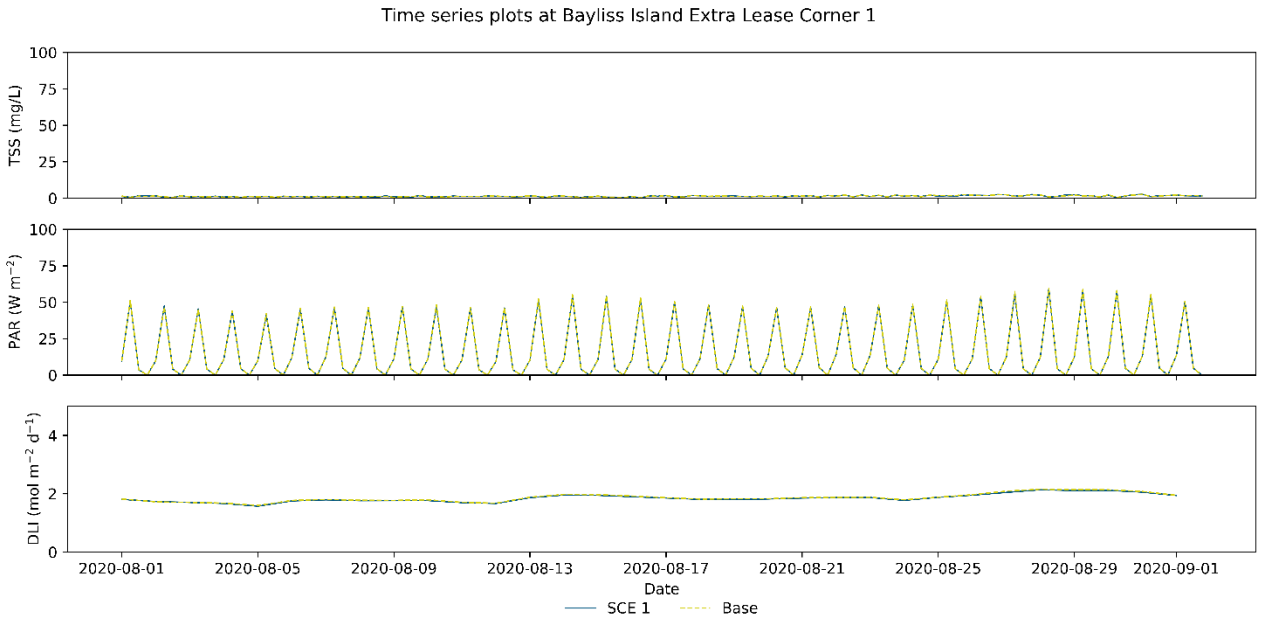

Figure 4.67 Modelled TSS (top), PAR (middle) and DLI (bottom) at Bayliss Extra corner 1 site for the base case and Scenario 1 during August 2021 (winter)

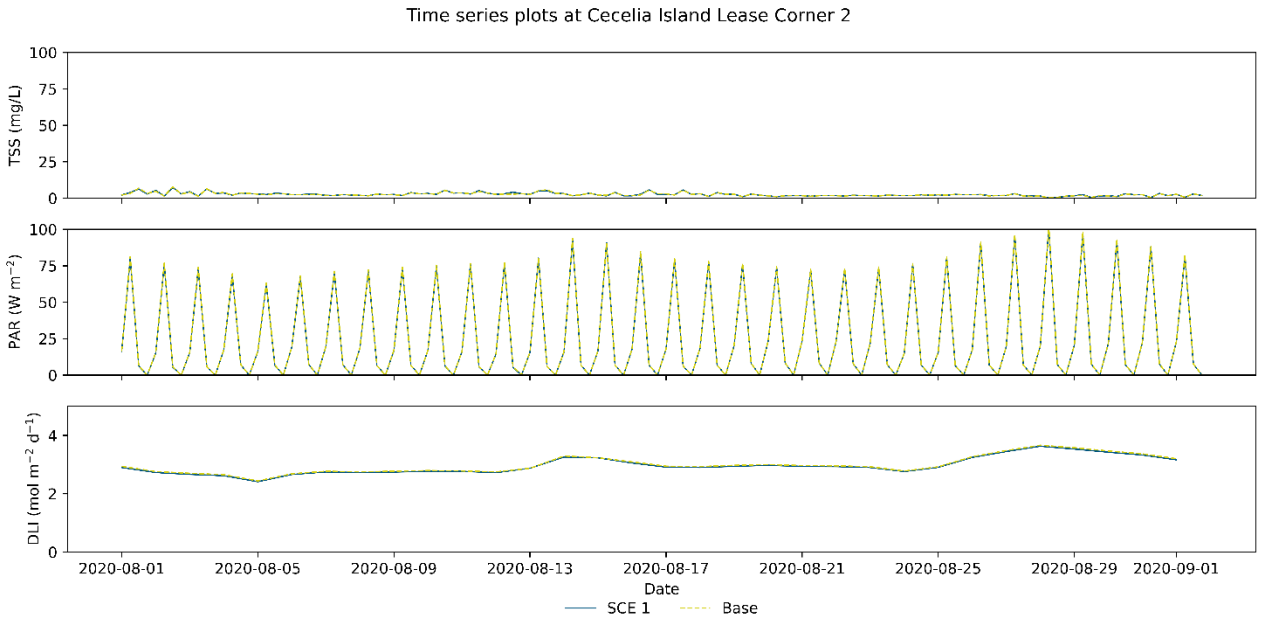

Figure 4.68 Modelled TSS (top), PAR (middle) and DLI (bottom) at Cecelia Island corner 2 site for the base case and Scenario 1 during August 2021 (winter)

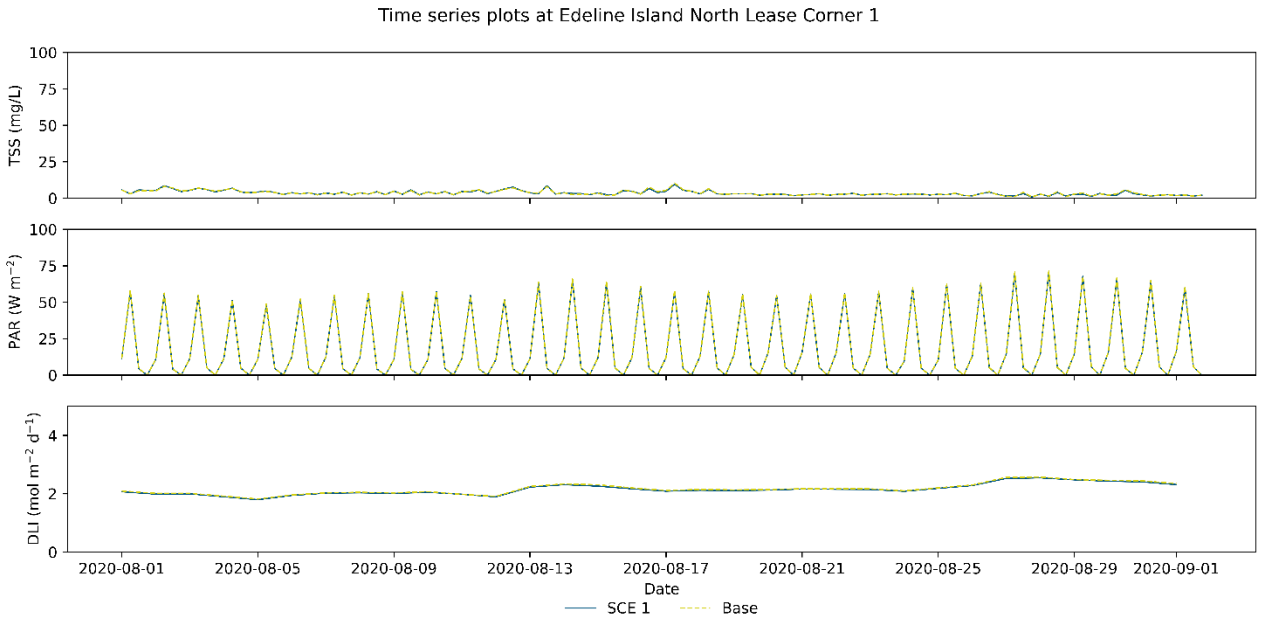

Figure 4.69 Modelled TSS (top), PAR (middle) and DLI (bottom) at Edeline North corner 1 site for the base case and Scenario 1 during August 2021 (winter)

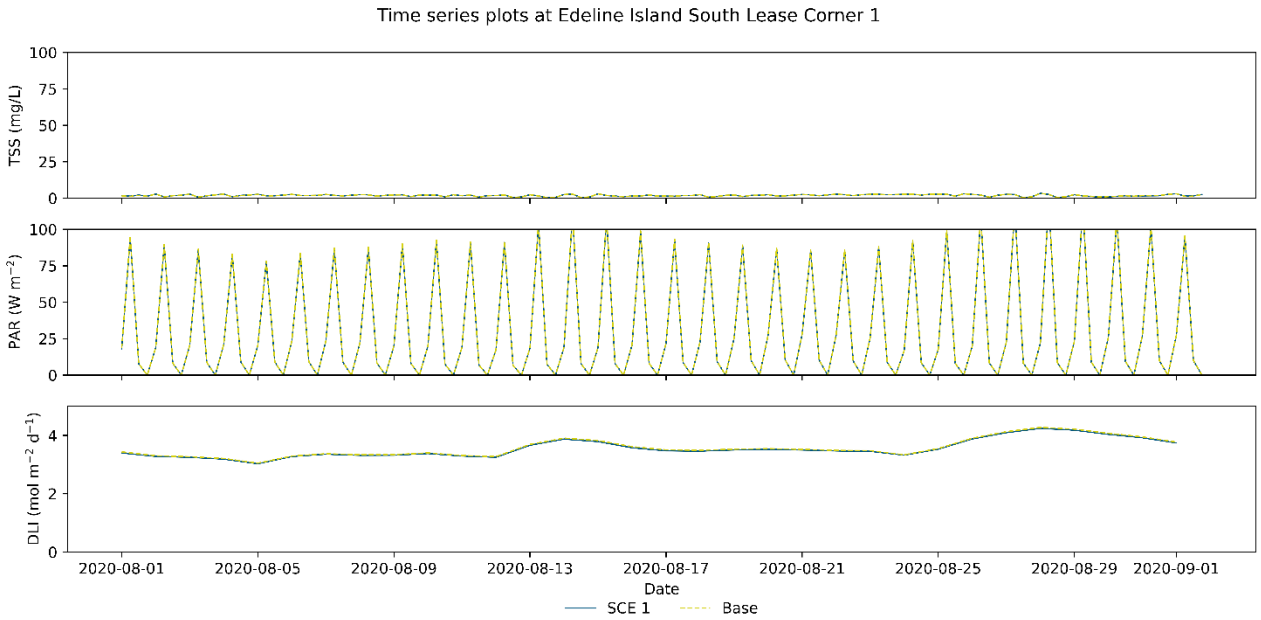

Figure 4.70 Modelled TSS (top), PAR (middle) and DLI (bottom) at Edeline South corner 1 site for the base case and Scenario 1 during August 2021 (winter)

4.5 Sediment Quality

4.5.1 Deposition footprint

Waste deposition footprints were mapped as waste accumulation per square meter over a 12-month period or waste area density (g/m^2/year). A regional view of the waste deposition footprints for Scenario 1 (Figure 4.71) and Scenario 2 (Figure 4.72) depicts the influence of local hydrodynamics on the dispersion of particulate waste.

Most particulate wastes were projected to be deposited within the leases by the end of the 12-month simulation. Projections of waste deposition on the seabed for incremental biomass operational scenarios indicate that lower FCRs lead to lower footprints compared to higher FCRs.

After 12 months, the maximum density directly beneath the pen was estimated to be just above 20,000 g/m^2/year. However, the areas where sediment deposition exceeded 20,000 g/m^2/year were minimal. Significant smothering impacts occur when sediment deposition surpasses 20 mg/cm^2/day at any point during the modelled period. The deposition footprint of 20,000 g/m^2/year corresponds to approximately 5.48 mg/cm^2/day. Under this impact assessment, the waste deposition footprint is expected to remain below the smothering threshold levels for both scenarios.

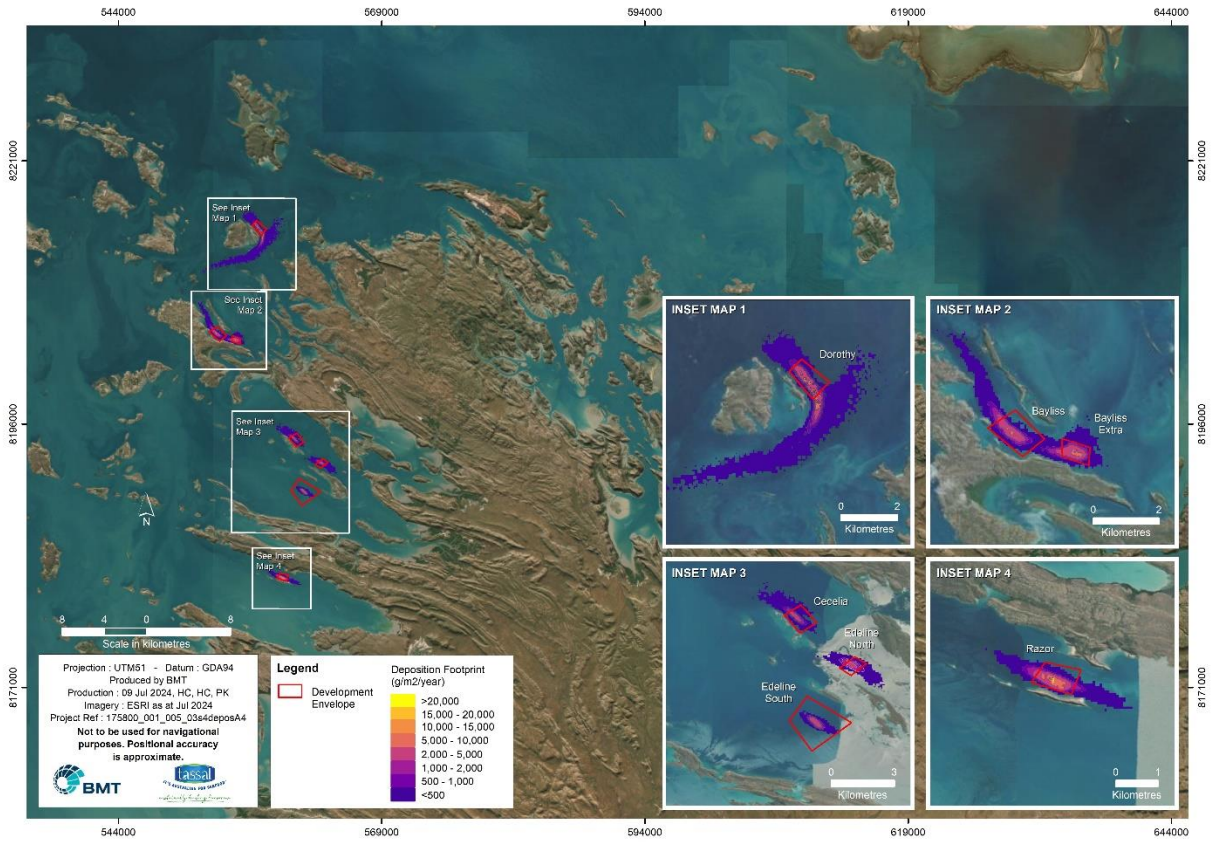

Figure 4.71 Waste deposition footprint (g/m^2/year) after 12 months of simulation at seven proposed farm locations for Scenario 1 (FCR 1.5).

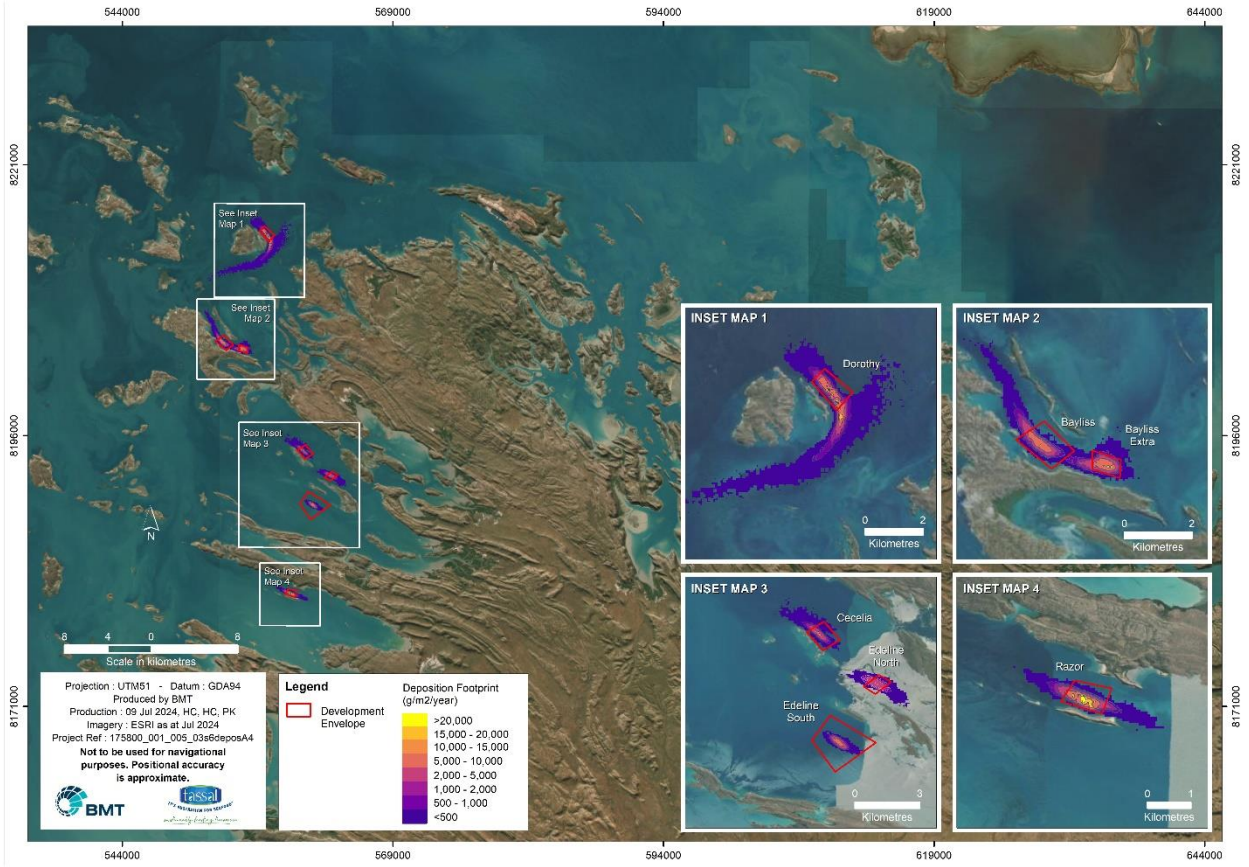

Figure 4.72 Waste deposition footprint (g/m^2/year) after 12 months of simulation at seven proposed farm locations for Scenario 2 (FCR 2.3).

4.5.2 Soft sediments (dissolved oxygen and sulphide content)

Figure 4.73 to Figure 4.77 show the projected extent of changes to dissolved oxygen and sulphide content in soft sediments as a result of deposition from the finfish pens; after one, two and five years of continuous (i.e. assuming no fallowing) operations respectively. Major increases in hydrogen sulphide content and subsequent decreases in dissolved oxygen content are generally only projected to occur directly beneath the sea-pens. Some moderate changes are predicted at the edges of the proposed limits and beyond for a subset of the leases. This is particularly the case for those leases which are situated in areas of significant hydrodynamic flushing, such as Dorothy Island or Bayliss Islands, where depositional material will be distributed over a large area.

For the most part, the predicted extent of impacts does not change substantially between one and two years of operations, with only small changes in the extent of impacts predicted after operations for five years.

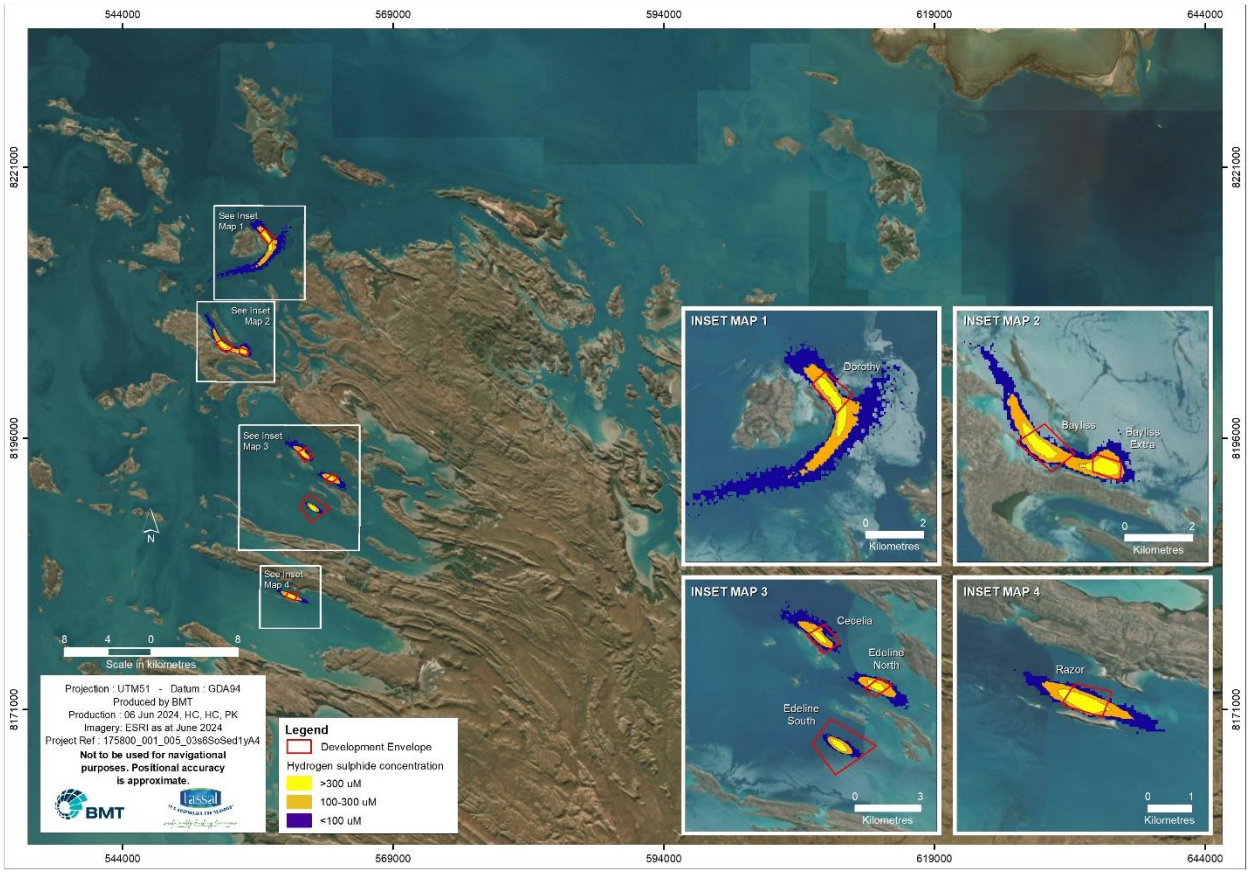

Figure 4.73 Soft sediment impact footprints after 1 year of operations under Scenario 1.

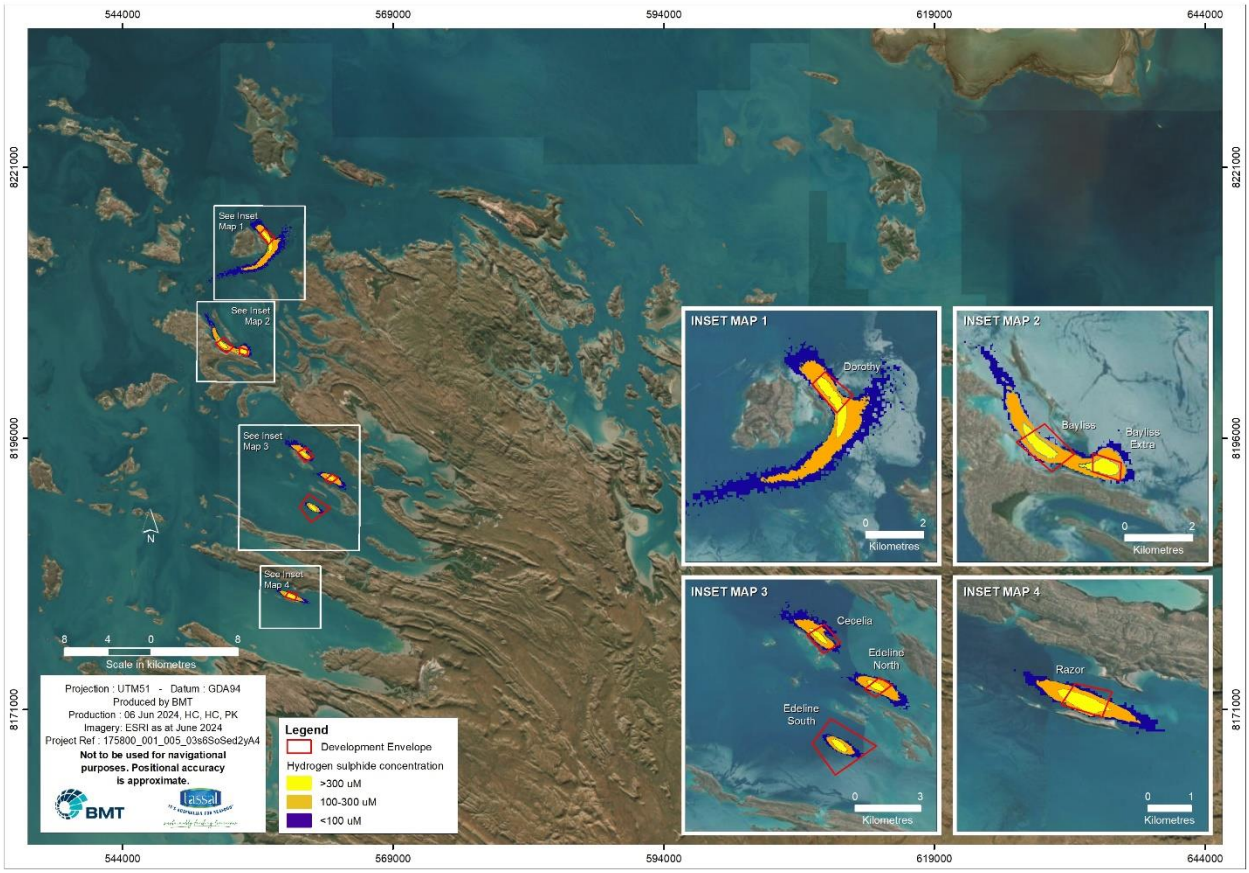

Figure 4.74 Soft sediment impact footprints after 2 years of operations under Scenario 1.

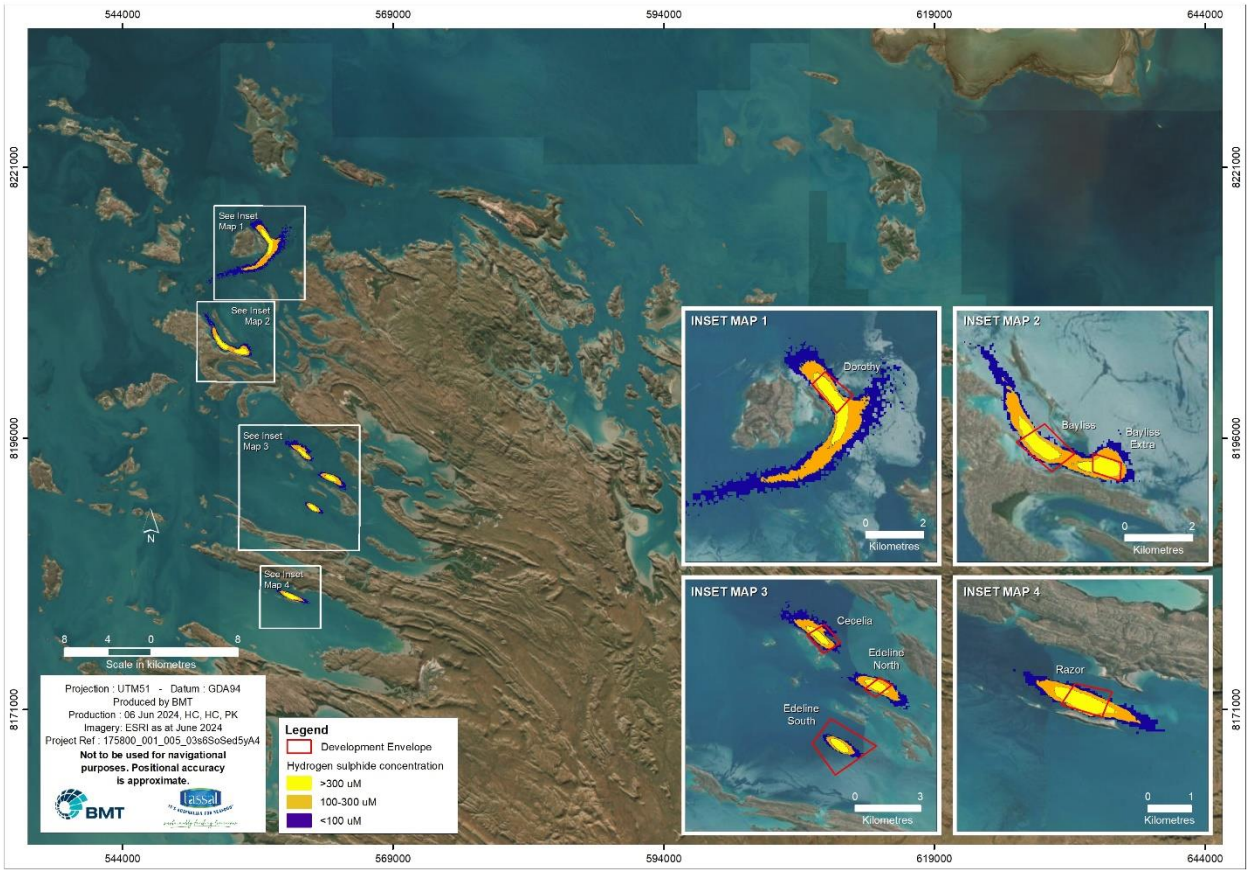

Figure 4.75 Soft sediment impact footprints after 5 years of operations under Scenario 1.

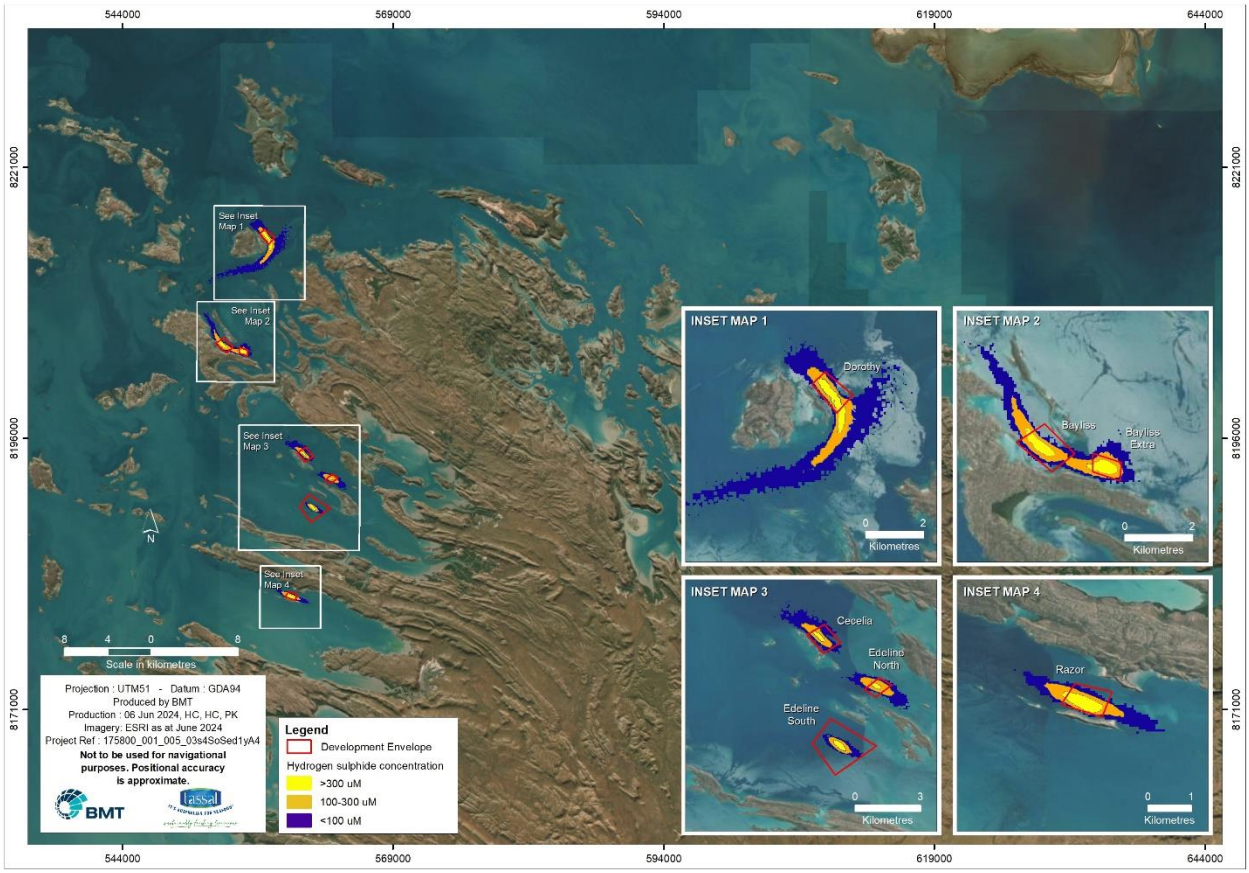

Figure 4.76 Soft sediment impact footprints after 1 years of operations under Scenario 2.

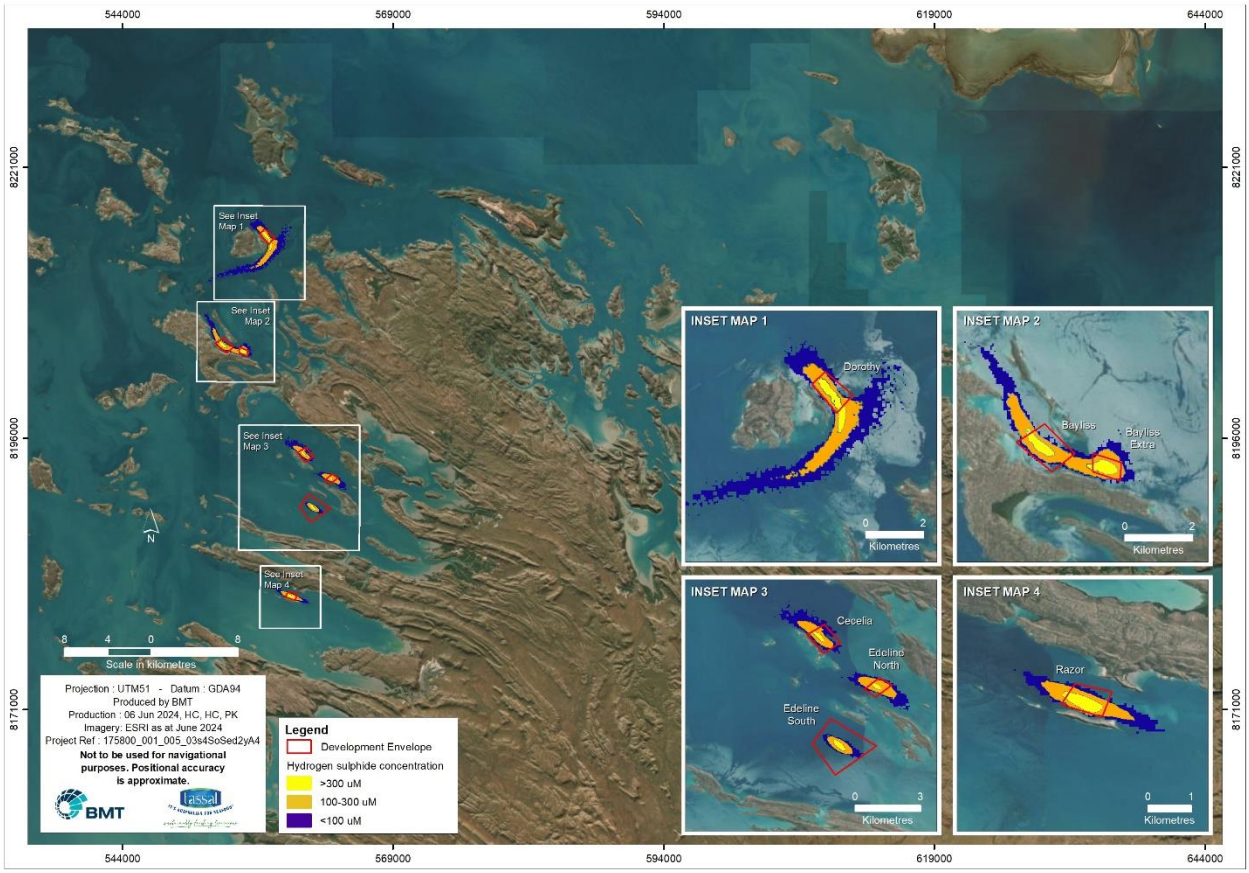

Figure 4.77 Soft sediment impact footprints after 2 years of operations under Scenario 2.

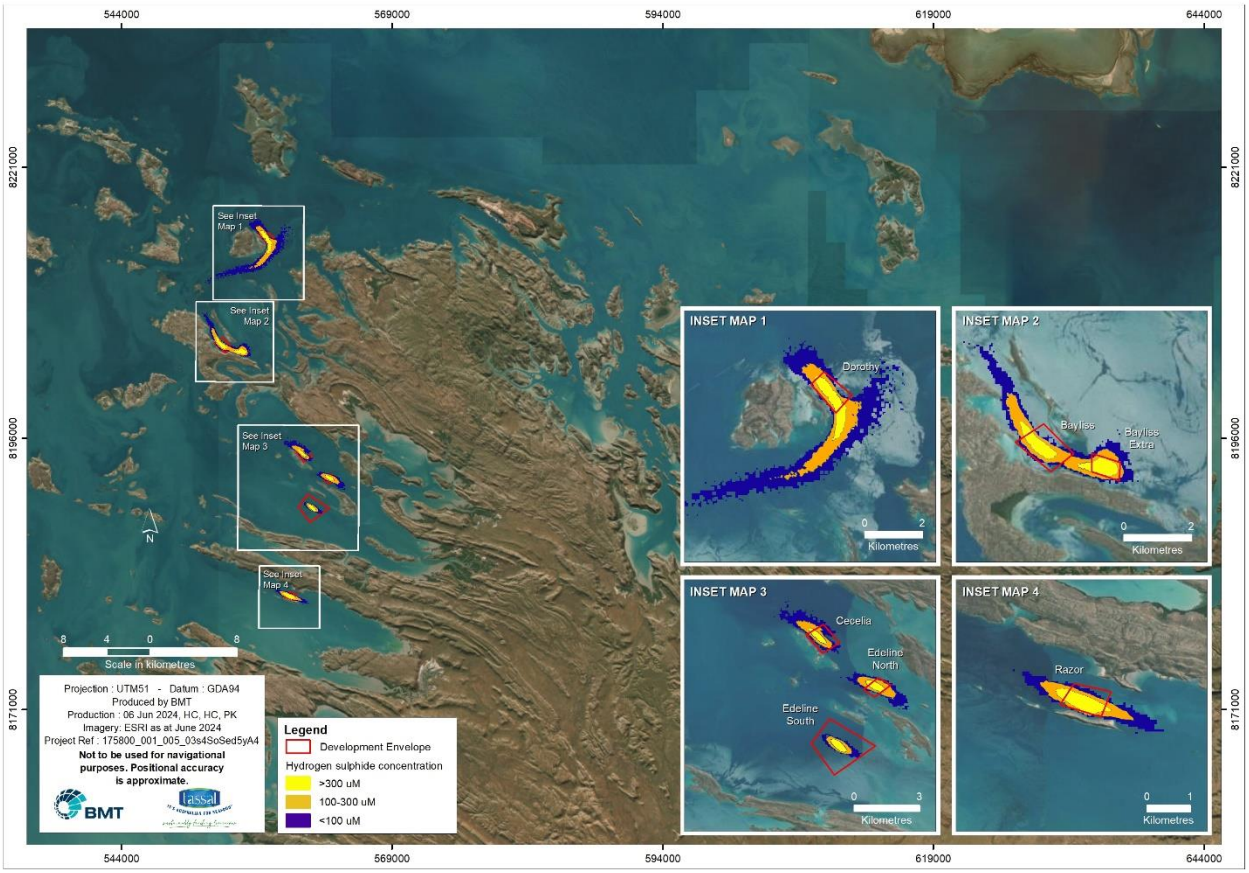

Figure 4.78 Soft sediment impact footprints after 5 years of operations under Scenario 2

5 References

Apogee Instruments (2016) Conversion - PPFD to Watts, [Accessed on 2024 Feb 18] https://www.apogeeinstruments.com/conversion-ppfd-to-watts/

Apogee Instruments (2024) Daily Light Integral Measurement, [Accessed on 2024 Feb 18] https://www.apogeeinstruments.com/daily-light-integral-measurement/

Boudreau BP (1997) Diagenetic models and their implementation. Heidelberg, Springer

Boudreau BP (1996) A method-of-lines code for carbon and nutrient diagenesis in aquatic sediments. Computers & Geosciences, 22(5): 479-496

Brigolin DR, Pastres TD, Nickell CJ, Cromey DR, Aguilera and P Regnier (2009) Modelling the impact of aquaculture on early diagenetic processes in sea loch sediments. Marine Ecology-Progress Series 388: 63-80

Brooks KM, Stierns AR, Backman C (2004) Seven year remediation study at the Carrie Bay Atlantic salmon (Salmo salar) farm in the Broughton Archipelago, British Columbia, Canada. Aquaculture 239: 81-123

BMT (2024a) Ocean Barramundi Expansion Project - Calibration Modelling Report. Prepared by BMT for Tassal. Report No. 175801.000_4

BMT (2024b) Ocean Barramundi Expansion Project - Baseline Marine Environmental Quality Report, Prepared by BMT for Tassal. Report No. 175801.000_3

BMT (2024c) Ocean Barramundi Expansion Project – S38 Referral Supporting Report. Prepared by BMT for Tassal. Report No. 175801.000_1.

BMT (2020) TUFLOW FV User Manual, Build 2020.01, Sediment Transport and Particle tracking modules

BMT (2019) Delma Island Aquaculture Development Zone, Modelling Report, R.B22025.002.00.

BMT (2016) Modelling and Technical Studies in Support of the Mid-West Aquaculture Development Zone, Technical Report,1051_009/1_Rev3

Chen YS, Beveridge MCM, Telfer TC (1999) Settling rate characteristics and nutrient content of the faeces of Atlantic salmon, Salmo salar L., and the implications for modelling of solid waste dispersion, Aquaculture Research, 30:395-398

Cromey CJ, Nickell TD, Black KD (2002) DEPOMOD – modelling the deposition and biological effects of waste solids from marine pen farms, Aquaculture Vol 214: 211-239

DHI (2013) Kimberley Aquaculture Zone - Environmental Field Studies and Numerical Modelling in Support of an EIS. Final report prepared for the Western Australian Govt. Dept. of Fisheries, May 2013

Department of Environment and Science - DES (2018) Guidance on using Photosynthetically Active Radiation (PAR) as a method to measure light availability for aquatic photosynthetic organisms facing

acute impacts, Environmental Protection (Water) Policy 2009 - Monitoring and Sampling Manual, Biological assessment, Version: February 2018, https://environment.des.qld.gov.au/__data/assets/pdf_file/0017/90512/biological-assessment-measuring-light-using-par.pdf

Department of Water and Environmental Regulation (DWER) (2021): http://wir.water.wa.gov.au/Pages/Water-Information-Reporting.aspx, Water levels – flow and Water quality data, accessed 16 September 2021

EPA (2016) Technical Guidance – Protection of Benthic Communities and Habitats, Environmental Protection Authority. Perth, Western Australia, December 2016

EPA (2017) Environmental Quality Criteria Reference Document for Cockburn Sound – A Supporting Document to the State Environmental (Cockburn Sound) Policy 2015. Environmental Protection Authority, Perth, Western Australia, April 2017

EPA (2021) Technical Guidance – Environmental impact assessment of marine dredging proposals, EPA, Western Australia, September 2021

Falkowski PG, & Raven JA (2013). *Aquatic photosynthesis*. Princeton University Press.

Felsing M, Telfer T, Glencross B (2005) 15N-enrichment of an aquaculture diet and tracing of pen culture waste in an estuarine environment. J. App. Icthyology 22: 419-426

Fernandes M & Tanner J (2008) Modelling of nitrogen loads from the farming of yellowtail kingfish Seriola lalandi (Valenciennes, 1833). *Aquaculture Research*, *39*(12), 1328-1338.

FES2014 (2016), FES2014 was produced by Noveltis, Legos and CLS and distributed by Aviso+, with support from Cnes (https://www.aviso.altimetry.fr/)

Flather RA & Davies AM (1976) Note on a preliminary scheme for storm surge prediction using numerical models. *Quarterly Journal of the Royal Meteorological Society*, *102*(431), 123-132.

Gattuso JP, Gentili B, Duarte CM, Kleypas JA, Middelburg JJ, & Antoine D (2006) Light availability in the coastal ocean: impact on the distribution of benthic photosynthetic organisms and their contribution to primary production. *Biogeosciences*, *3*(4), 489-513.

Gunaratne GL, Carmody H, Crisp J, McCall E and Bruce L (2021) A decision support tool for environmental impact assessment in mariculture; An integrated modelling approach, MODSIM2021, 24th International Congress on Modelling and Simulation. Modelling and Simulation Society of Australia and New Zealand, December 2021, ISBN: 978-0-9872143-8-6.

Herbeck LS, Unger D, Wu Y.& Jennerjahn T (2013) Effluent, nutrient and organic matter export from shrimp and fish ponds causing eutrophication in coastal and back-reef waters in NE Hainan, tropical China. Cont Shelf.

Hipsey MR, Bruce LC & Hamilton DP (2013) Aquatic Ecodynamics (AED) Model Library, Science Manual, https://aed.see.uwa.edu.au/research/models/aed/downloads/AED_ScienceManual_v4_draft.pdf

HYCOM 3.1, Global Ocean Forecasting System (GOFS) 3.1 output on the GLBy0.08 grid, https://www.hycom.org/dataserver/gofs-3pt1/analysis

Macleod C, & Forbes S (2004) Guide to the assessment of sediment condition at marine finfish farms in Tasmania. Tasmanian Aquaculture and Fisheries Institute, University of Tasmania.

Moccia R, Bevan D, Reid G (2007) Composition of Fecal Waste from Commercial Trout Farms in Ontario: Macro and Micro Nutrient Analyses and Recommendations for Recycling. Final Report Submitted to the Ontario Sustainable Aquaculture Working Group Environment Canada, 22pp

Moran D, Pether S, Lee PS (2009) Growth, feed conversion and faecal discharge of yellowtail kingfish (Seriola lalandi) fed three commercial diets. New Zealand Journal of Marine and Freshwater Research, 2009, Vol. 43: 917-927

Murray JW (2000) The oceans. In International Geophysics, Vol. 72, pp. 230-278.

NASA Earth Observations (2014) NASA Goddard Space Flight Center, Ocean Ecology Laboratory, Ocean Biology Processing Group. NASA OB.DAAC, Greenbelt, MD, USA. doi: 10.5067/AQUA/MODIS/L3B/CHL/2014. https://neo.gsfc.nasa.gov/view.php?datasetId=MY1DMM_CHLORA. Accessed 2021/08/25. Maintained by NASA Earth Observations (NEO) in coordination with Gene Feldman and Norman Kuring, NASA Goddard Ocean Color Group.

O2Marine (2021) s38 Referral Supporting Document Rev1, Appendix Q; Water Quality Desktop Review Report; Ashburton Infrastructure Project, prepared for Mineral Resources Limited.

Paraska DW, MR Hipsey and SU Salmon (2014) Sediment diagenesis models: Review of approaches, challenges, and opportunities. Environmental Modelling & Software 61(0): 297-325

Paraska DW, Bruce L and MR Hipsey (2015) Midwest Zone Aquaculture Modelling; Sediment quality impact assessment, Technical Report, The University of Western Australia (UWA) & BMT Oceanica

Riley JP & Skirrow G (1974) Chemistry Oceanography, vol. 1,(translated by Liu Guang, et al., 1982).

Rodela T (2013) The Humble Beginnings of The Study of Nitrogen Excretion in Fish. Journal of Experimental Biology 2013 216: 162-163; doi: 10.1242/jeb.076109

Skretting (2024) Nova FF for Barramundi and native species, Standard energy floating feed for optimal conditions.

Strydom S, McMahon K, & Lavery P (2017) Response of the seagrass *Halophila ovalis* to altered light quality in a simulated dredge plume. Marine Pollution Bulletin 121 (2017) 233-330

Tanner JE & Fernandes M (2010) Environmental effects of yellowtail kingfish aquaculture in South Australia. *Aquaculture Environment Interactions*, *1*(2), 155-165.

Tanner JE, Clark TD, Fernandez M and Fitzgibbon Q (2007) Innovative solutions for aquaculture: spatial impacts and carrying capacity - further developing, refining and validating existing models of environmental effects of finfish farming. South Australian Research and Development Institute – Aquatic Sciences, Adelaide, Australia

Volkman J, Thompson P, Herzfeld M, Wild-Allen K, Blackburn S, Macleod C & Revill A (2009) A whole-of-ecosystem assessment of environmental issues for salmonid aquaculture. Aquafin CRC Final Report (CRC Project 4.2 (2)/FRDC Project 2004/074).

Wu Y, Chaffey J, Law B, Greenberg DA, Drozdowski A, Page F, Haigh S (2014) A threedimensional hydrodynamic model for aquaculture: a case study in the Bay of Fundy. Aquaculture Environmental Interactions 5: 235-248

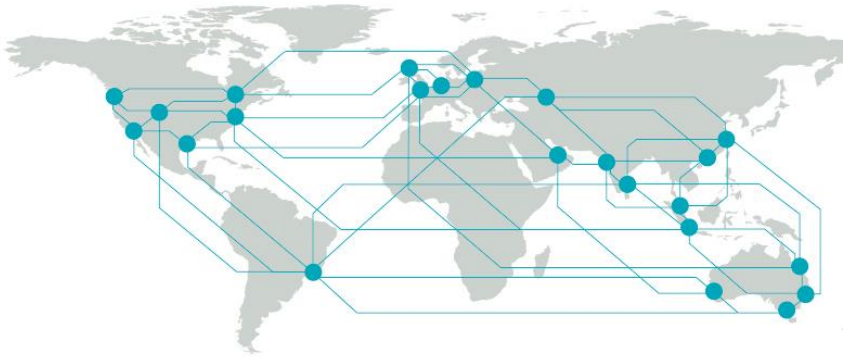

BMT is a leading design, engineering, science and management consultancy with a reputation for engineering excellence. We are driven by a belief that things can always be better, safer, faster and more efficient. BMT is an independent organisation held in trust for its employees.

Level 4
20 Parkland Rd
Osborne Park
WA 6017
Australia
+61 (8) 6163 4900

Registered in Australia
Registered no. 010 830 421
Registered office
Level 5, 348 Edward Street,
Brisbane QLD 4000 Australia

For your local BMT office visit www.bmt.org

Contact us

enquiries@bmtglobal.com

www.bmt.org

Follow us

www.bmt.org/linkedin

www.bmt.org/youtube

www.bmt.org/twitter

www.bmt.org/facebook